ISSN: 1813-1786 (Print)
ISSN: 2313-7770 (Online)
Volume No. 19
Indexed & Abstract in:
- PASTIC SCIENCE ABSTRACTS
- AGRIS DATABASE
- ProQuest Products

TECHNICAL JOURNAL

(Quarterly)

for online access please visit http://web.uettaxila.edu.pk/techjournal/index.html

2014

University of Engineering and Technology
Taxila, Pakistan

Vol: 19 **No. III (July - Sep)**

Technical Journal

A Quarterly Journal of University of Engineering & Technology (UET) Taxila, Pakistan
Recognized by Higher Education Commission (HEC)
Y Category

ISSN: 1813-1786 (Print) ISSN: 2313-7770 (Online)
Volume No. 19 (Quarterly)
No. III (July - September)
2014

Phone: 92 - 51 - 9047298 **Fax: 92 - 51 - 9047420** **E-Mail: technical.journal@uettaxila.edu.pk**

Technical Journal is abstracted and indexed in ProQuest Products, Agris, Pakistan Science Abstract, Ulrich periodic directory plus Pastic Indexing Service.

EDITORIAL OFFICE:
Editor Technical Journal
Central Library, University of Engineering and Technology (UET) Taxila, Pakistan

EDITORIAL BOARD

CONTENTS

Numerical Simulation of Vortex Induced Vibration and Related Parameters in Cross Flow Shell and Tubes Heat Exchanger: A Review

A. Khan[1], S. Khushnood[2], N. U. Saqib[3], I. S. Shahid[4], R. Khalid[5], H. Elahi[6]

[1,2,3,5,6]*Mechanical Engineering Department UET Taxila, Pakistan*
[4]*Mechanical Engineering Department HITEC University Taxila, Pakistan*
[1]asif_shaheen22@yahoo.com

Abstract-This paper presents a brief review of studies on cross flow induced vortices in downside of tubes which leads to vibration. Two types of vibrations have been studied for tubes in cross flow: first vibration of the tube due to vortex shedding which is important primarily in cross flow but this vibration disappears in slug flow or froth flow regions which are important in numerous heat exchangers, secondly fluid elastic excitation which is most dangerous mechanism in heat exchanger tube bundles. The paper also presents the other parameters such as temperature variation on tube, pressure effect, lift and drag generation and their influence on heat exchanger tubes, different models comparison and tube size effect of tubes for vortices.

Keywords-Resonance, Slug Flow, Vortex Shedding, Fluid Elastic Excitation, Lift Coefficient

I. INTRODUCTION

The shell and tube heat exchangers have high surface area and volume ratio among all other types of heat exchangers and are easy to manufacture. Flow induced vibrations is a phenomena that can be found in many engineering fields such as aircraft wings, turbine blades, shell and tube heat exchangers, power transmission lines, centrifugal pumps, hydraulic gates and valves.

Turbulent buffeting is one the main cause of the tube excitation in heat exchangers. Vibration at or close to shedding frequency has a strong effect on the wake. Vorticity is a constant and discrete phenomenon. The important parameter defining the vortex shedding is Strouhal number. Strouhal number is the constant number between the frequency of vortex shedding and free flow velocity of the fluid. Fluid-elastic instability is by far the most hazardous excitation mechanism and the mainly general source of tube collapse.This instability is distinctive of self-exited vibration in that it results from the relations of tube motion and flow. The main reason behind acoustic resonance is that some flow excitation (possibly vortex shedding) having a frequency, which equals with the natural frequency of the heat exchanger cavity.

CFD is the simulation of systems concerning fluid flow, transfer of heat and coupled phenomena such as chemical reactions by means of computer-based simulation. The current paper presents the review of past papers of flow over tubes and cylinders creating vortices and vibration in the tubes.

A. Nomenclature

fvs	Frequency of vortex shedding
U_∞, U	Free stream flow velocity (m/s)
d	Diameter of tube (mm)
St	Strouhal number
Re	Reynolds number
T/D	Transverse pitch to dia ratio
P/D	Pitch to diameter ratio
L	Tube length (m)
λn	Frequency factor
ρ_m	Tube material density (kg/m3)
ρ_w	Water density (kg/m3)
γ	Bending stiffness (N/m)

B. Abbreviations

CFD	Computational fluid dynamics
FFT	Fast Fourier Transform
FIV	Flow induced vibrations
LES	Large Eddy simulations
FDM	Finite difference method
FVM	Finite volume method
FEM	Finite element method
DNS	Direct numerical simulation
RANS	Reynold's average navier stroke model

II. REVIEW

A brief review of the work done by various previous researchers has been presented here.

2.1 Fluid Elastic Excitation

Fluid-elastic instability is the most hazardous excitation method in heat exchanger tubes and the most ordinary reason of tube fracture. When the tubes vibrate forces generated and these forces have a linked with fluid-elastic instability. The fluid-elastic instability is characterized as the feedback mechanism between fluid forced and the structural motion [i]. A small displacement in structure due to instability effects the flow pattern, creates a change in fluid forces. This results to an auxiliary displacement of tubes and so on. If this displacement increases, the significant phase difference started to occur, leading to the fluid-elastic instability. There are three different ways in which energy is extract by cylinder from flow. These are

1. There must be difference in phases of cylinder displacement and fluid force generated.
2. There should be at least two degree of freedom phase difference between cylinder and flow
3. Since the fluid force is hysteretic due to non - linearities and its magnitude depends on the direction of cylinder motion.

A substantial hypothetical and experimental research has been undertaken in the past three decades to enter at a secure and consistent design criterion against fluid-elastic instability. The topic has been discussed on ordinary basis from time to time by different researchers focusing on tube failure caused by fluid elastic instability [ii, iii, iv, v].

Eulerian porous medium formation was developed to model the fluid structure interaction of tube bundle [vi]. They results that porous medium model is used to represent the two way coupling which is assessed by comparing its predictions to DNS predictions of Laminar cross flow.

2.2 Vorticity Excitation

There are series of vortices produced across the tube as the fluid passes the tube and flow divides from the opposite sides of the tube. This shedding of vortices produces discontinuous forces, which arise more commonly as the free stream velocity increases. For a single cylinder, f_{vs} frequency of vortex shedding is given below by dimension less Strouhal number.

$$f_{vs} = \frac{StU}{d_o} \quad (1)$$

Locked-in phenomena occur in tubes when frequency of vortex shedding becomes equal to the natural frequency of of tubes vibrating freely even when we increase the free stream velocity [vii].

The value of Strouhal number becomes a constant of about 0.2 for a single cylinder [viii]. The accurance Vortex shedding for the ranges of Reynolds number 100 < Re <5x105 and > 2 x 106 while it dies out in-between. The gap is due to a transfer of the flow division point in vortices in the transitional trans-critical Reynolds number range. There is an excitation in the tubes when vortex shedding frequency matches with the natural frequency of the tubes.

Reference [ix] by simulating a circular cylinder found that by contrasting the flow at low Reynolds's number could generate the vortex shedding. There is a very wide wake when the flow is passed through a cooled cylinder due to more influence of the fluid which is ambient. A plot that clearly demarcated zones of the vortex shedding of Reynolds's number against Strouhal number is shown in Fig. 1.

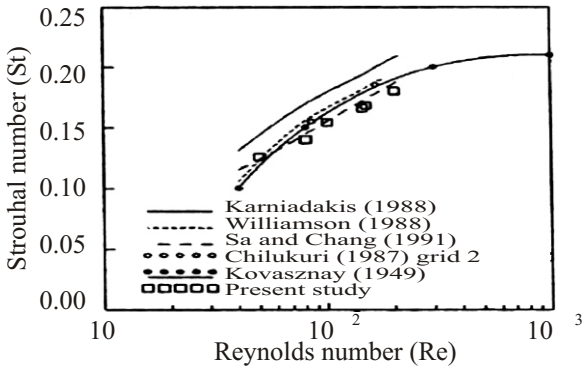

Fig. 1. Comparison of Strouhal number against Reynolds number. [ix]

Flow induced vibrations were investigated [x] by vortex shedding phenomena in underwater cylinder that leads to the damage in nuclear power plant components. Various numerical simulations and experiments have been conducted to predict the vibration phenomena. Three tests have been carried out including flow past a rigid circular cylinder, inline oscillations of the circular cylinder and flow induced vibrations with unidirectional motion to prove the projected numerical methods.

Reference [xi] studied the vortex shedding characteristics and the drag force acting on the circular cylinder attached with the splitter plate. The splitter plate is forced to oscillate harmonically at the Reynolds number of 100. The Fig. 2 presents the geometry and kinematics of the cylinder and the splitter plate.

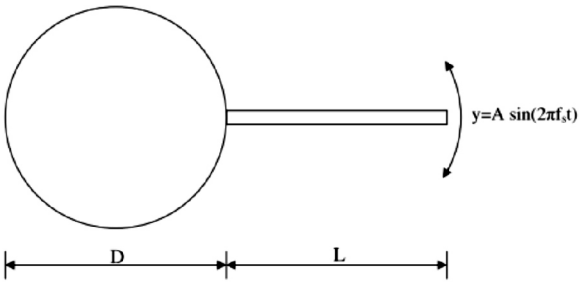

Fig. 2. Geometry of the cylinder and the splitter plate [xi]

Careful observation suggests that there are three patterns of vortex shedding observed in the wake of circular cylinder which mainly depends on the frequency and the amplitude of vibration of the oscillator plate, normal shedding, chain of vortices and shedding from the splitter plate. The results suggest that the shorter splitter plate with obligatory oscillations can be used to suppress vibrations.

A numerical technique was used, called hybrid discrete vortex method, to simulate flow around circular cylinder in a planar oscillatory flow [xii]. Number of techniques is examined for estimating the forces on the cylinder. The comparison of different techniques shows that the Wu's method gives more accurate predictions in which surface pressure is predicted more perfectly than other numerical techniques.

Same discrete vortex method was used [xiii] to investigate the hydro elastic interaction between oscillating cylinder and the fluid forces. The calculations are compared with the results obtained by the quasi-steady theory. The results show that transition of vibration mode occurs with the varying reduced velocity.

A single cylinder can show a large amplitude response even with a small velocity change. There is a certain vibration of the cylinder in elliptical orbits beyond the critical value [xiv]. The displacement in different cylinders with respect to velocity is shown in Fig. 3.

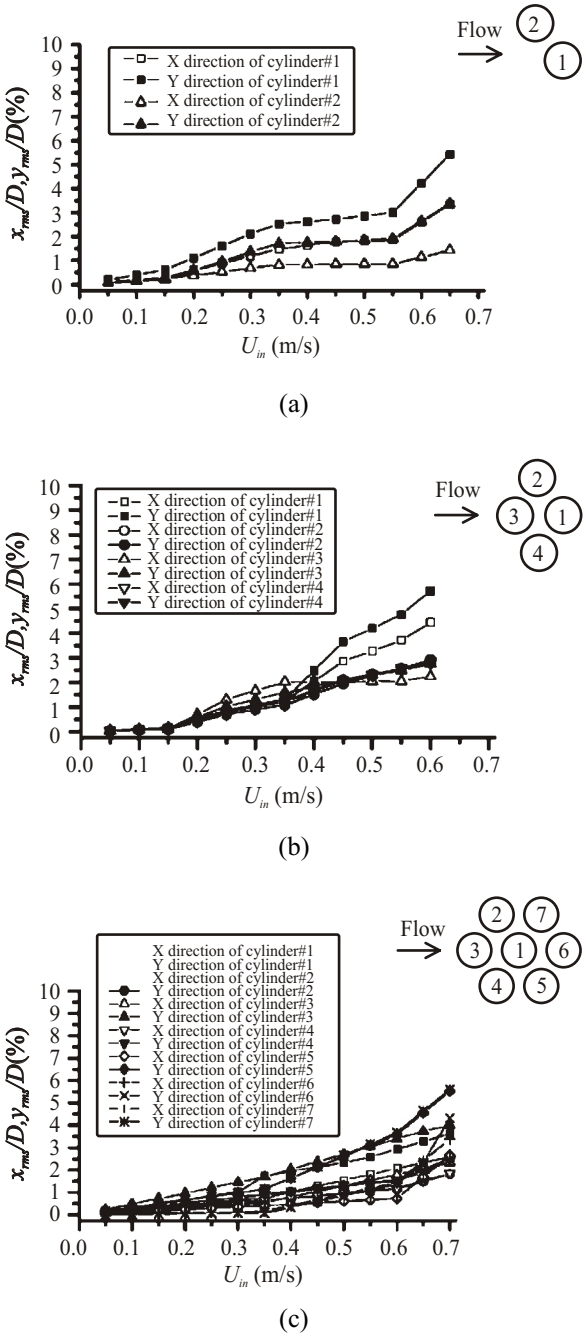

Fig. 3. (a), (b), (c) Displacement in different cylinders with respect to velocity [xiv]

Reference [xv] were the first who results analytically the vortex shedding frequencies in in-line tube bank in which he introduced different tube spacing and results that tube spacing has major effect on Strouhal number.

There exist vortex shedding in two cylinders when we arrange them parallel and perpendicular to free stream velocity [xvi, xvii].

Reference [xviii] carried out research on the turbulence response of the tubes due to excessive vibrations in many industries. They concluded the response of the tube, impact ratio and contact ratio in non-dimensionless form. There is a decrease in root mean square impact forces due to increase in support clearance which is a permanent level of excitation and centered tubes. Also there is a reduction in raise reaction of the tube for a series of clearances.

A numerical simulation was performed [xix] on two side by side tubes at different transverse gap ratio and results that at Re = 100 and Thickness/Diameter= 1.5 there is a biased flow pattern which is bi stable behind both cylinder. At different flow pattern and different flow velocities a wide and thin wake section develops behind each of the cylinders. Fig. 4 shows the flow characteristics of two side by side cylinders.

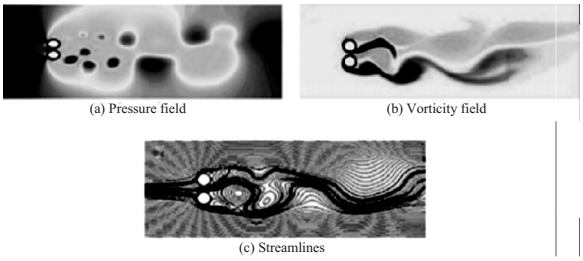

Fig. 4. Flow characteristics of two side by side cylinder at Re =100 T/D =1.5 tU/D = 65. [xix]

A simulation was performed for the flow behavior in a tube bundle and viewed that in the flow bundles [xx], when we know about the flow structure it can support in alleviating tribulations which are related by noise and vibrations induced by flow technique.

Analysis of fleeting flow behavior in the bundle of tubes with rounded and quadratic cross sections at dissimilar Reynolds numbers depends upon the inlet velocity and at different angle of attack. Results describes that a lean shear layers on the edge is resolved which becomes unsteady and this may result in the formation of co and contradict revolving vertices [xxi].

Research on surface vorticity method describes that while the tubes are fixed or rigid, stream in the region of the tubes is in ordinary pattern in a path around the tubes [xxii] as shown in Fig. 5.

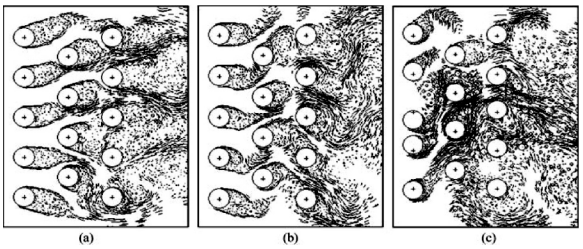

Fig. 5. Vorticity map of rigid and flexible cylinders (A) Rigid; (b) Flexible at SG =1.29, M =10 9; (c) Flexible at SG =0.516 , M=4. [xxii]

For tube banks strouhal number is not a unique value but changes with the pitch between the tubes [xxiii, xxiv]. Typical values for Strouhal number in-line and staggered tube bundle geometries are given in Fig. 6.

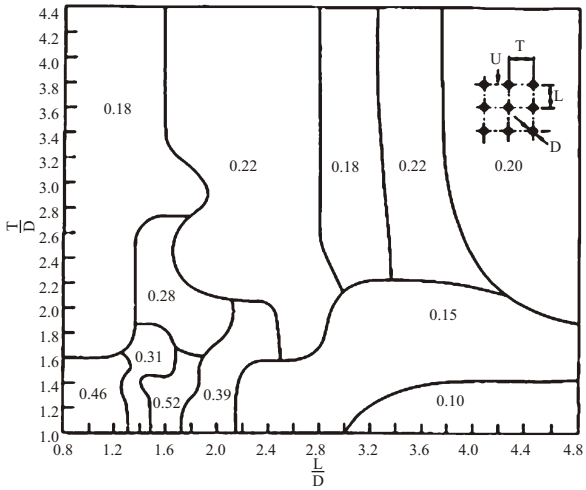

(a)

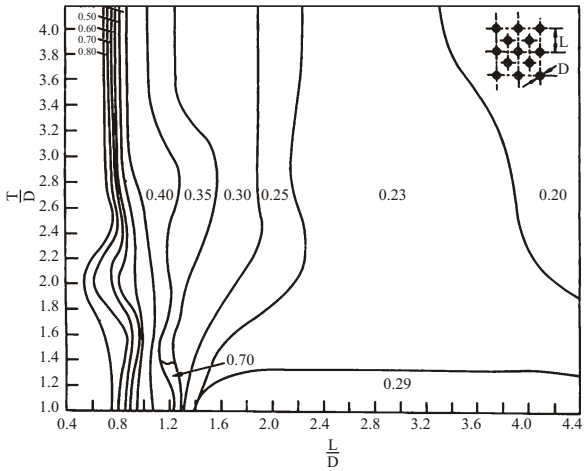

(b)

Fig. 6. (a) Strouhal numbers for in-line tube banks (b) Strouhal numbers for staggered tube banks [xxiii,xxiv]

Reference [xxv] have results numerically the effect of space between tubes on the vortex shedding of streamline flow over the inline tube array. The study consists a six row in-line tube bank having P/D = 8, with Navier-Strokes continuity equation based unstructured code. They wrote the incompressible navier-strokes equation in tensorial Cartesian form as given in equation (2) and (3)

$$\delta u_i / \delta x_i = 0 \quad (2)$$

$$\delta u_i/\delta t + \delta u_i u_j/\delta x_j = - \delta p/\rho \, \delta x_i + \nu \, \delta^2 u_i / \delta x_j \, \delta xj \quad (3)$$

A significant spacing range between 3.0 and 3.6 is identified at which displacement is maximum for the mean lift and drag coefficients. Also at critical spacing, there is 180° phase difference in the shedding cycle between succeeding cylinders and the vortices travel a distance twice the tube spacing within one period of shedding.

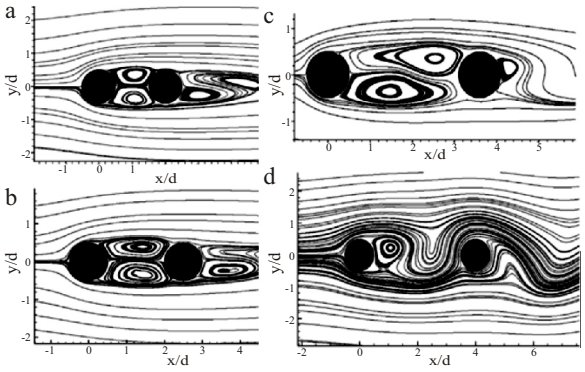

Fig. 7. Instantaneous response of two in line cylinders in tandem arrangement: (a) s=2, (b) s=2.5, (c) s=3.6 and (d) s=4.0. [xxv]

The review and summary of the basic results and discoveries associated to vortex induce vibrations with meticulous prominence to vortex dynamics and energy transfer that give rise to vibrations. They given the importance of mass and damping and the concept of "critical mass", "effective elasticity" and the liaison between force and vorticity. They results that that as the vibrating structural mass decreases, velocity stream (non-dimensional) having large amplitude vibration rises [xxvi].

The results of simulation in relation among vortex shedding and acoustic resonance in boiler plant for tube banks to illuminate the interactive properties of vortex shedding and acoustic resonance. At the Reynolds number range (1100-10000) it is observed that there is sporadic velocity fluctuation due to vortex shedding in tube banks [xxvii]. Areview stated that it is important to control vibrations induced by vortex shedding in realistic applications where active or passive control could be applied [xxviii].

Simulation results on vortex shedding relative with the acoustic resonance in staggered tube banks and examine three Strouhal number (0.29, 0.22 and 0.19). The vortices of 0.29 and 0.22 components on the other hand occasionally originated [xxix].

The discussion and overviewed procedures and recommended design guidelines for periodic wave shedding in addition to other flow induced vibration considerations for tube bundles concludes that the variable forces due to sporadic gesture shedding depends on the number of considerations like numerical configuration of tube bundles, its position Reynolds number, turbulence, density of fluid and pitch to diameter P/D ratio [xxx].

Reference [xxxi] tested different tube arrays and apply numerical method to different industry devices. Transient flow behaviour with tubes of circular, square and twice cruciform at different Reynolds number using different angles of attacks is studied. Results show that at high Reynolds no Re > 500 two dimensional effects are less important than three dimensional and it becomes necessary to us to simulate the detailed three dimension devices.

By using the URANS model show that flow is instable across tube bundles and there is a high pressure on the tube which is on the inlet flow of water and these results are taken from the distribution of pressure around the tubes [xxxii].

Turbulent flow computation in the cylinder arrays shows that there is a different flow regimes in line and circular cylinder even at same Reynolds's number. There is a different vortex form and a jet shear layer of vortices is present in the inline cylinder. In the rotated array vortices are generated by periodic shedding off the boundary. Due to these vortices rotated cylinder arrays have higher lift and drag coefficient [xxxiii].

Simulate the fluid structure interaction in a tube array shows that cylinder spontaneously displays an oscillatory motion which first corresponds to vortex induced vibration associated to a lock-in mechanism for low values of the reduced velocity and secondly develops Movement Induced Vibration, MIV, for higher values of the reduced velocity [xxxiv].

Analysis of the flow induced vibration of PWR steam generator used the fully coupled model of fluid dynamics and structure for the fluid structure problems and results that single tube gives more vibration as compared to bundles [xxxv].

2.3 Temperature Distribution And Heat Transfer Around Tubes:

Reference [xxxvi] reviewed that different arrangement of heated rod bundles found the introduction of different distribution of the temperature at the wall of the rods and its value depends upon the structure of the geometry. When conditions of the flow are the same, the flow which is on the downside of the rods is at higher wall temperature than the flow which is on the upper side. Also there is a smallest temperature of the wall at hexagonal geometry frame.

Research finds that there is an increase in heat transfer at high air velocity and decrease in pressure loss in the layer with delta winglet eddy generators [xxxvii].

2.4 Pressure Creation And Fall On Tubes

Research on the effect of increasing and decreasing baffle cuts on the pressure drop results that decrease the baffle plates cut, pressure drop across the heat exchanger decreases. They pointed out that this effect is due to baffle plate length the fluid crossing

it [xxxviii]. A research on plate fin heat exchanger to calculate the pressure fall break up of stainless steel heat exchanger calculated that the actual case has almost sixteen percent higher drop in pressure than ideal one which has a jagged curved at the inlet channel of heat exchanger [xxxix].

Reference [xl] performed a numerical study and concluded that there is a wake switching effect and rotatory eddy flaking in a tube bank which is to be staggered. They concluded that there is a spontaneous develops in the transient flow. Due to transient nature, pressure related quantities have a large shock. Also there is a large fluctuation of pressure acting on tube walls which is to be due to triode like effect. Reference [xli] carried our research on simulation of flow of fluid for the reduction of pressure drop across polymer tube bundles. Results shows that to make the streamline cylinder more slender there is a increase in the drag reduction. They results that there is a significant reduction in pressure drop when we use elliptical cylinder instead of circular cylinder.

Reference [xlii] carried out research that how pressure is drop in rheological and algebraic forms in the tubes. Their simulation describes that velocity is high in the centre of the tubes away from the walls. Due to the low additional stress point there is a low twisting rate occurs in the tubes.

Reference [xliii] carried out research on the different inlet velocity and oscillatory flow past a cylinder and concluded that there are several computational aspects at Reynold = 160. Results describes that there is a decrease in moment domain of nusselt number and root mean square values while increase in time domain drag coefficient with the increase in temperature values at the surface.

The investigation of turbulent flow crosses the heat exchanger tubes flow velocity in near wall passages have higher velocity and higher temperature. They results that heat transfer coefficients are lower near to wall tubes as compared to other tubes [xliv].

2.5 Effect of Size of Tubes

Reference [xlv] perform a numerical evaluation of heat exchanger and views that by alternating the sizes of the tube, there is a repression of the eddy flaking mechanism. The configuration of unequal cylinders that has been placed longitude and transverse pitches les to a raise in heat transfer.

A research on helically coil tubes find that there is a vibration and freeting wear which is due to potential flow. They concluded that by increasing the diameter of coil or the number of turns of the coil there is a reduction in normal frequency. The response of the amplitude to the highly disorder vibration induces by flow increases as the space rate or diameter of the coil increases [xlvi].

A research on the two phase bubby flow views that bubble trajectory in tube rods depends on the size of the bubble and the geometry of the rod [xlvii].

Reference [xlviii] concluded that at Re = 100 over cylinder and Length/Diameter = 2.5 in between the cylinders, there is no vortices on upstream cylinder shed and the cut off coating from the cylinder separation are going to reattach on the face of the downstream one. There is a decaying trend due to viscosity in the lift coefficient which is used to stabilize the flow. When we increase the Reynolds no and L/D ratio there is a more unstable behavior of flow.

Reference [xlix] using a number of techniques to find the cylinder forces and reviews that pressure which acts on the cylinder is considered by using the ordinary vortices slope at the surface with the use of Poisson's equation.

Reference [l] shows the Uncertainty reduction of the heat exchanger tubes along with the different complex issues which are responsible for the stability analysis. They actually gives us a review of real flows which are subjected to turbulent as well as vortex shedding.

Reference [li] pointed out that the turbulence is responsible to reduce the fluid flexible stable boundary and these stable boundary is defined by an unsteady divergence.

Reference [lii] reviewed that Spiral tube bundles are used in heat exchanger for the enhancement of the heat transfer and shows that in tube heat exchanger there is a significant effect due to cone angle and cross section and there is a little influence on the tube heat exchanger due to helical pitch. The inferior fluid flow turns into serious due to the raise of twist.

2.6 Formation of Lift and Drag on the Tube Bundles

Reference [liii] presented the Effect of Reynolds no on the drag and lift forces and results that there is a apparent periodic oscillations in lift coefficient. These oscillations are shown in Fig. 8.

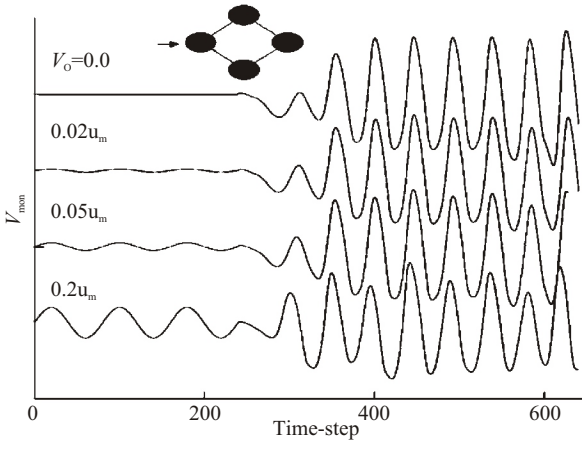

Fig. 8. Effect of Re on the lift coefficient. [liii]

Reference [liv] have perform a numerical study on the time proof of drag and lift forces, acting on the bundle of tubes and power spectral density. They concluded that it is possible to provide a mathematical approximation of the significant stream speed for the threshold of fluid flexible instability from the numerical results without using any results from experiment.

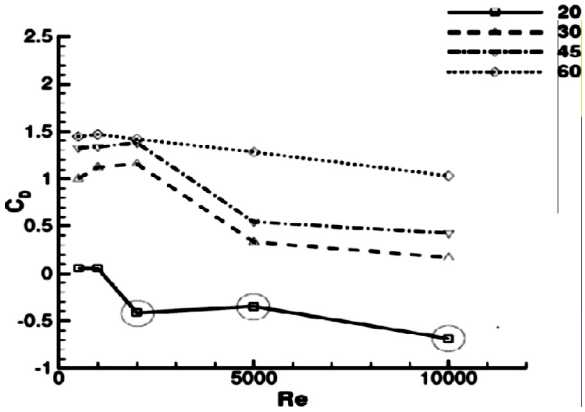

Fig. 9. Values of coefficient of drag at different Reynold's number. [liv]

Reference [lv] have performed the flow characteristics on staggered and non staggered tube bundles. The conservative forms incompressible energy, continuity and momentum equations which were used in their research are shown in equation (4), (5), and (6)

Continuity $$\frac{\partial y}{\partial t} + \nabla(\rho V) = 0 \quad (4)$$

Momentum $$\rho\frac{DV}{Dt} = \nabla.\tau_{ij} - \nabla p + \rho F \quad (5)$$

Energy $$\rho\frac{De}{Dt} + p(\nabla V) = \quad (6) \quad (6)$$

These equations are solved at every node of the the mesh for the drag and lift. The results shows that at high Reynolds number, the power range density results of the drag and lift forces are dissimilar on different tube rows are flooded onto a single curve.

A research on surface pressure measurement on the deformed tubes finds that when we integrate the exterior pressure allocation at a position which is at an angle, there is gradient in coefficient of lift and drag forces with respect to neighboring tube displacement and these parameters are free from Reynolds's number. They also concluded that tube spacing in the heat exchanger tubes effects the vortex shedding [lvi].

Reference [lvii] by using different method and set of laws to find the Navier stocks and continuity equations views that there is a critical spacing where average drag along with lift co-efficient for cylinders are maximum when cylinders are placed at last. By further increasing the spacing there is a decrease in force statistics.

Numerical simulation on the triangular arrays of tubes results that the lift coefficient of the root mean square and the time average drag coefficient take their maximum charge for the time in position for the cylinder. In the wake of the cylinder volumetric portion of the gaseous phase has a greater value [lviii].

Reference [lix] describes that flow patterns has a great effect on the vibration of tubes and concluded that by using mathematical study we have an inflection phenomenon which occurs at a lower excitation frequency in case of two cylinder than at a single cylinder. There is a higher drag and root mean square values in oscillating cylinders than at stationary cylinders.

2.7 Comparison of Different Models

Research to compare the different technique reviewed that these techniques gives the results of LES models on a mesh which is to be fined with the DNS model shown a sensible conformity even with a course mesh. Also the results shown that the 2D RSTM model is physically irrational which produced strong vortex shedding in the tubes [lx]. Reference [lxi] carried out research on Characteristics of gas pass a cylinder pointed out that the rebound tendency of the particulate is suppress by the high reynolds's no of the gas flows . A research which gives us a well-built relationship of the coherent velocity fluctuations which is to be found from the extent of two point space point relationship. This results is very suitable when the value of the Reynolds no are taken to be higher and the systems which are more complex [lxiii].

TABLE I
TUBE NATURAL FREQUENCIES MACDUFF AND FEGLAR [lxiii]

Formula/Procedure	Conditions
$f_n = \left(\frac{1}{2\pi}\right)\frac{\lambda_n}{l^2}\left(\frac{EI}{m}\right)^{1/2}$ (Jones, 1970)	Straight beams /single span n is the mode number and λ_n is a frequency factor which depends upon the end conditions
$f_n = \frac{1}{2\pi}\lambda_n\left(\frac{1}{R\alpha}\right)\left(\frac{EI}{m}\right)^{1/2}$ (Archer, 1960)	Curved beams/ single span λ_n is a frequency factor R is the radius of curvature and α is the subtended angle
$f_n = 59.55\frac{C_u}{L^2}\left(\frac{EI}{M_e}\right)^{0.5}$ (TEMA Standards, 1978)	U-tube curved C_u is the first mode U-tube constant

Formula/Procedure	Conditions
Experimental/computer Program $f_n = \frac{(\beta_n L)^2}{2\pi L^2}\sqrt{\frac{EIg}{W}}$ (Lowery and Moretti, 1975)	Straight/multiple, free-free spans (1-5 span tests); idealized support conditions, $(\beta_n L)^2$ is eigen value
FEM in-plane and out of plane Experimental/analytical (Elliott and Pick, 1973)	Straight/curved
Beams immersed in liquids, air, kerosene, and oil (Jones, 1970)	Straight/simply supported/clamped
Out of plane: $f_n = 3.13\frac{\lambda_n}{R^2}\sqrt{\frac{C}{\gamma A}}$ $\lambda_n = \frac{n(n^2-1)}{\sqrt{1+kn^2}}$ (Ojalvo and Newmann,1964)	Clamped ring segments n is mode number; k is bending stiffness γ is specific weight; C is the torsional stiffness. A is cross-sectional area
Graphical in-plane and out of plane (Wambsganss et al., 1974)	Straight/curved, single span /multiple span
Analytical/experimental (Khushnood et al., 2000)	Straight tubes single/multiple spans with damped/ fixed boundaries, Experimentation on refinery research exchanger (in-service)
Plucking and transient decay (Simpson and Harlten, 1974)	Tubes were not fully straightened. Wind tunnel determination of fluid-elastic thresholds Tubes were found sensitive to temperature.

III CONCLUSIONS

1. Fluid-elastic instability is characterized as the feedback mechanism between fluid forced and the structural motion.
2. At Reynold's number of Re > 40 amplitudes of coefficient of lift begins to develop which generate vortex shedding in the tube.
3. When the tubes are fixed, stream in the region of the tubes is in ordinary pattern in a path around the tubes.
4. The value of Strouhal number changes as the pitch and tube diameter changes.
5. Hexagonal geometry frame has a smallest temperature of the wall as compared to other geometry arrangement.
6. Pressure drop across the heat exchanger decreases as we decrease the baffle plates cut.
7. Reduction in pressure drop is dependent on the geometry of cylinder, by using elliptical cylinder instead of circular cylinder there is a significant decrease in pressure drop.

REFRENCES

[i] S. J. Price., (1995). A review of theoretical models for fluid-elastic instability of cylinder arrays in cross-flow. *Journal of Fluids and Structures, Vol. 9,* pp. 463-518. Available:http://www.sciencedirect.com/science/article/pii/S0889974685710092

[ii] M. P. Paidoussis., (1981). Fluid-elastic vibration of cylinder arrays in axial and cross-flow: State of the art. *Journal of Sound and Vibration, Vol.76,* pp. 329-360. Available:http://www.sciencedirect.com/science/article/pii/0022460X81905162

[iii] M. P. Paidoussis., (1982). A review of flow-induced vibrations in reactors and reactor components. *Nuclear Engineering and Design, Vol. 74,* pp. 36-40. Available:http://www.sciencedirect.com/science/article/pii/0029549383901383

[iv] M. P. Paidoussis., (1987). A review of flow-induced vibrations in reactors and reactor components. *Nuclear Engineering and Design, Vol. 74,* pp. 31-60. Available:http://www.sciencedirect.com/science/article/pii/0029549383901383

[v] M. P. Paidoussis., (1987). Flow-induced instabilities of cylindrical structures. *Applied Mechanics Reviews, Vol. 40,* pp. 163-175. Available:http://appliedmechanicsreviews.asmedigitalcollection.asme.org/article.aspx?articleid=1393931

[vi] E.Tixier, École Polytechnique de Montréal; Cédric Béguin, École Polytechnique de Montréal; Stephane Etienne, École Polytechnique de Montréal; Dominique Pelletier, École Polytechnique de Montréal; Alexander Hay, École Polytechnique de Montréal and Guillaume Ricciardi, cea cadarache. (2014). Fluid-Structure Interactions in a Tube Bundle Subject to Cross-Flow. Part A: Porous Medium Approach. Available**:**http://arc.aiaa.org/doi/abs/10.2514/6.2014-1455

[vii] R. D. Blevins., Flow-induced vibration. Van Nostrand Reinhold Company, 1997. Available:http://adsabs.harvard.edu/abs/1977vnr.book

[viii] J. M Chenoweth., Chisholm, D., Cowie, R. C., Harris, D., Illingworth, A., Loncaster, J. F., Morris, M., Murray, I., North, C., Ruiz, C., Saunders, E. A. D., Shipes, K.V., Dennis Usher, and Webb, R. L. Heat Exchanger Design Handbook HEDH, Hemisphere Publishing Corporation, 1993.
Available:http://scholar.google.com.pk/scholar

[ix] V. Patnaik, and A. Narayana. (1999). Numerical simulation of vortex shedding past a circular cylinder under the influence of buoyancy. *International journal of heat and mass transfer 42(18)*: 3495-3507.
Available:http://www.sciencedirect.com/science/article/pii/S0017931098003731

[x] H. B. Lee., Lee, T. R. and Chang, Y. S. (2012). Numerical simulation of flow-induced bi-directional oscillations. *Journal of Fluids and Structures*.
Available:http://www.sciencedirect.com/science/article/pii/S0889974612001788

[xi] Y. Sudhakar. and Vengadesan, S. (2012). Vortex shedding characteristics of a circular cylinder with an oscillating wake splitter plate. *Computers & Fluids Vol.53,* pp. 40-52.
Available:www.sciencedirect.com/science/article/pii/S0045793011002787

[xii] X. W. Lin., Bearman, P. W. and Graham, J. M. R. (1996). A Numerical Study Of Oscillatory Flow About A Circular Cylinder For Low Values Of Beta Parameter. *Journal of Fluids and Structures*, 10:501-526.
Available:http://www.sciencedirect.com/science/article/pii/S0889974696900341

[xiii] C. T. Yamamoto., Meneghini, J. R., Saltara, F., Fregonesi, R. A. and Ferrari, J. A. (2004). Numerical simulations of vortex-induced vibration on flexible cylinders. *Journal of Fluids and Structures, 19*:467-489.
Available:http://www.sciencedirect.com/science/article/pii/S0889974604000374

[xiv] M. H. Yu., & Lin, T. K. 920050. A numerical study of fluid elastic vibrations of multiple cylinders in cross flow. *Journal of the Chinese institute of engineers, 28(1)*, 101-110.
Available:http://www.tandfonline.com/doi/abs/10.1080/02533839.2005.9670976#.UycFEoUny50

[xv] B. J. Grotz., and Arnold, F. R., (1956). Flow-induced vibration in heat exchangers. TN No. 31 to office of Naval Research from Stanford, A. D 104508.
Available:http://scholar.google.com.pk/scholar?q=related:fqHj2HBsAXgJ:scholar.google.com/&hl=en&as_sdt=1,5

[xvi] H. M Sipvack., (1946). Vortex frequency and flow pattern in the wake of two parallel cylinders at varied spacing normal to an air stream. *Journal of the Aeronautical Sciences,* pp. 289-301.
Available:http://arc.aiaa.org/doi/abs/10.2514/8.11375?journalCode=jans

[xvii] D. G. Thomas., and Kraus, K. A. (1964). "Interaction of vortex streets. *Journal of Applied Physics, Vol. 35,* p. 3458-3459.
Available:http://scitation.aip.org/content/aip/journal/jap/35/12/10.1063/1.1713250

[xviii] M. Hassan., Weaver, D., & Dokainish, M. (2002). A simulation of the turbulence response of heat exchanger tubes in lattice-bar supports. *Journal of fluids and structures, 16(8)*, 1145-1176.
Available:http://www.sciencedirect.com/science/article/pii/S0889974602904688

[xix] B. G. Dehkordi., Moghaddam, H. S., & Jafari, H. H. (2011). Numerical simulation of flow over two circular cylinders in tandem arrangement. *Journal of Hydrodynamics, Ser. B, 23*(1), 114-126.
Available:http://www.sciencedirect.com/science/article/pii/S1001605810600959

[xx] Y. Hassan., & Barsamian, H. (2001). New-wall modeling for complex flows using the large eddy simulation technique in curvilinear coordinates. *International Journal of Heat and Mass Transfer, 44(21),* 4009-4026
Available:http://www.sciencedirect.com/science/article/pii/S0017931001000473

[xxi] K. Schneider., (2005). Numerical simulation of the transient flow behaviour in chemical reactors using a penalisation method. *Computers & fluids, 34(10),* 1223-1238.
Available:http://www.sciencedirect.com/science/article/pii/S0045793004001343

[xxii] F. Wang., Jiang, G., & Lin, J. Z. (2008). Simulation of cross-flow-induced vibration of tube bundle by surface vorticity method. *Frontiers of Energy and Power Engineering in China, 2(3),* 243-248.

[xxiii] J. H. Lienhard. (1966). Synopsis of lift, drag and vortex frequency data for rigid circular cylinders, Washington State University, College of Engineering Research Division, Bulletin, 300.
Available:http://link.springer.com/article/10.1007/s11708-008-0049-7#page-1

[xxiv] Th. Karaman, (1912). Uber den mechanismus des Widerstandes den ein bewegter Korper in einen Flussigkeit Erfahrt", Nachr. Konigl. Gesellschaft.
Available: https://eudml.org/doc/58812

[xxv] C. Liang., Papadakis, G., & Luo, X. (2009). Effect of tube spacing on the vortex shedding characteristics of laminar ?ow past an inline tube array: *A numerical study," Computers & Fluids, 38,*950-964.

[xxvi] C. H. K. Williamson., & Govardhan, R. (2008). A Brief Review Of Recent Results In Vortex-Induced Vibrations. *Journal of Wind Engineering and Industrial Aerodynamics, 96,* 713-735. Available:http://www.sciencedirect.com/science/article/pii/S0167610507001262

[xxvii]H. Hamakawa., & Matsue, H. (2008). Acoustic Resonance and vortex shedding from tube banks of Boiler Plant. *Journal of Science and Technology, Vol.6,* No. 3. Available:http://adsabs.harvard.edu/abs/2008JFST....3..805H

[xxviii]A. R. Kumar., Sohn, H. C., & Gowda, H. L. (2008) Passive Control Of Vortex-Induced Vibrations: An Overview. *Recent Patents on Mechanical Engineering 1,* 1-11. Available:http://benthamscience.com/journal/index.php?journalID=rpmengsamples/meng%201-1/Kumar.pdf

[xxix] H. Hamakawa., & Fukano, T. 2006 "Effect Of Flow Induced Acoustic Resonance On Vortex Shedding From Staggered Tube Arrays," JSME International Journal, Vol.49. Available:

[xxx] M. J. Pettigrew., & Taylor, C. E. (2003). Vibration Analysis Of Shell-And-Tube Heat Exchangers: An OverviewPart 2: Vibration Response, Fretting-Wear, Guidelines. *Journal of Fluids and Structures, 18,*485-500. Available:http://www.sciencedirect.com/science/article/pii/S088997460300121X

[xxxi] K. Schneider., & Farge, M. (2005). Numerical simulation of the transient flow behaviour in tube bundles using a volume penalization method. *Journal of Fluids and Structures, 20(4),* 555-566. Available:http://www.sciencedirect.com/science/article/pii/S088997460500040X

[xxxii]M. A. Dalila. , P. A. Lahouari and A. Yacine simulation of turbulent flow across in-line tube bundle using different urans models. Available:http://cfd.mace.manchester.ac.uk/twiki/pub/CfdTm/ResPub231/Publi-Master.pdf

[xxxiii]N. K. -R Kevlahan., & Ghidaglia, J.-M. (2001). Computation of turbulent flow past an array of cylinders using a spectral method with Brinkman penalization. *European Journal of Mechanics-B/Fluids, 20(3),* 333-350. Available:http://www.sciencedirect.com/science/article/pii/S0997754600011213

[xxxiv]V. Shinde, T. Marcelb, Y. Hoarauc, T. Delozeb, G. Harranb, F. Bajd, J.Cardolacciad, J. P. Magnaudd, E. Longattea and M. Braza. (2014). Numerical simulation of the fluidstructure interaction in a tube array under cross flow at moderate and high Reynolds number. Journal of Fluids and Structures. Volume 47, May 2014, Pages 99-113.

[xxxv]Z. WENSHENG ., FEI XUEB, GUOGANG SHUC, MEIQING LIUA, LEI LINB, ZHAOXI WANGD AND ZHIHUAI XIAOA. (2014). Analysis of flow-induced vibration of steam generator tubes subjected to cross flow. Nuclear Engineering and Design. Volume 275, August 2014, Pages 375-381. Available**:**http://www.sciencedirect.com/science/article/pii/s0029549314003173.

[xxxvi]Z. Shang. (2009). CFD investigation of vertical rod bundles of super critical water-cooled nuclear reactor. *Nuclear Engineering and Design, 239(11),*2562-2572. Available:http://www.sciencedirect.com/science/article/pii/S0029549309003501

[xxxvii]S. W. Hwang., et al. (2012). CFD analysis of fin tube heat exchanger with a pair of delta winglet vortex generators. *Journal of mechanical science and technology 26(9):* 2949-2958. Available:http://link.springer.com/article/10.1007/s12206-012-0702-2#page-1

[xxxviii]V. Prithiviraj., & Andrews, M. (1998). Three dimensional numerical simulation of shell-and-tube heat exchangers. Part I: Foundation and fluid mechanics. *Numerical Heat Transfer, Part A Applications, 33(8),* 799-816. Available:http://www.tandfonline.com/doi/abs/10.1080/10407789808913967#.UycoVYUny50

[xxxix]L. Sheik Ismail., C. Ranganayakulu and R. K. Shah (2009). Numerical study of flow patterns of compact plate-fin heat exchangers and generation of design data for offset and wavy fins. *International journal of heat and mass transfer 52(17):* 3972-3983. Available:http://www.sciencedirect.com/science/article/pii/S0017931009002099

[xl] S. Beale., & Spalding, D. (1999). A numerical study of unsteady fluid flow in in-line and staggered tube banks. *Journal of fluids and structures, 13(6),* 723-754. Available:http://scholar.google.com.pk/scholar?qG=&hl=en&as_sdt=1%2C5

[xli] Li, Z.,Davidson, j. H, & Mantell, S. C. (2004). Heat transfer enhancement using shaped polymer tubes:fin analysis. *journal of heat transfer,126(2),* 211-218. Available**:**http://heattransfer.asmedigitalcollection.asme.org/article.aspx?articleid=1447158

[xlii] A. O. Nieckele., Naccache, M. F., & Souza Mendes, P. R. (1998). Crossflow of viscoplastic materials through tube bundles. *Journal of non-newtonian fluid mechanics, 75(1),* 43-54. Available:http://www.sciencedirect.com/science/article/pii/S0377025797000797

[xliii] B Bolló., & Baranyi, L. Numerical simulation of

oscillatory flow past and heat transfer from a cylinder. Available:http://publikacio.uni-miskolc.hu/data/ME-PUB-43494/.CUTAFLUP-22.pdf

[xliv] Li Xiaowei , Xinxin Wu and Shuyan He (2014). Numerical investigation of the turbulent cross flow and heat transfer in a wall bounded tube bundle. Journal of Fluids and Structures. Volume 47, May 2014, Pages 99-113.

[xlv] S. G. Mavridou., And D. G. Bouris (2012). Numerical evaluation of a heat exchanger with inline tubes of different size for reduced fouling rates. *International Journal of Heat and Mass Transfer 55(19):* 5185-5195. Available:http://www.sciencedirect.com/science/article/pii/S0017931012003419

[xlvi] J. C. Jo., And M. J. Jhung (2008). Flow-induced vibration and fretting-wear predictions of steam generator helical tubes. *Nuclear Engineering and Design 238(4):* 890-903. Available:http://www.sciencedirect.com/science/article/pii/S002954930600656X

[xlvii] A. Serizawa., K. Huda, Y. Yamada and I. Kataoka (1997). Experiment and numerical simulation of bubbly two-phase flow across horizontal and inclined rod bundles. *Nuclear engineering and design 175(1):* 131-146. Available:http://www.sciencedirect.com/science/article/pii/S0029549397001696

[xlviii] D. B. Ghadiri., M. H. Sarvghad and J. H. Houri (2011). Numerical simulation of flow over two circular cylinders in tandem arrangement. *journal of hydrodynamics 1*: 019. Available:http://www.cnki.com.cn/Article/CJFDTotal-SDYW201101019.htm

[xlix] X. Lin., P. Bearman and J. Graham (1996). A numerical study of oscillatory flow about a circular cylinder for low values of beta parameter. *Journal of Fluids and Structures 10(5):* 501-526. Available:http://www.sciencedirect.com/science/article/pii/S0889974696900341

[l] E. Longatte., F. Baj, Y. Hoarau, M. Braza, D. Ruiz and C. Canteneur (2013). Advanced numerical methods for uncertainty reduction when predicting heat exchanger dynamic stability limits: Review and perspectives. *Nuclear Engineering and Design 258:* 164-175. Available:http://www.sciencedirect.com/science/article/pii/S0029549312005845

[li] G. Rzentkowski., And J. Lever (1998). An effect of turbulence on fluidelastic instability in tube bundles: a nonlinear analysis. *Journal of Fluids and Structures 12(5):* 561-590. Available:http://www.sciencedirect.com/science/article/pii/S0889974698901554

[lii] Y., Ke, et al. (2011). Numerical simulation on heat transfer characteristic of conical spiral tube bundle. *Applied Thermal Engineering 31(2):* 284-292. Available:http://www.sciencedirect.com/science/article/pii/S1359431110003959

[liii] H. R. Gohel., B. A. Shah and A. M. Lakdawala (2013). Numerical Investigation of Flow Induced Vibration for the Triangular Array of Circular Cylinder. *Procedia Engineering 51:* 644-649. Available:http://www.sciencedirect.com/science/article/pii/S1877705813000921

[liv] E. Longatte., Z. Bendjeddou and M. Souli (2003). Methods for numerical study of tube bundle vibrations in cross-flows. *Journal of fluids and structures 18(5):* 513-528. Available:http://www.sciencedirect.com/science/article/pii/S0889974603001233

[lv] H. Barsamian., And Y. Hassan (1997). Large eddy simulation of turbulent crossflow in tube bundles. *Nuclear Engineering and Design 172(1):* 103-122. Available:http://www.sciencedirect.com/science/article/pii/S0029549397000344

[lvi] d. Keogh. And c. Meskell. measurement of surface pressure on neighbouring tubes in a deformed normal triangular tube array. Available:http://scholar.google.com.pk/scholar

[lvii] C. Liang., G. Papadakis and X. Luo (2009). Effect of tube spacing on the vortex shedding characteristics of laminar flow past an inline tube array: a numerical study. *Computers & Fluids 38(4):* 950-964. Available:http://www.sciencedirect.com/science/article/pii/S0045793008002016

[lviii] H. R., Gohel., B. A. Shah and A. M. Lakdawala (2013). Numerical Investigation of Flow Induced Vibration for the Triangular Array of Circular Cylinder. *Procedia Engineering 51:* 644-649. Available**:**http://www.sciencedirect.com/science/article/pii/S1877705813000921

[lix] D. S. Lee., M. Y. Ha, H. S. Yoon and S. Balachandar (2009). A numerical study on the flow patterns of two oscillating cylinders. *Journal of Fluids and Structures 25(2):* 263-283. Available:http://www.sciencedirect.com/science/article/pii/S0889974608000790

[lx] S. Benhamadouche., & Laurence, D. (2003). LES, coarse LES, and transient RANS comparisons on the flow across a tube bundle. *International Journal of Heat and Fluid Flow, 24(4),* 470-479. Available:http://www.sciencedirect.com/science/article/pii/S0142727X03000602

[lxi] Y. Morsi., Tu, J., Yeoh, G., & Yang, W. (2004). Principal characteristics of turbulent gas-particulate flow in the vicinity of single tube and

tube bundle structure. *Chemical engineering science, 59(15),* 3141-3157. Available:http://www.sciencedirect.com/science/article/pii/S0009250904002611

[lxii] D. Chang., And S. Tavoularis (2007). Numerical simulation of turbulent flow in a 37-rod bundle. *Nuclear Engineering and Design 237(6):* 575-590. Available:http://www.sciencedirect.com/science/article/pii/S0029549306004705.

[lxiii] J. N. MacDuff., Feglar, R. P., 1957, "Vibration Design Charts" Trans. ASME, Vol. 79, pp. 1455-1474.

An Eco-friendly Approach for Sodium Chloride Free Cotton Dyeing

T. Umer[1], I. A. Shaikh[2], S. Munir[3], E. Suhail[4], M. Zameer[5], I. Ahmad[6]

[1,2,3,4,5,6]College of Earth and Environmental Sciences, University of the Punjab, Lahore
[4]erham_great@hotmail.com

Abstract-Present study was conducted with an aim to develop an environmental friendly method of dyeing cotton as an alternative to standard reactive dyeing process that requires high level of salt. When dyeing was carried out in the absence of sodium chloride (NaCl), an extremely lighter depth of shade was experienced, and hence this particular research was focused on the reduction of the total colour difference (ΔE*) to a minimum level. Instead of adding any other chemical or any additional process like cationization, salt-free reactive dyeing was carried out by varying three common process parameters (dyes, alkali, and process time) to achieve required depth of shade. The results obtained were compared with those of conventionally dyed fabrics in terms of depth of shade (ΔL*), total colour difference (ΔE*), washing fastness, and rubbing fastness. The results were found to be promising and comparable to those dyed with using NaCl. Moreover, the investigated method showed a significant reduction of Total Dissolved Solids (TDS) and Electrical Conductivity (EC) in the wastewater, and thus proved to be an environment friendly process.

Keywords-Cotton, Reactive Dyes, Salt-free Dying, Colour, Wastewater

I. INTRODUCTION

Industries uses large amount of water and chemicals, and textile industry is no exception. Textile processes consume large amount of water, and in return, produce huge volume of wastewater containing large number of pollutants such as coloured effluent, residual chemicals, high pH, Chemical Oxygen Demand (COD), Biological Oxygen Demand (BOD), and high amount of Total Suspended Solids (TSS) and Total Dissolved Solids (TDS) [i].

Dyes such as reactive, direct, vat, and sulphur are extensively used in the dyeing of cellulosic materials, however, reactive dyes are high in demand due to its advantageous properties like excellent brightness, wide gamut of colours available, and excellent wash fastness due to the formation of covalent bonds between dye and fibre [ii]. Use of reactive dyes is also proved to be an expensive and time consuming process because it requires high amount of electrolytes (salt and alkali), extensive rinsing and hot washing-off steps after dyeing for the removal of unfixed dyes. All this creates a large volume of wastewater containing elevated amount of salt and alkali [iii].

Electrolytes (NaCl or Na_2CO_3) are required in the process of reactive dyeing to overcome the large repulsive forces (zeta potential) between anionic reactive dye and negatively charged cotton fiber [iv]. Concentration of electrolyte depends upon the required depth of colour and type of dye structure, and can be varied up to 100 grams per liter [v].

Several researchers reported different methods to achieve salt-free dyeing, including modification of reactive dyes [v], pre-treatment of cotton with chitosan derivatives [vi], polyvinylamine chloride [vii], cationic modification of cotton [viii], dendrimer use to modify the dyeing behavior [ii], NBP-NH2 to graft cotton fiber [ix] and use of organic salt [x].

The aim of the present work was to develop a salt-free dyeing method which can produce similar depth of shade compared to that of standard dyeing method. It was also of interest to find the reduction of the pollution load associated with the excessive usage of electrolytes in standard textile dyeing process. To achieve this goal, numbers of salt-free dyeing were performed by varying only common process parameters (dyes, alkali, and process time).

II. MATERIALS AND METHODS

2.1 Materials

A 100% Cotton knitted fabric (single jersey) made of 30's yarn and having 200 GSM (Grams per Square Meter) was used in the study. The reactive dyes Synozol Black B 150% (CI Reactive Black 5), Synozol Red HF-6BN (CI Reactive Red 195), and Synozol Yellow HF-2GR (CI Reactive Yellow 145) were supplied by KISCO Corporation (Korea). Structural formulas of dyes are given in Fig. 1. Auxiliary chemicals, sodium chloride (NaCl), sodium hydroxide (NaOH), and acetic acid (CH_3COOH), used were of commercial grade and used without any dilution.

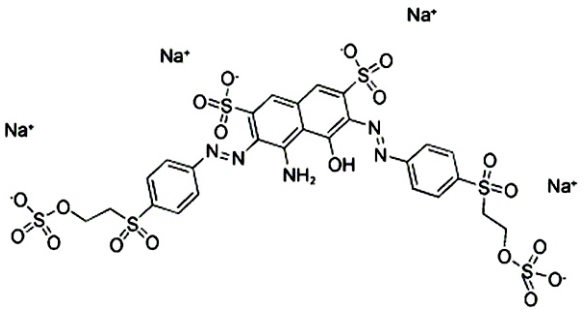

a) Reactive Black 5

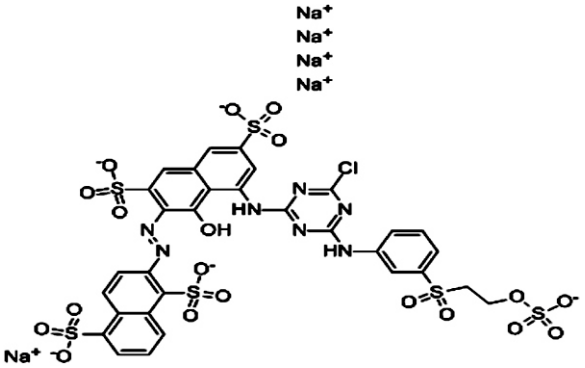

b) Reactive Red 195

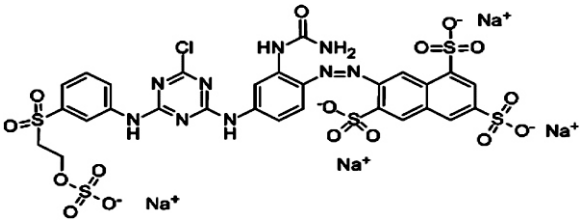

c) Reactive Yellow 145

Fig. 1. Structural formulas of dyes

2.2 Dyeing and wash-off Conditions

10 gram fabric samples were dyed according to exhaust dyeing method (ALL-IN-ONE) for shade depth of 5% o.w.f at a liquor ratio of 1:10. Dyeing was carried out at 60ºC for 60 min with 80g/L sodium chloride and 20g/L sodium carbonate. This dyed fabric was regarded as standard sample. Dyeing trials with 0 g/L salt were carried out the similar way as standard dyeing process. At the completion of dyeing, fabric was subjected to wash-off treatment that involved rinsing, neutralization, warm wash (60°C), hot wash (80°C), soaping/boil off (95°C) and rinsing. Each step was performed for 5 minutes.

Afterwards, fabric samples were removed from laboratory dyeing machine (AHIBA NUANCE, USA), squeezed, dried, and conditioned before evaluating for change of shade and colour fastness properties.

2.3 Measurements

Colour difference values (ΔL*, Δa*, Δb*, ΔC*, ΔH* and ΔE*) [11] were determined using a spectrophotometer (600 PLUS CT, Datacolour, USA) with illuminant D65/10° observer, specular reflectance included, and aperture size 30 mm settings. Colour fastness to washing and crocking were determined using test methods ISO 105-CO6 and ISO 105-X12, respectively, and reported in standard grey scale (marks 1-5, 1=poor, 5=excellent).

III. Results and Discussion

When dyeing was carried out in the absence of salt (0g/l) and compared to standard dyeing, the results were summarized in Fig. 2. The data clearly shows that the values of depth of shade (ΔL*) and total colour difference (ΔE*) were found to be on the higher side. In the case of Black 5, the salt-free dyeing was very light (ΔL*= 3.4) and less saturated (ΔC*= 2.68) compared to standard dyeing, thus resulting into huge total colour difference (ΔE*= 4.41). Salt-free dyeing of Yellow 145 yielded a lighter (ΔL*= 4.45), brighter (ΔC*= 4.52), and an off-shade (ΔE*= 8.63) dyeing. Fabric dyed with Red 195 in the absence of salt was also lighter (ΔL*= 7.33), duller (ΔC*= -6.52), and had a huge total colour difference (ΔE*= 9.81).

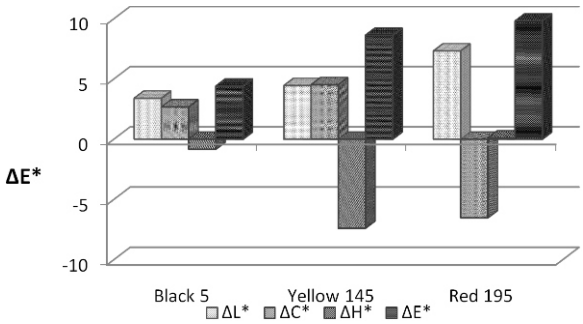

Fig. 2. CIELab Colour differences between standard and 0g/l salt dyeing

To minimize the colour difference between reference dyeing and salt-free dyeing, several dyeings were carried out with increased amount of sodium carbonate (20-40 g/L), and the results are summarized in Table I.

TABLE I
CIELAB VALUES OF SAMPLES WITH VARIED Na_2CO_3 CONCENTRATION

	ΔL*			ΔE*		
Name of dye	20g/l Na_2CO_3	30g/l Na_2CO_3	40g/l Na_2CO_3	20g/l Na_2CO_3	30g/l Na_2CO_3	40g/l Na_2CO_3
Black 5	3.4	1.6	0.47	4.41	1.45	0.49
Yellow 145	4.45	2.8	0.96	8.63	4.38	1.31
Red 195	7.33	4.3	2.28	9.81	6.23	2.92

When the concentration of Na_2CO_3 was limited to 20 g/l (with 0 g/l salt), all three shades were found extremely lighter and different to those of reference dyeing. However, when the concentration of Na_2CO_3 was increased to 30 and 40 g/l (with 0g/l salt), both depth of shade (ΔL*) and total colour difference (ΔE*) was minimized significantly. In case of Black 5, ΔL* and ΔE* were reduced to 0.47 and 0.49, respectively, when the concentration of Na_2CO_3 was increased to 40 g/l. For Yellow 145, both ΔL* and ΔE* were reduced to 0.96 and 1.31, respectively. However, in the case of Red 195, ΔL* was significantly improved from 7.33 to 2.28 and ΔE* from 9.81 to 2.92, but the final colour assessment cannot be regarded as a perfect match due to ΔE* difference greater than 1.0.

Dye concentration influences both dye fixation and the colour strength of the dyed fabric in the dyeing process [12]. Table II clearly demonstrates that colour depth (ΔL*) of the dyed fabric increased with increasing dye concentration, and thus total colour difference (ΔE*) was also reduced and colour fastness was found between 4 to 5. In case of Black 5, the depth of shade (ΔL*) was significantly increased from 3.4 to 0.74 when dye concentration was increased from 5 to 8% owf. Correspondingly, the total colour difference (ΔE*) was also reduced from 4.41 to 1.12. In the dyeing of Yellow 145 and Red 195, an improvement in ΔL* and ΔE* was clearly observed when dye concentration was gradually increased, however the shade difference was still far away from a commercially acceptable match. When the Na_2CO_3 concentration was also increased, from 20 to 40 g/l, along with increased dye concentration, both ΔL* and ΔE* improved significantly. Colour fastness properties of all dyes at all concentrations were almost same.

Table III shows that when the dyeing time was increased from 60 to 120 minutes along with increased dye concentration, an overall improvement in colour difference was observed. In case of Black 5, the lowest colour difference in terms of ΔL* and ΔE* were found to be 0.40 and 0.42, respectively. For Yellow 145, the best results (ΔL*=0.04 and ΔE*= 0.80) were achieved when the depth of shade and dyeing time were increased to 8% o.w.f and 120 minutes, respectively. The dyeing of Red 195 also followed the similar trend. When dyeing time was extended to 120 minutes along with increased dye and Na_2CO_3 concentrations, ΔL*values of -1.18, -0.62, and -0.49 were achieved for Black 5, Yellow 145, and Red 195, respectively. This showed that all samples were darker than those of dyed with zero salt dyeing. Colour fastness properties of all dyes for 2 hours dyeing were not much different from 60 min dyeing and ranges between 4.5 to 5, which are considered excellent colour fastness values.

This study also revealed that the total dissolved solids (TDS) and electrical conductivity (EC) concentration was decreased up to 40 to 50 % when dyeing was carried out in the absence of salt as shown in Table IV.

TABLE IV
VALUES OF TDS AND EC AT VARIOUS DYEING CONDITIONS

Process type	Dye concentration (%)	Waste water quality parameter	
		TDS(ppm)	EC
Standard dyeing	5	123000	174
Dyeing with 20 g/l	5	42000	62
Na_2Co_3	6	41000	60
	7	42000	63
	8	45000	64
Dyeing with 40 g/l	5	70000	73
Na_2Co_3	6	72000	82
	7	73000	81
	8	75000	81

IV. CONCLUSION

A Salt-free reactive dyeing method aiming a comparable colour yield and having minimum colour differences was investigated. No pre-treatment and no additional chemicals were added, and dyeings were carried out by varying common process parameters like dyes, alkali, and process time only. The optimum dyeing conditions are as follows: for Black 5, 5% owf, 40g/l Na_2CO_3, 60-minute dyeing time; 7% owf, 30 g/l Na_2CO_3, 60-minute dyeing time; 7% owf, 30g/l Na_2CO_3, 120-minute dyeing time; for Yellow 145, 5% owf, 40g/l Na_2CO_3, 60-minute dyeing time; 8% owf, 30g/l Na_2CO_3, 120-minute dyeing time; for Red 195, 7% owf, 40g/l Na_2CO_3, 120-minute dyeing time. At these conditions, a considerable decrease of total dissolved solids (TDS) and electrical conductivity (EC) in the wastewater was observed.

REFERENCES

[i] S. Tubtimhin (2002). *Pollution minimization and energy saving potentials in the cotton dyeing industry,* School of Environmental Resources and Development, Asian Institute of Technology, Thailand.

[ii] S. M. Burkinshaw, M. Mignanelli, P. E. Froehling and M. J. Bide, (2000, Dec). The use of dendrimers to modify the dyeing behaviour of reactive dyes on cotton. *Dyes Pigments*. [Online]. *47(3),* pp. 259-267. Available:http://www.sciencedirect.com/science/article/pii/S014372080000053X

[Iii] C. Zheng, A. Yuan, H. Wang and J. Sun. (2012, Jun). Dyeing properties of novel electrolyte-free reactive dyes on cotton fibre. *Color. Technol.* [Online]. *128(3),* pp. 204-207. Available: http://onlinelibrary.wiley.com/doi/10.1111/j.1478-4408.2012.003

[iv] D. Chattopadhyay, R. Chavan and J. Sharma. (2007, Sep). Salt-free reactive dyeing of cotton. *International J. Cloth. Sci. Tech.* [Online]. *19(2),* pp. 99-108. Available:http://www.emeraldinsight.com/journals.htm?articleid=1593600

[v] K. Srikulkit and P. Santifuengkul. (2000, Dec). Salt-free dyeing of cotton cellulose with a model cationic reactive dye. *Color. Technol.* [Online]. *116(12),* pp. 398-402. Available:http://onlinelibrary.wiley.com/doi/10.1111/j.1478-4408.2000.tb00017.x/pdf

[vi] S. H. Lim and S. H. Hudson. (2004, May). Application of a fibre-reactive chitosan derivative to cotton fabric as a zero-salt dyeing auxiliary. *Color. Technol.* [Online]. *120(3),* pp. 108-113. Available:http://onlinelibrary.wiley.com/doi/10.1111/j.1478-4408.2004.tb00215.x/pdf

[vii] W. Ma, S. Zhang, B. Tang and J. Yang. (2005, Jul). Pretreatment of cotton with poly (vinylamine chloride) for salt-free dyeing with reactive dyes. *Color. Technol.* [Online]. *121(4),* pp. 193-197. Available:http://onlinelibrary.wiley.com/doi/10.1111/j.1478-4408.2005.tb00272.x/pdf

[viii] M. Montazer, R. Malek and A. Rahimi. (2007, Dec). Salt free reactive dyeing of cationized cotton. *Fiber Polym.* [Online]. *8(6),* pp. 608-612. Available:http://link.springer.com/article/10.1007%2FBF02875997

[ix] F. Zhang, Y. Chen, H. Lin, H. Wang and B. Zhao. (2008, Oct). HBP-NH2 grafted cotton fiber: Preparation and salt-free dyeing properties. *Carbohydr. Polym.* [Online]. *74(2),* pp. 250-256. Available:http://www.sciencedirect.com/science/article/pii/S0144861708000878

[x] N. S. Ahmed, (2005, Jun). The use of sodium edate in the dyeing of cotton with reactive dyes. *Dyes Pigments*. [Online]. *65(3),* pp. 221-225. Available:http://www.sciencedirect.com/science/article/pii/S0143720804001780

[xi] M. S. Alam, G. A. Khan, S. A. Razzaque, M. J. Hossain, M. Minhaz-ul-Haque and S. Zebsyn, (2008, Mar). Dyeing of cotton fabrics with reactive dyes and their physico-chemical properties. *Indian J. Fibre Text.* [Online]. *33(1),* pp. 66-71. Available:http://nopr.niscair.res.in/handle/123456789/372

[xii] Y. Deng, B. Tang, H. Zhao, J. Xu, J. Xiao, X. Zhang,. . . S. Zhang. (2013, Apr). Dyeing method and properties of polymaleic acid dyes on cotton. *Color. Technol.* [Online]. *129(2),* pp. 144-149. Available:http://onlinelibrary.wiley.com/doi/10.1111/cote.12013/full

TABLE II
CIELAB VALUES OF SAMPLES WITH VARIED DYES AND Na_2CO_3 CONCENTRATION

Dyes	Conc. of dye (%)	ΔL*			ΔE*			Staining of cotton	
		20g/l Na_2CO_3	30g/l Na_2CO_3	40g/l Na_2CO_3	20g/l Na_2CO_3	30g/l Na_2CO_3	40g/l Na_2CO_3	20g/l Na_2CO_3	40g/l Na_2CO_3
Black 5	6	2.17	0.95	-0.05	3.27	0.98	0.15	4	5
	7	0.75	0.45	-0.28	1.34	0.49	0.50	5	5
	8	0.74	0.42	-0.81	1.12	0.45	1.63	4.5	5
Yellow 145	6	4.04	3.22	2.33	7.61	4.50	3.52	5	4.5
	7	2.90	2.60	2.50	6.69	4.63	4.03	5	4
	8	2.78	2.10	1.89	5.42	4.30	3.05	4.5	5
Red 195	6	5.58	3.28	2.48	7.29	4.90	3.68	4.5	5
	7	5.00	3.12	2.99	5.91	4.53	3.87	4	5
	8	3.85	2.74	2.28	4.91	3.67	2.92	5	4.5

TABLE III
CIELAB VALUES OF SAMPLES WITH VARIED DYE AND NA_2CO_3 CONCENTRATION USING 2-HOUR DYEING TIME

Dyes	Conc. Of dye (%)	ΔL*			ΔE*			Staining on cotton	
		20g/l Na_2CO_3	30g/l Na_2CO_3	40g/l Na_2CO_3	20g/l Na_2CO_3	30g/l Na_2CO_3	20g/l Na_2CO_3	20g/l Na_2CO_3	40g/l Na_2CO_3
Black 5	5	3.53	2.19	1.34	4.29	2.58	1.81	4.5	5
	6	1.50	0.56	-0.21	1.82	0.64	0.40	4.5	5
	7	0.45	0.12	-0.40	0.45	0.10	0.73	5	5
	8	0.40	-0.32	-1.18	0.42	0.45	1.63	5	5
Yellow 145	5	1.31	1.10	0.57	2.50	1.39	0.87	4.5	4.5
	6	1.19	0.78	-0.16	2.76	0.83	0.80	5	4.5
	7	1.06	0.54	-0.38	1.93	0.65	0.46	5	5
	8	0.04	0.15	-0.62	0.8	0.45	0.89	4.5	4.5
Red 195	5	4.05	2.99	2.09	5.54	3.10	2.72	5	4.5
	6	3.26	1.86	0.64	4.23	1.79	0.71	5	5
	7	2.75	0.97	0.04	3.53	0.87	0.42	5	5
	8	1.92	0.76	-0.49	2.4	0.49	1.49	4.5	5

Leverage of Advanced Manufacturing Effectiveness: A Case of Apparel Industry

G. Asghar[1], M. Jahanzaib[2], M. Noman[3]

[1,2,3]Industrial Engineering Department, University of Engineering and Technology Taxila, Pakistan
[2]jahan.zaib@uettaxila.edu.pk

Abstract-This study is about the effectiveness of latest technology flexible machines in apparel manufacturing. Techniques to justify the advanced manufacturing systems, break-even and sensitivity analysis have been developed to analyze the significance between the conventional as well as the latest flexible machines. Payback Period (PP) and Return on Investment (ROI) are renowned methods to validate the investments. These terms are calculated for both conventional model machines and for latest model. The comparison is made between them. The production rate and annual profit of each model has been calculated and compared. The break-even analysis showed that the profit margin is increased by using the latest flexible machines while producing the same quantity as with the conventional machines. It is analyzed that the break-even is achieved earlier by using latest flexible machines as compared to the conventional ones. The sensitivity analysis verified the outcomes of break-even analysis. It has been learned that the advanced manufacturing improves the performance of the system and is justified in the manufacturing environment.

Keywords-Advanced Manufacturing, Break-Even, Payback Period, Return on Investment, Sensitivity Analysis.

I. INTRODUCTION

This work is a specific study of apparel manufacturing which has been taken for the analysis of advanced manufacturing effectiveness of latest technology. It consists of comparison of conventional machines versus the latest flexible machines in terms of productivity and the financial benefits gained by companies. This comparison is only in terms of financial benefits; it does not cover the strategic & other benefits gained by the firms adopting the latest technology flexible machines/equipments. A leading apparel manufacturing company was having a unit of 220 conventional machines of model GL714 previously. It has recently established a new unit of 220 machines of latest model GL546. This case study would evaluate the benefits gained by the company in monetary terms. First, the conventional financial figures are calculated for each of the models separately, and then the comparison is made between these figures of two models. It is also analyzed with the help of break-even analysis that how much profit could be earned by the company against the specified production quantities. The sensitivity analysis has been carried out to verify the recommendations of break-even analysis.

II. LITERATURE REVIEW

Methods have been developed for justifying investment in advanced manufacturing systems. It is discussed [i] that the adoption of advanced manufacturing technology (AMT) involves major investment and a high degree of uncertainty and, hence, warrants considerable attention within a manufacturing firm at the strategic level. Researchers [i-iii] reported that justification of investments in advanced manufacturing systems can be grouped into three categories; (i) The economic approach involving the classical financial justification techniques of Payback Period (PP), Return on Investment (ROI), Internal Rate of Return (IRR), and Net Present Value (NPV); (ii) The strategic approach involving analysis of competitive advantage, business objectives, research and development objectives and technical importance; (iii) The analytic approach involving value analysis, portfolio analysis and Risk Analysis (RA).

These methods vary significantly from each other due to non-monetary factors [iv]. Economic justification methods of manufacturing investments are discussed [v]. The authors [vi] stated that the economic justification of advanced technology has been a very popular approach and they also reported that the cost/benefit analysis is also utilized for AMT project appraisals. These attempts aim to improve a firm's ability to account for costs and benefits. It is reported [vii] that the Payback period (PP) technique was the most popular method of AMT appraisal in his study of the machine tool industry. He also investigated that Return on Investment (ROI) was the second most popular technique being used for AMT appraisal.

They [viii] found that PP techniques continue to be popular in the USA, the UK and the Czech Republic. As the payback methods are generally effective for short-term perspective on investments, which can be dangerous for AMT projects. It would be quite interesting to note that the Japanese [ix] also use the payback method most frequently; it serves more as a performance measurement tool than as a rigid financial criterion. However, it is suggested [x] that this method has more disadvantages than the payback method because it does not measure the economic value of the project.

It is analyzed [x-xi] that the firms where the level of risk and uncertainty make up the most critical elements of the justification process, it is observed that risk sensitivity analysis is the most appropriate evaluation technique. They [xii] investigated that in comparing conventional projects for installation of robots, the flexibility and reprogram ability of the robot merits a lower hurdle rate. Works cited by the authors [xiii-xiv] have identified several barriers that may encounter manufacturing companies to adopt AMT successfully. Researchers [xv] investigated machine rates and prioritized different process parameters for developing technology driven manufacturing strategy. Authors [xvi] discussed the financial and accounting methods used by the managers for decision making as well as for the justification of AMT. Studies conducted by researchers [xvii] in Czech Republic revealed the problems associated with adoption of AMT from the management point of view. It is reported [xviii] that Analytical Hierarchical Process (AHP) is very effective in multi-criterion decision making for the selection and evaluation of AMT. The steady conducted by [xix] assessed the critical factors which influence the adoption of AMT in small and medium-sized enterprises (SMEs). Researchers [xx] found that Flexible Manufacturing System (FMS) has the greatest impact on producer's value due to its high effects on quality and cost while Just-in-Time is found to be the most successfully employed AMT. A number of studies also advocated by the authors [xxi] that a collaborative approach of Concurrent Engineering (CE) product delivery approach is better suited than the conventional Product Delivery Process (PDP) and this approach is valid and successfully implemented in manufacturing organizations for the delivery of products at lower cost. A significant work has been carried out by the researchers [xxii] in prioritizing the different activities of a business environment according to the manufacturing strategy adopted by the manufacturing firm.

The mathematical relationships have been developed using well established techniques and the parameters of interested are defined in section III and numerical values have been calculated. Model is presented in next section followed by methodology and coherently scenarios with results and recommendations.

III. System Model

A. Abbreviations and Acronyms

The following abbreviations have been used;

T_a = Available Time or Number of machine hours available per day at 85% efficiency
T_o = Time required for making one piece
N = Number of units (pieces)produced per day
N_p = Number of pairs produced per day
$N_{d/d}$ = Number of dozens produced per day
R_p = Hourly Production rate of complete unit
TM = Total number of machines (220 machines)
NM = No. of machines operated by one operator(8 m/c)
M = Number of operators needed
M_t = No. of operators needed for three shifts
$R_{p/m}$ = Production rate of each Machine
$R_{p/mnth}$ = Monthly production rate
$R_{p/annl}$ = Annual production rate
S_p = Unit Sale Price
S_{mnth} = Monthly sales (revenue)
S_{annl} = Annual sales (revenue)
LC_m = Total salary paid per month
LC_d = Labor cost per dozen
VC = Variable Cost per Unit
VC_d = Variable cost per dozen
VC_{annl} = Annual variable cost
FC = Fixed Cost
TC_{annl} = Total Annual Cost
P_{annl} = Annual Profit
ROI_{annl} = Annual Return on Investment

B. Mathematical Relationships

Number of dozens produced per day would be;

$$N_{d/d} = \frac{T_a}{24T_o} \quad (1)$$

And the hourly production rate of the complete unit of 220 machines would be;

$$R_p = \frac{T_a}{576T_o} \quad (2)$$

Number of operators needed for three shifts are;

$$M_t = \frac{TM}{NM} \times 3 \times 1.30 \quad (3)$$

In the above equation 1.30 is multiplied because 30% extra work force is needed to compensate the leaves and absenteeism.

Production Rate of each Machine could be;

$$R_{p/m} = \frac{T_a}{576 \times 220T_o} \quad (4)$$

Monthly production rate of the complete unit (220 m/c) would be;

$$R_{p/mnth} = \frac{T_a}{576T_o} \times 24 \times 30 \quad (5)$$

It is to be noted here that 24 and 30 denote the 24 hours per day and 30 days in a month.

Annual production rate of the complete unit (220 m/c) would be;

$$R_{p/annl} = \frac{T_a}{576T_o} \times 24 \times 30 \times 12 \quad (6)$$

In the above equation 12 shows the number of months in a year.

Monthly sales (revenue) generated would be;

$$S_{mnth} = \frac{T_a}{576T_o} \times 24 \times 30 \times S_p \quad (7)$$

Annual sales (revenue) generated would be;

$$S_{annl} = \frac{T_a}{576T_o} \times 24 \times 30 \times 12 \times S_p \quad (8)$$

The labor cost in terms of salary paid to the worker would be;

$$LC_d = \frac{LC_m}{\frac{T_a}{576T_o} \times 24 \times 30} \quad (9)$$

The variable cost of one dozen would be;

$$VC_d = VC + LC_d \quad (10)$$

Annual variable cost will be;

$$VC_{annl} = VC + 12LC_m \quad (11)$$

Total annual Cost will be;

$$TC_{annl} = FC + VC + 12LC_m \quad (12)$$

Annual profit will be;

$$P_{annl} = S_{annl} - (FC + VC + 12LC_m) \quad (13)$$

Annual return on investment (ROI) will be;

$$ROI_{annl} = \frac{P_{annl}}{TC_{annl}} \quad (14)$$

Payback period (PBP) could be;

$$PBP = \frac{\text{Break even Quantity}}{N_{d/d}} \quad (15)$$

IV. Research Methodology

This study focuses on the determination of break-even point and sensitivity analysis, for the specified units of conventional and latest flexible knitting machines of apparel manufacturing. Leading apparel manufacturing company has installed a new unit of 220 knitting machines of latest model GL546. Previously, it had also another unit of 220 knitting machines of model GL714. The management has taken this step due to the increasing orders /demand of fashion articles by the customers. Conduct the financial analysis and benefits gained by the company. Scrap rate is 5% and the production efficiency is 85%. There are three main types of socks (i) Crew Socks, (ii) Quarter Socks and (iii) No Show/Low Cut/Ankle Socks. The conventional knitting machines are of Model GL714. The word G stands for Goal and L for Lonati, 7 means 3.5 inch cylinder diameter, 1 means single feed machine and 4 means four colors feeds. Therefore the maximum possible variation of colors is up to five colors. The latest knitting machines are of model GL546. The digit 5 means 4 inch cylinder diameter, 4 means four main feeds and 6 means six colors feeds. So, the possible variation of colors is up to ten colors in the product. There are two scenarios under study which have been discussed.

Scenario I for Model GL714

The price of single feed knitting machine of Model GL714 equals $ 20,370, with total price of 220 machines equals $4.4814million and the fixed by adding the installation and basic infrastructure cost like building, land etc. would be equals $5.0 million. The variable cost (including materials means yarn, energy consumption, processing materials, finishing and packing costs & all other miscellaneous) equals $ 8/dzn. The average sales price of one dozen socks of plain/ non fashion article equals $ 20/dzn. The cycle time for crew, quarter and low cut socks are 166 sec/piece, 156 sec/piece, and 148 sec/piece respectively. The average cycle time is 156.67 sec/piece or 2.61 minutes/piece. There are 3 shifts and 8 hours per shift and machines are operated round the clock means 24 hours. Therefore number of machine hours equals 5,280 hours and at 85% efficiency 4488 hours.

The production rate of 220 machines is 178.67 dozens/hour. But as we know that the scrap rate is 5%, so the good quality production rate is 170.16 dozens/hour. One operator operates 8 machines so 28 operators would be required for one shift. As 30% extra work force is maintained to manage the rests and absenteeism of the operators. So to operate one shift the operators needed would be 37 operators and for three shifts 110 operators would be enough. These 110 operators also include the helpers, which feed the yarn to the machines and change the cones when required. These helpers which feed the yarn to the machines are called bobbin keepers. In-spite of the above mentioned workforce, there would be 21 technicians required to keep up the maintenance of the machines and also to rectify the malfunctioning of the machines and to minimize the break-downs. These 21 technical members team consists of 5 line in-charges and 15 shifts mechanics and one head of this technical staff. Production rate of each machine equals 0.7735 dzns/hr/m/c. Monthly production rate of the complete unit (220 m/c) is equals 122,517.30 dzns/month. Annual production rate equals 1,470,207.6 dzns / yr.

Monthly and yearly sales (revenue) generated are $2.45 million and $29.404 million respectively. The total salary paid to the workers of a complete unit equals $14,445/month. Therefore the labor cost per dozen would be $0.1179 and the variable cost per dozen would become $8.1179. The annual variable cost is $11.935 million/year and the total annual cost (by adding the fixed and variable) equals $16.934998 million/year. The annual profit (which is the difference of annual sales and total annual cost) is equals $12.469153 million/year. Annual return on investment (ROI) would be 73.63%.

TABLE I
CALCULATION OF COSTS AND SALES AGAINST DIFFERENT QUANTITIES FOR MODEL GL714

Quantity (Q) (1000)	Fixed Cost ($)	Variable Cost ($)	Total Cost ($)	Sales ($)
50	5,000,000	405,895	5,405,895	1,000,000
100	5,000,000	811,790	5,811,790	2,000,000
150	5,000,000	1,217,685	6,217,685	3,000,000
200	5,000,000	1,623,580	6,623,580	4,000,000
250	5,000,000	2,029,475	7,029,475	5,000,000
300	5,000,000	2,435,370	7,435,370	6,000,000
350	5,000,000	2,841,265	7,841,265	7,000,000
400	5,000,000	3,247,160	8,247,160	8,000,000
450	5,000,000	3,653,055	8,653,055	9,000,000
500	5,000,000	4,058,950	9,058,950	10,000,000
550	5,000,000	4,464,845	9,464,845	11,000,000
600	5,000,000	4,870,740	9,870,740	12,000,000

In Table I different quantities in thousands have been taken and the variable cost, total cost and the sales against these quantities are calculated. It is noted that the fixed cost would be same for all the quantities.

Break Even Analysis Model GL714

According to the values calculated in Table I, the break-even point is plotted below as;

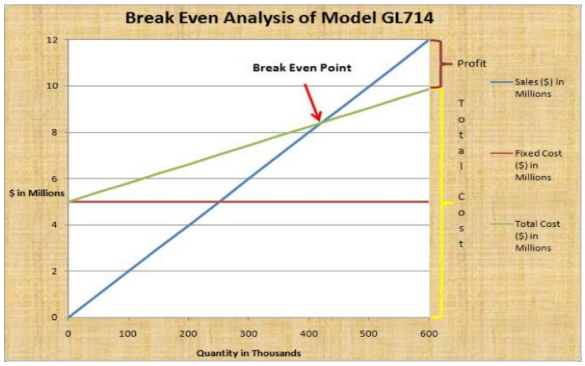

Fig. 1. Break Even Analysis of Model GL714

As the above given Fig.1 shows that the break-even point is achieved at 420,000 dozen in terms of manufacturing quantity or 8.40 million dollars in monetary terms. Using either of these above figures, the payback period is calculated according to equation (18), which is 103 days for the conventional model machines of GL714.

Scenario II for Model GL546

The price of four feed knitting machine of Model GL546 equals $ 23,150, with total price of 220 machines equals $5.093 million and the fixed by adding the installation and basic infrastructure cost like building, land etc. would be equals $5.6116 million. The variable cost (including materials means yarn, energy consumption, processing materials, finishing and packing costs and all other miscellaneous) equals $10/dzn. The average sales price of one dozen socks of fashion socks (Article) equals $28/dzn. The cycle time for crew, quarter and low cut socks are 90 sec/piece, 82 sec/piece, and 76 sec/piece respectively. So the average cycle time is 82.67 sec/piece or 1.38 minutes/piece. There are three shifts and 8 hours per shift and machines are operated round the clock means 24 hours. Therefore number of machine hours equals 5,280 hours and at 85% efficiency 4488 hours. The production rate of 220 machines is 337.89 dozens/hour. But as we know that the scrap rate is 5%, so the good quality production rate is 321.8 dozens/hour. One operator operates 8 machines so 28 operators would be required for one shift. As 30% extra work force is maintained to manage the rests and absenteeism of the operators. To operate one shift the operators needed would be 37 operators and for three shifts 110 operators would be enough. These 110 operators also include the helpers, which feed the yarn to the machines and change the cones when required. These helpers which feed the yarn to the machines are called bobbin keepers. In-spite of the above mentioned workforce, there would be 21 technicians required to keep up the maintenance of the machines and also to rectify the malfunctioning of the machines and to minimize the break-downs. These 21 technical members team consists of five line in-charges and 15 shifts mechanics and one head of this technical staff. Production rate of each machine equals 1.463 dzns/hr/m/c. Monthly production rate of the complete unit (220 m/c) equals 231,717.30 dzns/month. Annual production rate equals 2,780,607.6 dzns / yr.

Monthly and yearly sales (revenue) generated are $6.4880844 million and $77.857012 million respectively. The total salary paid to the workers of a complete unit equals $14,445/month. Therefore the labor cost per dozen would be $0.06234 and the variable cost per dozen would become $10.06234. The annual variable cost is $27.980 million/year and the total annual cost (by adding the fixed and variable) equals $33.591019 million/year. The annual profit (which is the difference of annual sales and total annual cost) equals $44.265993 million/year. Annual return on investment (ROI) would be 131.78%.

TABLE II
CALCULATION OF COSTS & SALES AGAINST DIFFERENT QUANTITIES FOR MODEL GL546

Quantity (Q) (1000)	Fixed Cost ($)	Variable Cost ($)	Total Cost ($)	Sales ($)
50	5,611,600	503,117	6,114,717	1,400,000
100	5,611,600	1,006,234	6,617,834	2,800,000
150	5,611,600	1,509,351	7,120,951	4,200,000
200	5,611,600	2,012,468	7,624,068	5,600,000
250	5,611,600	2,515,585	8,127,185	7,000,000
300	5,611,600	3,018,702	8,630,302	8,400,000
350	5,611,600	3,521,819	9,133,419	9,800,000
400	5,611,600	4,024,936	9,636,536	11,200,000
450	5,611,600	4,528,053	10,139,653	12,600,000
500	5,611,600	5,031,170	10,642,770	14,000,000
550	5,611,600	5,534,287	11,145,887	15,400,000
600	5,611,600	6,037,404	11,649,004	16,800,000

The above Table II shows the calculations of fixed, variable and total costs and sales against different Quantities for the latest flexible knitting machines of Model GL546.

Break Even Analysis of Model GL546

According to the values calculated in Table II, the breakeven point for latest model machines is plotted below as;

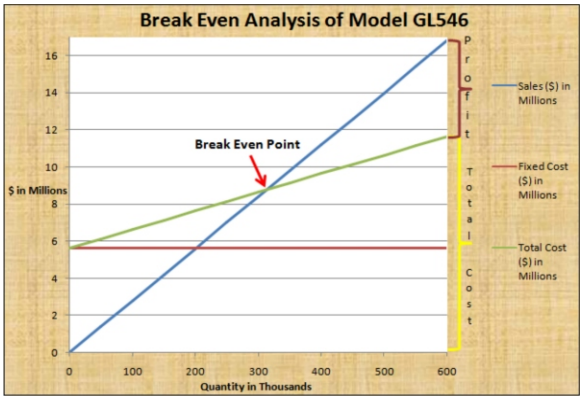

Fig. 2. Break-even Analysis of Model GL546

As the above given Fig. 2 shows that the break-even point is achieved at 313,000 dozen in terms of manufacturing quantity or 8.80 million dollars in monetary terms. Using either of these above figures, the payback period is calculated according to equation (18), which is 41 days for the latest model machines of GL546.

Comparison of Models

TABLE III
COMPARISON DIFFERENT VALUES OF BOTH MODELS

Comparison		
Value	**Model GL714**	**Model GL546**
Fixed Cost	$ 5.0 Millions	$ 5.6116 Millions
Variable Cost/year	$ 11.935 Millions	$ 27.980 Millions
Sales/year	$ 29.404 Millions	$ 77.857 Millions
Profit/year	$ 12.469 Millions	$ 44.266 Millions
Production Rate/hr	170.16 dzn/hr	321.80 dzn/hr
Production Rate/operator	6.07 dzn/hr	11.49 dzn/hr
Production Rate/machine	0.7735 dzn/hr	1.463 dzn/hr
Annual Rate of Return	73.63%	131.78%
Payback Period	103 days	41 days

In the above Table III, the comparison of both models is made, which shows that the fixed and variable is high for the latest model machines. At the same time the annual sales and profit is also very high for the latest machines. The production rate of latest model is better than the conventional machines.

Comparison of Break-evens of Models

As the comparison is made between different values of both models of conventional and latest model machines in Table III, in the same way, comparison would be made between breakeven points of both models as given below in Fig.3.

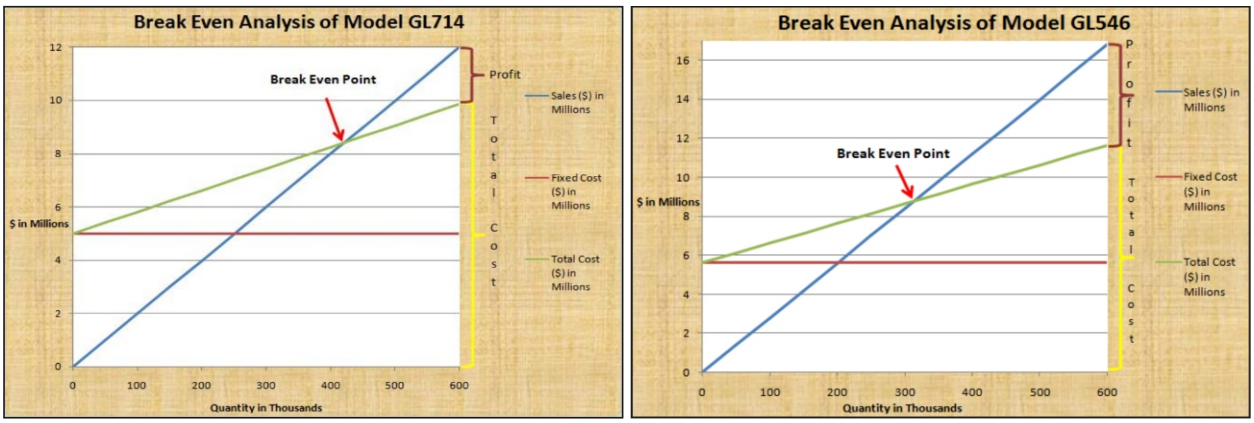

Fig. 3. Comparison of Break-evens

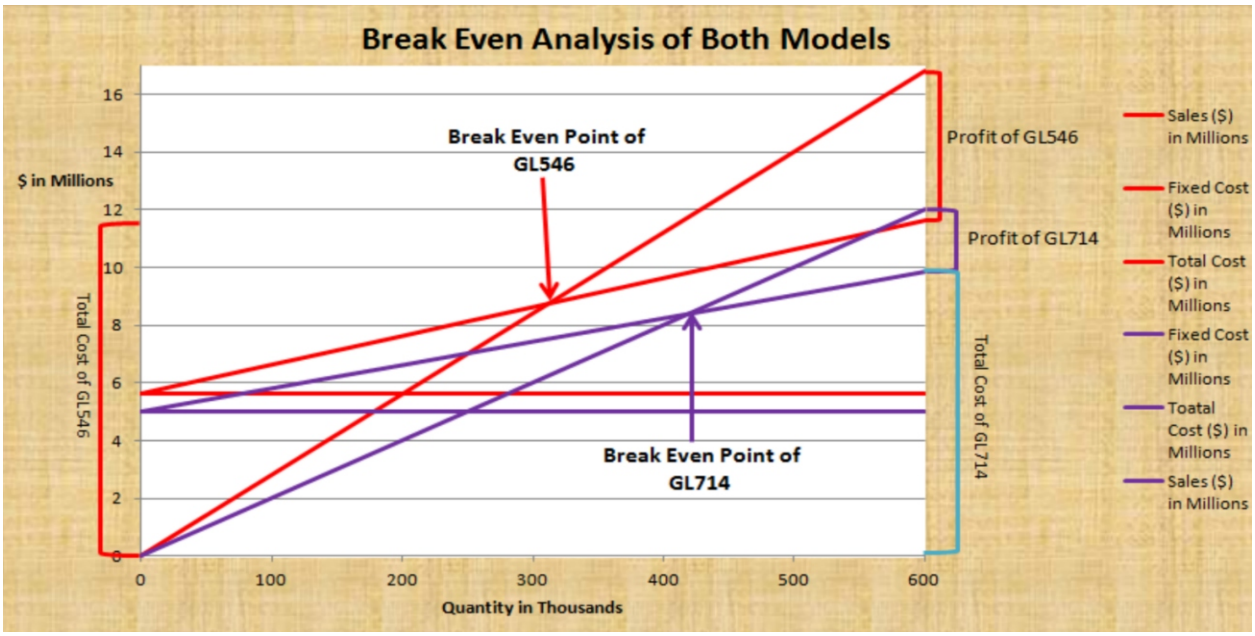

Fig. 4. Overlapped view of the Break-evens

The comparison of break-evens in Fig.3 demonstrates that for model GL714 machines, 420,000 dzns should be produced to reach at no profit and no loss situation and for model GL546 machines, only 313,000 dzns should be produced to reach at break-even point.

In Fig. 4, the red colored lines are used for the values of Model GL546 and purple colored lines are used for Model GL714. This graph shows that the break-even for Model GL546 is achieved earlier as compared to the Model GL714. It is also depicted by this graph that the profit area is much wider for Model GL546 than for the Model GL714 for the same production Quantity for both the models.

Sensitivity Analysis

The objective of sensitivity analysis is to select the better suited machine's model between two alternatives (Model GL714 and Model GL546). There are six important variables, which have direct effect on the selection of model's machines. These variables are Fixed Cost, Variable Cost, Sales/Revenue, Production Quantity, Quality and Profit. All the mentioned terms have been selected as variables because the values of these terms have been computed previously in two scenarios. The comparison has also been made between these terms. An analysis has been carried out in AHP™ to prioritize the selected variables.

Fig. 5. Prioritization of Variables w.r.t. Machine's Model Selection

There are three options in Expert Choice™ (AHP) to prioritize the selected variables. These options are pairwise numerical comparisons, pairwise verbal comparisons and pairwise graphical comparisons. The pairwise graphical comparisons method is used to prioritize the selected variables. The above Fig.5 shows the priorities with respect to the goal, which is selection of better machine's model. The top priority has been given to the profit maximization which is obviously the core objective of organization. In the same way all other variables have been prioritized.

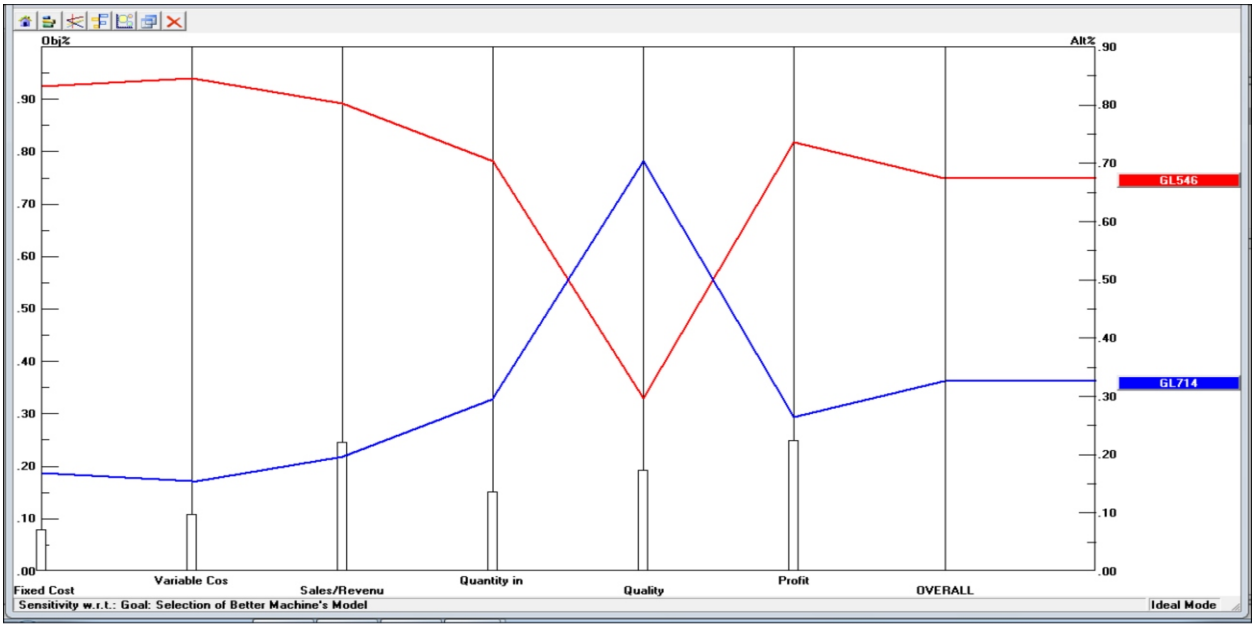

Fig. 6. Performance Sensitivity for Nodes

The above Fig. 6 of performance sensitivity for nodes shows that the model GL546 is 67% prioritized and model GL714 is given 33% priority. The weighted sensitivity analysis in Fig. 7 illustrates that all the variable will favor the selection of model GL546 machines except the quality. As demonstrated by the trends in Fig. 7, the quality has negative trend, which means that the selection of model GL546 will have inverse impact on the quality of the product.

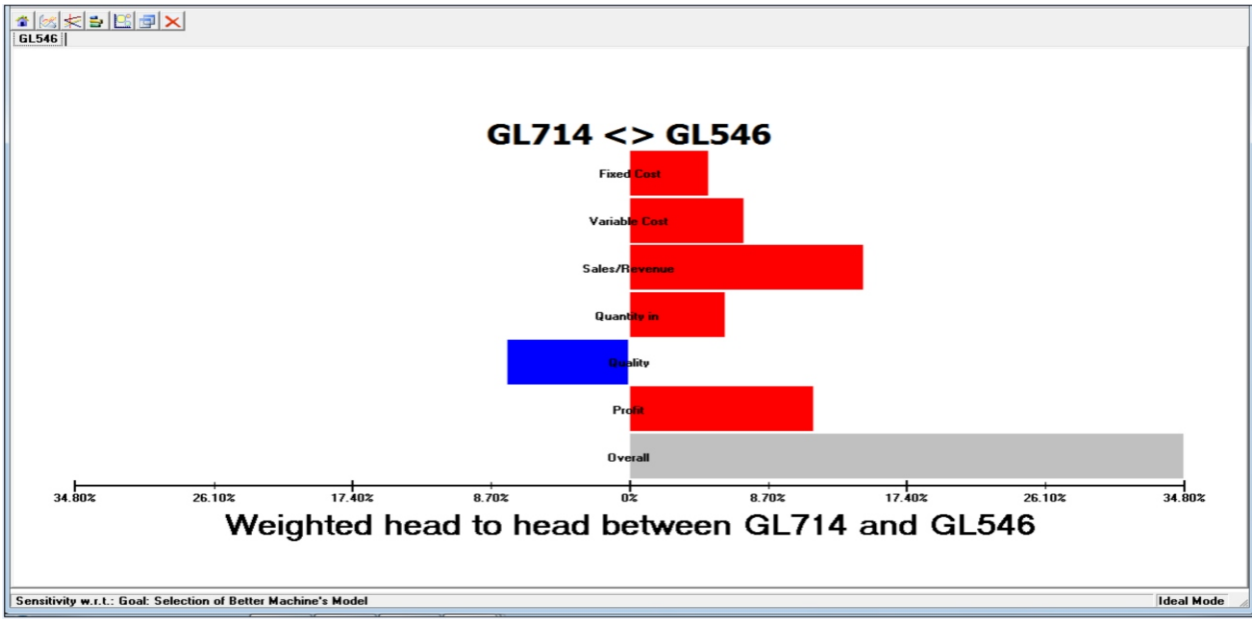

Fig. 7. Weighted Head to Head Sensitivity Analysis of Models

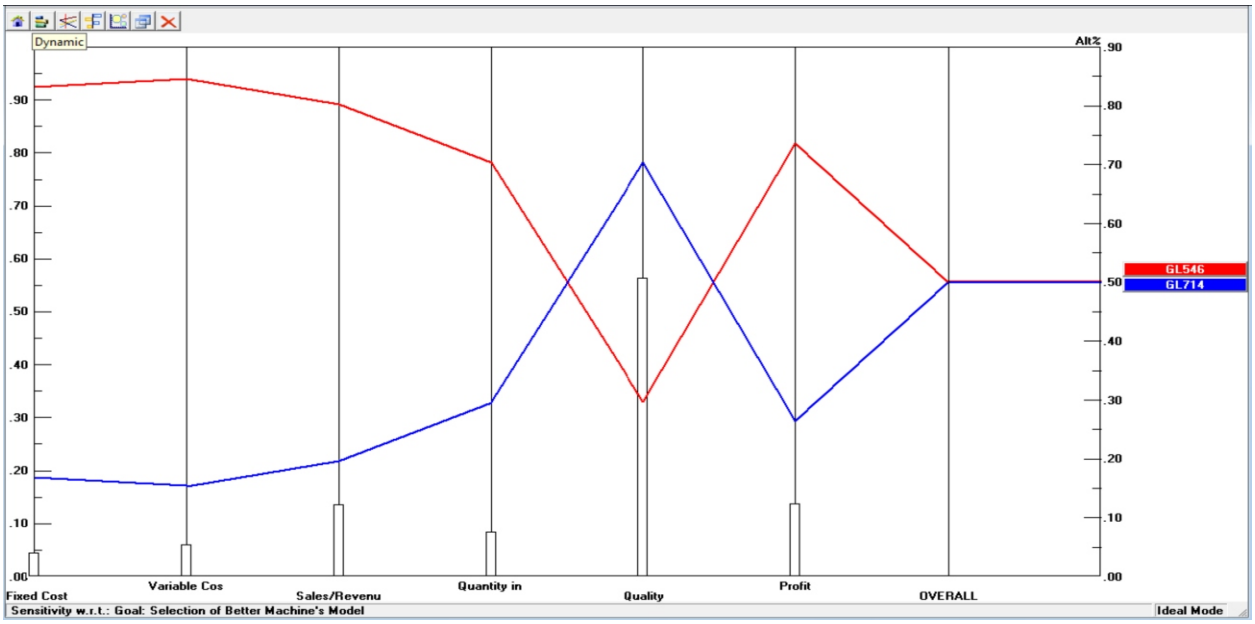

Fig. 8. Sensitivity Analysis for Quality at 58% Rating

The above Fig. 8 shows that if the quality is given 58% rating then both the models has equal chances of selection. But at 58% rating of quality the value of profit has been decreased from 24.5% to 12%. This describes that the profit margin squeezed up by rating the higher value of quality than the default value. In the same way the quality rating also has impact on the quantity and sales, which have been decreased from 14.7% and 24.2% to 8% and 14% respectively.

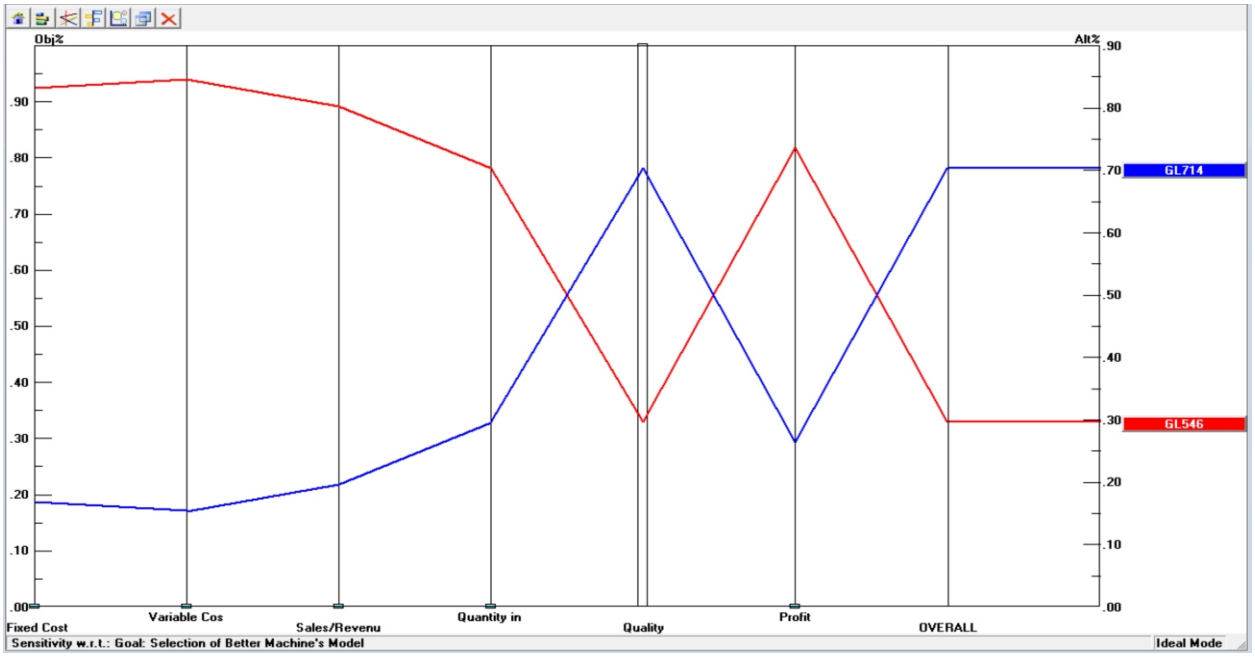

Fig. 9. Sensitivity Analysis for Quality at 100% Rating

The above Fig. 9 describes that if hundred percent rating will be given to the quality, then the suggested alternative would be totally opposite to the original decision. Then the most suitable alternative would be model GL714 machines with 71% rating and the rating of model GL546 would be only 30%. The reason for the quality to be sensitive is that as the production rate of model GL546 is very high therefore the rejection quantity would also be very high.

The quality of the product is checked and controlled by the quality control (QC) department which is a separate dedicated department to control the quality of the product at every stage and all the quality standards are followed (like ISO-9001, ISO-14001, ISO-17025, WARP, OKEOTEX-100, Fair Trade etc.). Means that the quality is not only managed through the machines but also it is managed through proper quality control department, which maintains the product quality from knitting to the packing stages. At the end, the quality assurance (QA) department again verifies the product quality before shipping to the customer. Therefore the quality would not be an issue.

V. Results and Discussion

Break even for GL714 shows that the quantity of 420,000 dzn should be produced to reach at no profit and no loss situation.

Break even for GL546 shows that we have produce 313,000 dzn to reach at no profit and no loss situation.

The break even analysis also shows that if we produce 600,000 dzn by using machines of GL714, then the profit will be $ 2.130 Millions.

But if the machines of Model GL546 are used for the same quantity, then profit will be $ 5.151 Millions.

The annual profit of GL714 machines is $ 12.469 Millions and annual profit for GL546 is $ 44.266 Millions.

The payback period for Model GL714 is 103 days and the payback period for Model GL546 is 41 days.

The annual rate of return for GL714 is 73.63% and annual rate of return for GL546 is 131.71%.

There is not a significant difference in terms of fixed cost for both the models but the there is a considerable difference in variable costs between two models. Variable cost for GL714 is $ 11.935 Millions and for GL546 is $ 27.980 Millions.

There is also a lot of difference in production rates, as the production rate for GL714 is 170.16dzn/hr. and the production rate for GL546 is 321.80dzn/hr.

The sensitivity analysis of both the models also suggests that the most suited model would be GL546 of flexible machines.

VI. Conclusions

Leverage of AM has been carried out and established that it is the most beneficial for the company to use latest flexible machines for coping with the new design changes and an analysis based of financial terms recommended use of flexible machines of model GL546. Sensitivity analysis using AHP also recommended use of AM for fulfilling the demands of the customers. It is concluded that the latest/flexible machines have greater productivity; therefore this will automatically decrease the lead time to a significant extent.

References

[i] J. R. MEREDITH and N. C. SURESH, "Justification techniques for advanced manufacturing technologies," *International Journal of Production Research,* vol. 24, pp. 1043-1057, 1986.

[ii] F. Raafat, "A comprehensive bibliography on justification of advanced manufacturing systems," *International Journal of Production Economics,* vol. 79, pp. 197-208, 2002.

[iii] M. H. Small, "Justifying investment in advanced manufacturing technology: a portfolio analysis," *Industrial Management & Data Systems,* vol. 106, pp. 485-508, 2006.

[iv] Z. Banakar and F. Tahriri, "Justification and Classification of Issues for the Selection and Implementation of Advanced Manufacturing Technologies," *World Academy of Science, Engineering and Technology,* vol. 65, pp. 341-349, 2010.

[v] M. D. PROCTOR and J. R. CANADA, "Past and present methods of manufacturing investment evaluation: a review of the empirical and theoretical literature," *The Engineering Economist,* vol. 38, pp. 45-58, 1992.

[vi] M. H. Small and I. J. Chen, "Economic and strategic justification of AMT inferences from industrial practices," *International Journal of Production Economics,* vol. 49, pp. 65-75, 1997.

[vii] R. J. Fotsch, "Machine tool justification policies: their effect on productivity and profitability," *Journal of Manufacturing Systems,* vol. 3, pp. 169-195, 1984.

[viii] F. Lefley, F. Wharton, L. Hajek, J. Hynek, and V. Janecek, "Manufacturing investments in the Czech Republic:: An international comparison," *International Journal of Production Economics,* vol. 88, pp. 1-14, 2004.

[ix] P. Y. Huang and M. Sakurai, "Factor automation: the Japanese experience," *Engineering Management, IEEE Transactions on,* vol. 37, pp. 102-108, 1990.

[x] P. L. Primrose, *Investment in manufacturing technology*: Chapman & Hall, 1991.

[xi] P. M. Swamidass and M. A. Waller, "A classification of approaches to planning and justifying new manufacturing technologies," *Journal of Manufacturing Systems,* vol. 9, pp. 181-193, 1990.

[xii] K. Jenkins, P. Smith, and A. Raedels, "The financial evaluation of robotics installations," *Robotics,* vol. 3, pp. 213-219, 1987.

[xiii] F. Chan, M. Chan, H. Lau, and R. Ip, "Investment appraisal techniques for advanced manufacturing technology (AMT): a literature review," Integrated Manufacturing Systems, vol. 12, pp. 35-47, 2001.

[xiv] A. S. Sohal, R. Schroder, E. O. Uliana, and W. Maguire, "Adoption of AMT by South African manufacturers," Integrated Manufacturing Systems, vol. 12, pp. 15-34, 2001.

[xv] M. Jahanzaib and K. Akhtar, "Technology driven strategy (TDS) using machine automation cost in discrete parts manufacturing," KUWAIT JOURNAL OF SCIENCE AND ENGINEERING, vol. 34, p. 207, 2007.

[xvi] J. Hynek and V. Janeček, "Economic Justification of Advanced Manufacturing Technology," in Proceedings of the 2nd WSEAS Int. Conf. on Management, Marketing and Finances (MMF'08), 2008, pp. 103-108.

[xvii] J. Hynek, V. Janeček, and L. Svobodová, "Problems associated with investment in advanced manufacturing technology from the management point of view," WSEAS Transactions on Systems, vol. 8, pp. 753-762, 2009.

[xviii] Z. Taha, Z. Banakar, and F. Tahriri, "Analytical hierarchy process for the selection of advanced manufacturing technology in an aircraft industry," International Journal of Applied Decision Sciences, vol. 4, pp. 148-170, 2011.

[xix] M. Darbanhosseiniamirkhiz and W. K. Wan Ismail, "Advanced Manufacturing Technology Adoption in SMEs: an Integrative Model," Journal of technology management & innovation, vol. 7, pp. 112-120, 2012.

[xx] R. Abdullah and M. G. Hassan, "Advanced Manufacturing Technology: The Perceived Impact on Producer's Value," The Asian Journal of Technology Management (AJTM), vol. 5, 2012.

[xxi] S. A. M. Mirza Jahanzaib, K. Akhtar, and T. Aslam, "Improvement in Subsisted Product Delivery Process of Manufacturing Organization using Concurrent Engineering," Life Science Journal, vol. 10, 2013.

[xxii] S. A. Masood, M. Jahanzaib, and K. Akhtar, "Key Performance Indicators Prioritization in Whole Business Process: A Case of Manufacturing Industry," Life Science Journal, vol. 10, 2012.

Experimental Study of Silty Clay Stabilization With Cement and Lime in Multan, Pakistan

T. Sultan[1], A. Latif [2], M. U. Rashid[3], U. Ghani[4], T. A. Khan[5], K. Khader[6]

[1,2,5]*Civil Engineering Department, University College of Engineering and Technology BZU. Multan, Pakistan*
[3]*WR Division, NESPAK, Lahore, Pakistan*
[4]*Civil Engineering Department, University of Engineering and Technology, Taxila, Pakistan*
[6]*Civil Engineering Department, College of Engineering, Salman bin Abdul Aziz University, P. O. Box 655, AlKharj 11942, Saudi Arabia*
[1]tahirsultanch@hotmail.com

Abstract-Stabilization is valuable substitute for advancing the soil characteristics. The engineering features gained after stabilization differs broadly owing to non-uniformity in constitutions of soil. This study describes an assessment of cement and lime additives for advancing soils ventures. The effectiveness of lime and cement stabilization on geotechnical characteristics of the in situ soil has also been described in the paper. The additives like cement and lime were added in different dosage rates to examine the change in properties of the in situ soil. Cement addition caused an increase in unconfined compression strength (UCS) throughout from 4% to 16% of cement. Moreover, it has been observed that by adding lime, the early strength of clay increases up to 6% of lime but for long term strength i.e. 28 days maximum strengths is achieved for 4% of lime. It also confirms that with more percentage of lime and longer duration of curing, it expands. In addition to the strength behavior of samples at various percentages of cement and lime, the deflection at failure point was also examined. In order to make a straight comparison, both cement and lime stabilized soils were also tested in laboratory. Generally, the performance of Portland cement-stabilized soils was advanced to lime in the experiments performed.

Keywords-Atterberg Limits, Portland Cement, Unconfined Compressive Strength, Hydrated Lime, Soil Stabilization, Deflection.

I. INTRODUCTION

It is an eminent verity that, every building structure must rest upon the soil or be made up of various soils. It would be ideal to hit upon a soil to be suitable for the proposed use as it exists in nature at a precise construction field but unluckily, such a thing is of rare occurrence.

Stabilization of soil is only one of the several techniques available to the geotechnical engineers and its preference for any circumstances should be made only after a comparison with other techniques in terms of technical and economical parameters. Scientific methods of stabilization of soil have been initiated in recent years [i]. The two techniques to augment the properties of sandy soils i) mechanical stabilization and ii) mixing of stabilization agents into un-disturbed soils were discussed in detail by Reference [ii]. "Soil Stabilization, in an extensive sense, refers to the techniques utilized with a view to alter one or more properties of a soil so as to recover its engineering performance" [ii].

Soils when at a construction field are not fit or when contain objectionable possessions composing them inapt for exercise in a geotechnical tasks, they may need to be stabilized [iii]. Chemical stabilization includes the variation of characteristics of a native accessible soil to recover its engineering properties. Two most frequently utilizing chemical stabilization techniques are cement and lime stabilization. There are many stabilization techniques and methods presently in application. In accordance with Reference [iv] the type of methods to be selected for a certain field relies on the kind of the stabilizing soil, the kind of construction to be executed, extend of needed stabilization, on the environmental impact sand the accessibility of construction materials. Stabilized soil increases shearing conflict of the soil, conflict against wear and tear, reduces the quantity of soil and water permeability of unsealed pavements.

1.1. Stabilization of Soil with Cement and Lime

Stabilized soil is usually a merged material that results from amalgamation and optimization of characteristics in individual component materials [v]. Regarding soil stabilization using various additives like cement and lime, broad studies have been conducted by [vi]. Soil stabilization using lime or cement has extensively been utilized to enhance the mechanical properties of various soils for civil engineering functions [vii].

1.1.1. Lime Stabilization

Lime stabilization results in reducing maximum dry density and enhancing optimum moisture content,

Strength, fatigue intensity and elasticity modulus. Lime was initially utilized as a mean of soil stabilization in modern building construction in 1924 for little widening of road toughened by the accumulation of the hydrated. Laboratory testing shows that lime counters to average, modestly fine and fine sized soil particle sand increases workability, strength and reducing plasticity [viii]. Lime action augments optimum water content and reduces maximum dry density of soil. Many researchers have also exposed that optimum water content increase by advancing lime quantity [ix-x].

1.1.2. Cement Stabilization

Cement is a versatile material that has both adhesive and cohesive characteristics, facilitating it to bond mineral splinters into a firm mass. Soil stabilization with cement method has been in survival over a long period of time. Cement treatment affects chemical response parallel to lime and may be utilized for both soil stabilization and modification functions. Cement stabilization is more exclusive than lime. Reference [xi] presented that Portland cement has been deemed as one of the most flourishing soil stabilizers, due to its easy worth control and easy handling properties. Reference [xii] discovered that the larger will be the strength of the cement stabilized clayey soil, if the cement quantity increases. Several researches have revealed cement treatment is found to be more suitable for the grainy soils and also for clayey materials having low plasticity index [xiii].

The accumulation of cement also augments the optimum water content. However, it reduces the maximum dry density [x]. On the other hand, by ACI committee 230 (1990), a report describes that the intention of cement action affects the variation of optimum water content and maximum dry density. In supplement, cement dealing affects instantaneous reduces water content [xiv]. Consequences of a specific investigation revealed that, decreases in unconfined compressive strength were 10% to 20% and reaches up to 40% for four and 24 hours deferrals, respectively [xv].

1.2. Curing Time

The shear strength of lime-treated and cement treated soils enhances with the passage of time. In the starting periods of the curing time, the tempo of increase in strength is usually quick after that, as the time increases, the tempo of increase in strength declines. However, in the early stages, the rate of increase in strength for cement stabilized soil is more as compared to that of the lime stabilized soils. In both, the concrete and lime stabilized soils; the shear strength of cement stabilized clay augments with the passage of time [v].

II. Methodlogy and Data Collection

The soil sample used in the project was acquired from Bahadurpur Chowk near Bahauddin Zakariya University, Multan, where construction of road was in progress. Hydrated lime and Portland cement were exercised as the stabilizing agents at various dosage levels. The collected samples were treated with lime and cement at different mix ratios. The cement and lime were treated to the natural in situ soil by loose volume and dry mass of the soil respectively. Consequently, the treated soil samples were investigated for unconfined compression strength UCS values. Curing, without adjusting the temperature, was carried out in the laboratory.

2.1. DosageRate

The dosage rate is the amount of stabilizer mixed to the soil for stabilization purpose. Dosage values may be enumerated in various modes, but we utilized the dosage rates to be depended on the dry weight of soil to be stabilized.

The following dosages (%) of cement and lime were utilized in our study:

4, 6, 8, 10, 12, 14 and 16 percent cement by the dry weight of soil

4, 5, 6, 7 and 8 percent lime by the dry weight of soil

III. Environmental Investigations

3.1. Soil Characterization

Soil characterization tests, as a preliminary step, were carried out to appraise key soil characteristics to ascertain either it is appropriate for stabilization. Soil categorization tests were executed on soil specimen in agreement with approved ASTM standard methods. The brief explanation of each testing is as follows:

3.2. Soil Classification

Soil classification was done by employing the Unified Soil Classification System (USCS). Utilizing the Atterberg limits and the grain size distribution, the USCS appoints a dual letter indication and a group name for soil reorganization. A visual physical inspection method could also be employed to classify soil simply at the site; but, classification offered in this study was supported on laboratory testing depended method.

3.3. Specific Gravity

Specific gravity values of the soils were decided by inserting known weight of oven-dried soil in a flask and then adding water to fill the flask. The displaced water weight was then computed by contrasting the weight of the soil and water in the flask with the weight of flask having water in it, only. The specific gravity was then computed by dividing the dry weight of the

soil by the weight of the displaced water.

3.4. Particle Size Distribution

The mixture of particle sizes and the distribution of these sizes provide very useful knowledge about the engineering performances of the soil. The particle size distribution was determined by using the process of sieving analysis in the laboratory.

3.5. Atterberg Limit

For the determination of the plasticity of the soils, the liquid limit and plastic limit values were estimated. The Atterberg limits apparatus was employed to find the liquid limit, while the plastic limit was found by rolling 3 mm diameter threads of soil till they started to fracture.

3.6. Modified Proctor Compaction Test

Optimum moisture content (OMC) at maximum dry density (MDD) for the as-received soil without any stabilizers was established by testing. The test was carried out to calculate the degree of compaction in concern of its dry unit weight. The optimum moisture content then was measured. At least four density values were taken by which the optimum moisture content was obtained. The dry density of the soil specimen was calculated and plotted versus moisture content.

3.7. Unconfined Compression Strength (UCS)

Effect on stabilization was inspected by varying the dosage rates of Portland cement and lime on UCS of the soil sample. UCS tests were carried out on the same day, after 7, 14, 21 and 28 days. Unconfined compressive test uses a cylindrical soil sample with no lateral confinement. An axial compressive load was gradually employed on the soil until it started to fail. The load was applied quite rapidly (typically 1 minute to failure), thus produced an un-drained condition.

IV. Results and Discussions

4.1. Soil Classification

The soil classification and grain size analysis of the as-received soil are presented in Table I. Soil characteristics i.e. Atterberg limits, optimum moisture content (OMC) and maximum dry density (MDD) are shown in Table II. The OMC and MDD of the soil samples were determined using modified compactive effort.

TABLE I
Classification and Grain Size Analysis of As-received Soil

Sieve No.	Sieve Size (mm)	Retained Weight (gm)	% Retained Weight	Cumulative Retained On Each Sieve	% Finer
4	4.75	209	13.93	13.93	86.07
8	2.36	157	10.47	24.4	75.6
40	0.425	310	20.67	45.07	54.93
100	0.15	542	36.13	81.2	18.8
200	0.075	107	7.13	88.33	11.67
Pan	0.0	175	11.67	100	0

TABLE II
Classification of As-received Soil

Basic Characteristics	Soil	Test Standards
USCS Classification	CL-ML	ASTM D 2487
Liquid Limit (%)	24	ASTM D 4318
Plastic Limit (%)	18	ASTM D 4318
Plasticity Index (%)	6	ASTM D 4318
Specific Gravity	2.62	ASTM D 854
Optimum Moisture Content (%)	12.64	ASTM D1557
Maximum Dry Unit Weight (KN/m^3)	19.13	ASTM D1557

4.2. Unconfined Compressive Strength (UCS)

The UCS tests of stabilized/treated soils were then executed on various dosages of stabilizers to appraise the dosage of stabilizer, the technique (% dosage of stabilizer) required to gain the aimed strength rates and the aptness of the specific stabilizer for certain soils. Following results of USC were revealed when soil was treated with cement and lime at various dosage rates.

4.2.1. Results for Cement

The Fig. 1 exhibits the performance of soil (CL-ML) at various percentage dosages of cement. It shows the ultimate strength achieved at various percentage dosages of cement as a stabilizer. It has been observed that the ultimate strength of soil enhances by increasing the percentage dosage of cement. This increase in strength is monitored throughout from 4% of cement to 16%. In addition to the strength behavior of samples at different percentage dosages of cement the deflection at failure point have been examined. The failure deflections along with their respective percentage dosages of cement are given in Fig. 2. It may be seen from the figure that pattern of deflection cannot be easily examined and cannot be related accurately to any other factor like percentage dosage of cement and curing dates as it can be seen that while coming down from 4 to 8% dosage, deflection is first

decreasing and then rising up again. In the same way for the sample of all percentage dosages magnitude of deflection is first decreasing by increase of curing period and then increasing again. The decrease in deflections with the passage of time was observed (up to 15 days of adding cement) but after that deflections were increased (at 25 days). Increase in the deflection may be pointed towards the partial breakage of bond between the soil and stabilizer due to high increase in unconfined compressive strength. Also increase in deflection may be attributed to either environmental effects or due to mishandling of sample during compression test.

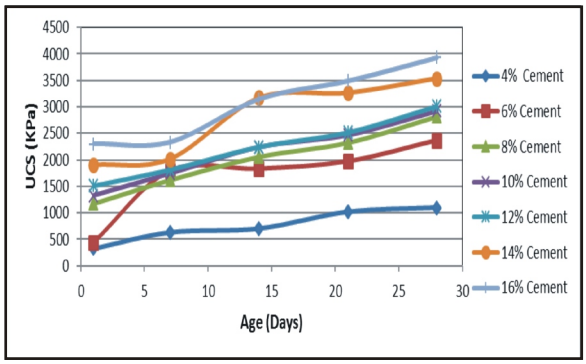

Fig. 1. Graph between UCS of Soil and Age at Different % of Cement

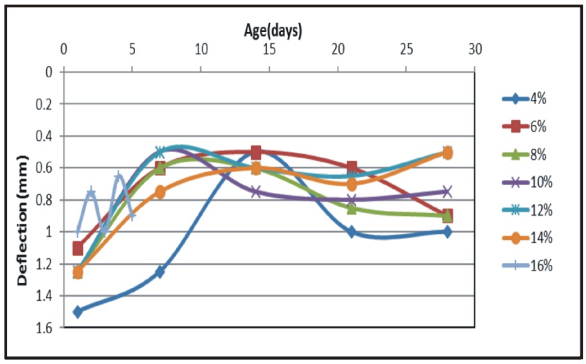

Fig. 2. Graph between Deflection of Soil and Age (Days) at Different %age of Cement

4.2.2. By Adding Lime

By adding lime following results from unconfined compression test were achieved:

From Fig. 3 it can be observed that early strength of soil increases up to 6% of lime but for longer term strength i.e. 28 days maximum strength is achieved for 4% of lime.

This is due to the reason that with more percentage of lime and longer duration of curing lime expands. Also, it can be perceived that for curing period up to 14 days 6% lime samples has the maximum value of strength. This was actually owing to fact that it was the optimum combination of percentage dosages of lime and curing period, as later this curing period of 14 days lime started to expand up to the point that its expansion affected the stability and consistency of soil samples and hence resulting in the loss of ultimate strength of soil. On the other hand, for percentage dosages more than 6% of lime sample started expansion in the premature days of the curing period and hence, showed less strength than 6% of lime and 14 days of appropriate curing the expansion became so much that sample were not able to stand stable enough for testing. In addition to the strength behavior of samples at different percentage dosages of lime the deflection at failure point have also been examined and shown in the Fig. 4. The deflection pattern determined from the figure with respect to curing periods for 4%, 5% and 6% of lime addition show decreasing trend. However, for 7% and 8% samples, there is a sudden increase of deflection from 7 to further days. The 14 and 28 days soil samples were found highly unstable and therefore, shown a sudden increase in deflection.

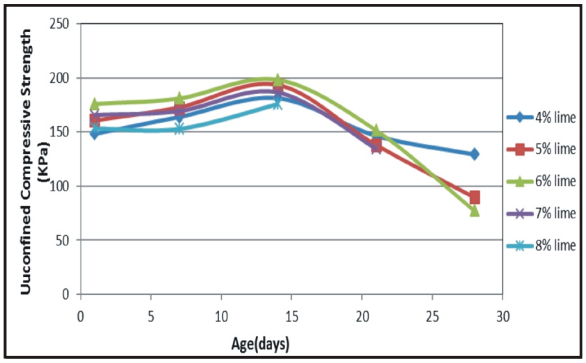

Fig. 3. Graph Between Unconfined Compressive Strength (UCS) of Soil (KPa) and Age (Days) at Different %age of Lime

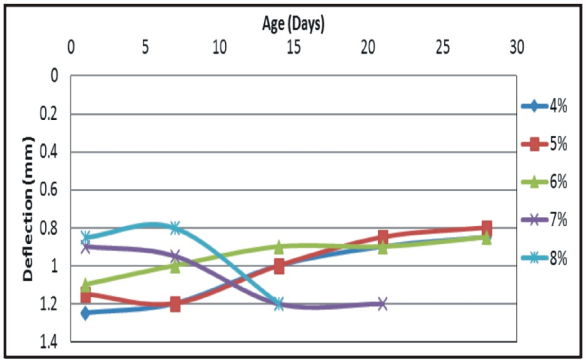

Fig. 4. Graph between deflection of soil and age (Days) at Different %age of Lime

V. CONCLUSIONS

This investigation was executed to appraise the performance of Portland cement and lime in stabilizing advanced engineering properties of particular soils by

probing unconfined compressive strength. The following usual terminations can be drawn based upon the investigation executed. The unconfined compressive strength (UCS) of soil stabilized with cement is always higher than that of lime-stabilized soil at all stages.

Results acquired from UCS test of Portland cement indicate that with the addition of Portland cement to soil, the UCS values increases. The UCS values also increase as the curing time for the stabilized soil samples increases. Values of UCS increase considerably after 7, 14, 21 and 28 days curing period. The strength gained continued throughout 28 days curing period. The maximum strength that can be achieved on 28 days of curing is 3928.6 Kpa.

Lime-stabilized soil begins weaker but attains strength with time. The increase in UCS of lime-stabilized soil is more reliant on curing time rather than dosage. The increase in performance with higher dosages of cement is clearly manifested. This proposed the dependence of pozzolani reaction for strength obtain in the soils with lime stabilization.

The strength gained continued upto 14 days curing period and then it starts decreasing. The maximum strength that can be achieved is 198.44 KPa for 6% addition of lime at 14 days.

VI. Recommendations

The following recommendations have been drawn from the study:

The additive assortment must depends on the efficiency of provided stabilizer/additive to enhance the physio-chemical characteristics of the exclusive soils. The initial assortment of the suitable stabilizer(s)/additive(s) for the stabilization of soil must ponder:

Soil uniformity, consistency and gradation

Soil constituents and its mineralogy

Required geotechnical engineering and soil mechanics characteristics

Functions of soil treatment

Methods of stabilization

Ecological situations and engineering finances

The selection of using lime or cement mixing depend upon; in situ moisture content, in-situ soil state, effectual of stabilizer to be used and the kind of execution to be required. Moreover, lime should not be spread dry during the windy weather because it will cause dusting problems. A sprinkling with water with lime will diminish dusting.

The recommended procedure of soil stabilization with cement at site is: i) Grade the area, ii) Scarify, pulverize and pre - wet soil as needed, iii) Re-grade the area, iv) Spread Portland cement and mix it with soil, v) Apply water and mix it, vi) Compact the soil, vii) Final grade the area, viii) Cure the area.

The recommended procedure of soil stabilization with lime at site is: i) Grade the area first, ii) Scarify and pulverize the soil, iii) Spread lime on the soil, iv) Add water during preliminary mixing, v) Rough grade with light compaction, vi) Preliminary cure, vii) Final rotary mix and pulverize the soil viii) Compact the soil, ix) Finally cure all area.

Some practical application of the study includes: Soil stabilization is applicable to diminish compressibility and permeability of soil strata in existing earthen structures and to augment the unit weight of soil. It is applicable to augment bearing capacity of foundation soil materials and to prevent seepage (through cracks, joints and porous zones) from foundation, basements, slopes and ditches. It is utilized to advance the natural soils for execution of airfields and highways. In a short interval of time it is utilized to make an area trafficable for emergency needs. Soil stabilization expands the shear strength of soil.

Refrerences

[i] C. D. F. Rogers, S. Glendinning, and T. E. J. Roff, "Modification of clay soils for construction expediency," *Geotechnical Engineering*, vol. 125, pp. 1-8, 1997.

[ii] H. F. Winterkorn, Soil Stabilization. "Chapter 8. In Foundation Engineering Handbook". *Winterkorn and Fang, eds., Van Nostrand Reinhold, New York, N. Y.*, pp. 312-336, 1975.

[iii] J. E. Bowles, "Foundation analysis and design," McGraw- Hill companies Inc., USA. 1996.

[iv] K. N. Derucher., G P., Korfitatis, A. S. Ezeldin, "Materials for Civil and Highway Engineers," Prentice-Hall. 1998

[v] E. A. Basha, R. Hashim, H. B. Mahmud, and A. S. Muntohar, "Stabilization of residual soil with rice husk ash and cement," *construction and Building Materials*, 19, 448-453, 2005.

[vi] A. A. Rawas, and M. F. A. Goosen, "Expansive soils-Recent advances in characterization and treatment," Taylor & Francis group, Balkema, London, UK. 2006.

[vii] P. Sherwood, "Soil stabilization with cement and lime," *State of the Art Review. London: Transport Research Laboratory, HMSO*. 1993.

[viii] D. N. Little, "Handbook for Stabilization of Pavement Subgrades and Base Courses with Lime," Kendall/Hunt, Iowa, 1995.

[ix] J. Mallela, H. V. Quintus, and K. Smith, "Consideration of lime-stabilized layers in mechanistic-empirical pavement design," *The National Lime Association*. 2004.

[x] A. M. Tabatabi, "Pavement [Roosazi Rah]", *University's publication center, Tehran, Iran.* 1997.

[xi] S. Y. Saitoh, Suzuki. and K. Shirai. "Hardening of Soil Improvement by Deep Mixing Method,"

Proc. of the 11th ISCMFE. San Franscico. Vol. 3. pp. 1745-1748, 1985.

[xii] B. B. Broms, "Stabilization of Soft Clay with Lime and Cement Columns in South-east Asia. Applied Research Project RP10/83," *Nanyang Technical Institute, Singapore.* 1986.

[xiii] D. D. Currin, J. J. Allen, and D. N. Little, "Validation of soil stabilization index system with manual development," *Report No. FJSRL-TR-0006, Frank J. Seisler Research Laboratory,* United States Air Force Academy, Colorado. 1976.

[xiv] D. T. Bergado, L. R. Anderson, N. iura, and A. S. Balasubramaniam, "Soft ground improvement," *ASCE Press*, 1996.

[xv] W. G White, and C. T. Gnanendran, "The influence of compaction method and density on the strength and modulus of cementitiously stabilized pavement material." *The International Journal of Pavement Engineering*, vol 6(2), pp. 97-110, 2005.

Investigation Regarding Bridge Expansion Joints Deterioration in Pakistan and its Remedial Measures

A. Ajwad[1], L. A. Qureshi[2], F. Tahir[3], J. Hussain[4]

[1,2]Environmental Engineering Department, University of Engineering and Technology Taxila, Pakistan
[3,4]Civil Engineering Department, University of Engineering and Technology Taxila, Pakistan
[1]ajwad1989@gmail.com

Abstract-The Concrete bridges are a vital part of highway infrastructure in Pakistan. The main problem that exists is the deterioration of most of them over the past 20 years or so. The main reason for this is the deviation from specified construction procedures and the negligence of the maintenance departments due to several reasons. At the moment National Highway Authority (NHA) owns about 5000 bridges in number across the country and according to a survey, about 30 percent of them are either not up to the mark or are out of service. The fund that NHA reserves every year for the maintenance purposes ranges from PKR 500 to 600 million which is very limited when it comes across the scope of the work. It means that expensive testing and retrofitting techniques that need to be implemented can never be achieved practically. This research is focused on case studies involving deterioration of bridge expansion joints only. All the deficiencies with their root causes and remedial measures are discussed in detail. The research is based upon wide experience of authors and will prove to be a cherished standard and beneficial reference article for working engineers engaged in fresh construction as well as renovation & repairs of concrete highway bridges.

Keywords-Bridge, Expansion Joints, NHA, Maintenance, Wearing Surface, Deterioration

I. INTRODUCTION

Ridges are considered as the spinal column of infrastructure for any country [i]. At the moment Pakistan is facing a big bridge crisis which means actions are required as soon as possible. The main problem is that the amount of resources available to meet the rehabilitation works are not even close to do all the repairs [ii]. Thus, the need for fast devotion to the suffered problems is required which would include a broad approach to bridge maintenance. This would include better repair and restoration methods. In current investigation work, the main objective was to define the current methods being followed in the maintenance of the bridges and to come up with such measures that will take the managing and monitoring abilities of the bridge engineers to the next level.It is well known fact that construction projects are meant to be designed as economical as possible. For this reason, design engineers have to design the bridges with taking into consideration only the reasonable loading conditions instead of designing for extraordinary one. It means that it is impossible to plan a bridge which has no risk involved at all. It can also be said that this planet has not good enough resources for such type of zero risk bridge [iii]. Any form of construction cannot last forever which includes Bridges. The consequences of degradation will start to emerge, sooner or later, it would not matter whatsoever method of construction is adopted and whichever supplies are used. There are many reasons which contribute to the type and degree of degradation which would include quality of construction, constructional materials, structural form, design and detailing, fire, scour, atmospheric environment, earthquakes, fatigue, weather, floods, intensity and nature of the traffic loading imposed upon it. Bridge management and maintenance can be defined as a method which includes going through all the necessary steps and checking each and every aspect, from the paperwork to its design, construction and finally the end of its useful life.

Bridge management approaches are being amended and enhanced to carry out required renovation and restoration work in a balanced manner The responsibility of maintaining and managing bridge stock economically, efficiently and effectively lies on the shoulders of bridge managers so that it would effectively sustain the imposed loads without loss of structural reliability or deterioration in its physical appearance. As part of their duty, they have to make vital choices concerning numerous doubts [iv].

There is a tremendous load of pending rehabilitation works on bridges in many developing countries like Pakistan. Such problems can be seen in most of the national highways in Pakistan. But as it is a known fact that that Pakistan has not sufficient funds to be allocated for bridge repairs and hence only PKR 500 to 600 million is assigned yearly to maintain and

renovate in total over 5000 bridges. In addition to this, the lack of expertise has led the local authorities like provincial and national highway departments into flattening the depreciated bridges. At some places, this demolishing was done for only the superstructures but most of the times the whole structure was flattened.

The main aim of this research work was basically to look ahead on defining damage problems observed in expansion joints of bridges and proposing remedial measures within the available financial resources based on the personal experience of authors which would then help bridge engineers. The methodology adopted for this research was based on some case studies regarding rehabilitation works on bridges in Pakistan. National Highway Authority conducted a survey in 2006 regarding prevailing conditions of service bridges in Pakistan. The paper is based on some recommendations about expansion joints based on their field experience and code practice.

II. Literature Review

An expansion joint can be defined as a device which supports the surfacing, and provides a running surface by filling up the gap between the adjacent bridge deck and abutment or the area between adjacent decks. Bridge expansion joints are designed to allow for continuous traffic between structures accommodating movement, shrinkage, temperature variations on reinforced and prestressed concrete, composite and steel structures. They stop the bridge from damages in extreme conditions and allow enough vertical movement to permit bearing replacement without the need to dismantle the bridge expansion joint [v]. There are various types, which can accommodate movement from 30 to 1000 mm.

The failure of the expansion joint serves as one of the main causes of bridge superstructure and substructure damage. The main problem occurs when expansion joints fail.They have to be repaired along the pier, abutment and decks as well which adds up to almost hundred times more as compared to the actual cost of bridge joints only.

Reference [vi] did research on expansion joints which looked at the problems and their causes. He came out with a conclusion that use of proper seals will contribute to long life of bridge joints. He also concluded that If Polymer Modified Asphalt joints are used, caution should be taken to use them in locations where there is less truck traffic and bridge movement is small. Reference [vii] inspected 150 expansion joints in Portugal and concluded that installment errors and lack of maintenance are the most frequent causes of pathology. Reference [viii] carried out research into the properties and service performance of bridge deck expansion joints and highlighted the quality of workmanship during installation as essential to ensure satisfactory performance. Reference [ix] revealed that roadway members inevitably deteriorate over time at different rates, and the life of some components is only 5-7 years or less. The main causes of deterioration are heavy traffic, water carrying deicing salts, and weather conditions. The main defects include leaking waterproofing and expansion joints. Reference [x] investigated silicone foam as a sealant for small movement expansion joints in brigde decks and revealed that the solid sealant recovered faster than the foam sealant after being subjected to prolonged compression at elevated temperature.

Different types of bridge expansion joints can be categorized as following;

Buried joint
Asphaltic plug joint (APJ)
Nosing joint (N)
Cantilever comb or tooth joint (CT)
Reinforced elastomeric joint (RE)
Elastomeric joint in metal runners (EMR)
Cantilever comb or tooth joint (CT)
Modular joints including finger and sliding plates.

A. Functional requirements

The properly designed and installed joints should offer/fulfill the following needs;

Outstanding traffic control
Extended lifespan
Less sound
Resistant to corrosion
No reaction especially horizontal
The surface under the joints should be protected
Should provide good resistance to changing loads including heavy duty loads
Adaptableness to all sort of surface structure
Installation process should be easy
Low maintenance and service cost
Can be replaceable quick and easy without imposing damage to the existing structure.

Fig. 1. View of the properly installed finger joint

III. Defects Noted on Bridges in Pakistan

As far as the basic requirements like low noise, comfort to the road users and durability are concerned, the best quality of expansion joints have been noted in Pakistan on Lahore-Islamabad Motorway (M2) and Islamabad-Peshawar Motorway (M1). Except these, numerous problems with expansion joints prevail on other main highways. Figures 2-10 show different problems that were noticed during the survey conducted in 2006 by NHA.

Fig. 2. Joint assembly is removed bridge without joint will not serve properly

Fig. 3. Improperly repaired joint with bituminous material has cracked and restricted the movement

Fig. 4. Joint assembly is dislodged, causing noise and damage to the deck concrete

Fig. 5. Improperly repaired joint with bituminous material has restricted the movement

Fig. 6. The damaged wearing course would damage the joint

Fig. 8. Improperly repaired joint with bituminous material has cracked and restricted the movement

Fig. 7. Neoprene seal removed, gap is being filled with debris

Fig. 9. Improperly repaired joint with bituminous material has restricted the movement

Fig. 10. Water flowing through the joint causing deterioration of the deck

IV. Reasons of Damage

The poor condition of the present joints on our national highways was found due to various reasons like:

Overloading due to single axle trucks

Rutting of the asphaltic wearing course. When the asphalt level is below the joint rail, heavy thrust / impact is transferred to the joint which tends to dislodge it.

Non adherence to the specified installation precautions as recommended by the manufacturers.

V. Remedial Actions

The following sequence of actions were successfully followed for the above narrated problems;

1) **Laying the asphalt:** The asphalt should be laid without any delay and in a continuous manner over the bridge gap and then compaction is to be done.
2) **Cutting out:** With the help of an asphalt cutting machine, cutting in the asphalt surface should be done according to the given width of the expansion joint.
3) **Levelling:** The break should then be sandblasted and the edge profile is mounted and shuttering placed.
4) **Installing:** To form a smooth carriageway surface, the polymer concrete should be mixed, poured and cured without leaving any cavities behind. No further compaction will be required.
5) **Inserting:** The sealing profile should be inserted which would make the expansion joint 100% impermeable to water.

Mageba (Switzerland) and Freyssinet (France) are manufacturing the quality expansion joints with variety and all requirements and are available in Pakistan easily. If all five steps mentioned above are followed and quality expansion joints are used, there will be less chance of expansion joints failure.

VI. Construction Precautions

1) While installing the expansion joints, it has been observed with experience that its top levels should be kept below the existing elevation of asphaltic wearing course by at least 2 to 3 mm as an allowance to accommodate the settlements in wearing course. This provision is made while pouring the bedding concrete.
2) Thickness of the slab is increased at the ends of the slab by at least 2 inches for better installation of the joint assembly and spacing of reinforcement is reduced in the design as shown in the below figure.

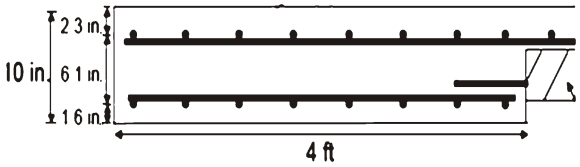

Fig. 11. Bridge deck Slab Cross-section

3) Literature and recommendations of the manufacturer should be strictly followed.
4) The process of installing the expansion joints should work as a team effort which means all the people related to the work e.g. engineer, main contractor and installer should work as a team. All of them should have complete access to the information and design details and it should be made sure that the whole procedure is followed in a professional and competent manner.
5) There should be a provision in the design of making the joint accessible from underneath the deck for inspection. Routine inspection of carriageway surfacing and the joint would mean that the different faults which occur such as rutted surface and blocked drainage can be detected in time and treated as soon as possible. This would help in avoiding the extra remedial work charges. The site engineer should be aware of different joint types and the defects it can have. For maximum service life, the interval between inspections should not exceed a time of one year and maintenance should be done accordingly for minimum disruption.
6) Another important aspect to be kept in mind is the adequate deck drainage. Water is believed to be a foe to any structure and hence the joint should be designed in such a way that water is removed from within and below the surface through drainage units placed in the decks.

7) The materials that should be used for the repairs should be according to NHA standards and should have good durability.

VI. Conclusions and Recommendations

Conclusions

1) The main reasons of weakening of bridges in Pakistan are due to meager and inadequate workmanship which mostly results in less concrete cover, honey combed concrete, improper drainage or water management. Another major cause of damage to concrete is the rebar corrosion which can take place in the presence of chlorides, carbonates and water.
2) A structure of decent features cannot be built without selection of appropriate supplies. The service life of a bridge can significantly be enhanced with the selection of proper and suitable materials.
3) The use of advanced construction methodologies is another way of increasing the safe service life of a bridge. If adequate concrete cover to reinforcement is provided, it can act like a key hurdle to the deterioration procedure.

Recommendations

1) The local establishments should give some devotion to the non-destructive analysis and the electrochemical investigation also.
2) Weekly or monthly assessment is necessary so that the problem can be controlled before it is too late and it reaches the point of no return. The rapid catastrophic event is the one that requires immediate action. Some of such events can be avoided if excellent systematic precautionary repairs are implemented.
3) Water is believed as a foe for any concrete structure and bridges are no different. It is the cause of many of the wears that affects our bridges. Not only does it precipitate corrosion directly if in the presence of oxygen, but it may carry destructive de-icing salts in solution to all parts of bridge through seepage. It tides over expansion joints, and it can seep through to bridge bearings.
4) One cheap and efficient way of guarding prevailing bridges from wear is consistent use of coatings. Such coatings can add up a life of up to 5-20 years depending on its kind and method of usage.
5) There are also numerous corrosion-inhibiting methods available in the market. These include rebar coatings, concrete admixtures and coatings applied to the concrete surface.

Acknowledgement

The authors are really grateful to the officers of National Highway Authorities (NHA) Pakistan, particularly Engr. Arshad Mehmood Choudhry, General Manager (BOT) and Engr. Asif Azam, Assistant Director (Bridges), for extending their complete assistance by providing the photographic data concerning bridges on main highways of Pakistan.

References

[i] P. Patros, Xanthakos, *Transportation Structures Series*, Prentice Hall PTR, upper saddle river, new jersy, 2000.

[ii] M. Mulherone,"*Durability of Bridges and Structures Module*," MSC Thesis in bridge engineering, dept. of civil engg.,University of Surrey, united kingdom, 2002.

[iii] G. TILLY, "*Conservation of Bridges*," 1ST edition, london: spon press, 2002, pp 299-332.

[iv] R. L. Duncan and R. V. Gevecker, Routine Maintenance of Concrete Bridges, American concrete institute, Rep. 345.IR-92, 2005.

[v] Freyssinet,. CIPEC expansion joints: design, build, maintain, 2014, [online]Available: Http://www.freyssinet.co.uk/pdfs/products/cipec_expansion_joints_(cv1).pdf

[vi] Luh-Maan Chang and Yao-Jong Lee, Evaluation and policy for bridge deck expansion joints, Indiana Department of transporation and Federal Highway administration, Rep. FHWA/IN/JTRP-2000/1, 2001.

[vii] Joao Marques and Jorge de Brito, *Inspection survey of 150 expansion joints in road bridges,*Engineering structures, Volume 31;5, 1077-1084, 2009.

[viii] Johnson and Mcandrew, *Research into the condition and performance of bridge deck expansion joints,* Transport research laboratory, Great Britain, 1993.

[ix] Kamaitis and Zanonas, *Deterioration of Bridge deck Roadway members. Part 1:Site Investigations,* Baltic journal of road and bridge engineering, Volume 1;4, 177-184, 2006.

[x] B. Ramesh Malla, R.Matu, Shrestha,*Temperature Aging, Compression Recovery, Creep, and Weathering of a Foam Silicone Sealant for Bridge Expansion Joints,*Journal Of Material In Civil Engineering, volume 23;3, 287-297, 2010.

Investigating the Suitability of Grid and Boundary Conditions on Simulation of A Curved Open Channel

U. Ghani[1], H. Nisar[2], A. Latif[3], N. Ejaz[4]

[1,2,4]Civil Engineering Department, University of Engineering and Technology Taxila, Pakistan
[3]Civil Engineering Department, University College of Engineering and Technology BZU. Multan, Pakistan
[1]usman.ghani@uettaxila.edu.pk

Abstract-This research paper presents results from a numerical modeling of an open channel flow. The channel investigated in this study had a semicircular section. The bed of the channel was rough. During this work, a three dimensional Computational Fluid Dynamics code Fluent has been used. The grid was developed with the help of Gambit. Three different grid shapes including structured, unstructured and structured with a boundary layer development were employed during the simulation work. Two different boundary conditions were considered to check their suitability in this numerical modelling. The first one was velocity inlet and pressure outlet boundary conditions whereas second one was periodic boundary conditions applied at the inlet and outlet of the channel. The results were presented in the shape of primary velocity contours. It was observed that the type of grid did not have any significant impact on the flow structure although structured grid with boundary layer in the vicinity of bed has given slightly better results. As far as boundary conditions are concerned, the periodic boundary condition has reduced the time consumption of the simulation work by reducing the domain size without compromising on the accuracy of the results. From this study it can be concluded that structured grid with boundary layer when used with periodic boundary conditions will produce accurate results with least simulation time and cost consumption.

Keywords-CFD, Fluent, Boundary Layer, Periodic Boundary Conditions, Turbulence Model

I. INTRODUCTION

In Computational Fluid Dynamics (CFD), selection of a suitable grid and application of appropriate boundary conditions are of prime importance to get proper simulation. Any problem in grid generation or wrong selection of boundary conditions will result in divergence and wrong solution. Proper results can only be obtained through good mesh and suitable boundary conditions.

Different researchers have worked on investigation of suitable boundary conditions for a particular problem. For example, reference [i] investigated the impact of boundary conditions on density dependent flow. Reference [ii] obtained different bench mark solutions in vertical channel flows under the action of varying boundary conditions. Some researchers conducted research work on geophysical flows with different boundary conditions [iii]. Reference [iv] performed research work on nonlinear flows in open channels with open boundary conditions. Reference [v] performed numerical modeling on levee failures using complex boundary conditions. Other researchers who investigated boundary conditions in different scenarios include research on two-dimensional tidal flows [vi] and investigation of incompressible flows with SPH [vii].

The open channel flows are very much complex especially during floods. In flood season, floodplains become inundated and water damages life and property. The flood flows are complex hydraulic processes due to a number of parameters. Among there are movement and deposition of sediments in the flow, presence of vegetation on the floodplains, variation of bed roughness from reach to reach and also in lateral direction over a cross section, varying cross section of the floodplains and main channel (such as converging or diverging channels), presence of floodplains on one or both sides of the main channel, etc. Flooding happens in different parts of the world every year. The river water overtops the main channel and starts flowing on the floodplain during floods. Hetrogeneous bed forms, strips and ridges exist in a variety of environments over floodplains such as in gravel-bed rivers and ephemeral stream beds. The research has been conducted by different investigators using numerical techniques and also through laboratory experimentation on open channel flow problems with above mentioned situations. Some of them include numerical modeling for cellular secondary currents and suspended sediment transport on smooth-rough bed strips[viii]. Similarly, reference [ix] worked on impact of non-uniform roughness on bedforms. Reference [x] conducted research on secondary flows in open

Channels.

This paper presents numerical modeling of an open channel comprised of a curved section. Different grids and boundary conditions were employed to get the most suitable for this particular case. A general purpose CFD code Fluent has been used for this purpose. Mesh was generated by Gambit 2.3. Results for different cases have been presented in the shape of primary velocity contours on different cross-sections along the length of the channel. The section II explains the governing equations of the CFD code, section III covers different options employed in numerical simulation. Section IV covers results and discussion which is followed by conclusions.

II. Governing Equations

The CFD code employed in this research work is a finite volume based model. It uses 3D incompressible momentum and continuity equations. These equations can be written as below [xi]

Continuity equation

$$\frac{\partial U_i}{\partial x_i} = 0$$

Momentum equation

$$U_j \frac{\partial}{\partial x_j}(U_i) = \frac{\nu}{\rho}\frac{\partial}{\partial x_j}\left(\frac{\partial U_i}{\partial x_j} + \frac{\partial U_j}{\partial x_i}\right) - \frac{1}{\rho}\frac{\partial P}{\partial x_i} + F_i + \left(-\overline{u_i u_j}\right)$$

Where ν and ρ are kinematic viscosity and density, P is pressure of the water, U_i is velocity vector in *ith* direction i.e. x, y, z directions, $u_i u_j$ are Reynolds stresses which are result of splitting instantaneous velocities into fluctuating components and average components of velocities.

III. Numerical Model Setup

The mesh was generated with the help of GAMBIT 2.3 software [xii] which is available with FLUENT 12 [xiii]. The meshes were comprised of quadrilateral, triangular and combination of two forms in three different cases as shown in Fig. 1, 4 and 6. Out of these Fig. 1 shows structured mesh, Fig. 4 depicts unstructured mesh whereas Fig. 6 indicates mesh comprising of structured elements and boundary layer regions. Once developed in Gambit, these meshes were exported to Fluent. The boundary conditions employed include, velocity inlet, pressure outlet, wall boundary condition on the bed and side walls and free surface was treated as symmetry plane. The velocity value at the inlet was taken as 0.39317 m/s. The roughness height at the bed and walls was taken as 3×10^{-6}. Atmospheric pressure was assumed at the outlet. In case of periodic boundary condition inlet and outlet were treated as periodic boundaries. For this periodic boundary condition, a value of mass flow rate of 1.645 kg/s was taken at the inlet/outlet. It was ensured that the y^+ distance was such that the first cell lied with in fully turbulent region and log-law exists in that part of the flow. The convergence criterion was set as 1×10^{-6}. The under-relaxation factors were set at their default values The SIMPLE algorithm was taken for pressure-velocity coupling. The first-order upwind scheme has been incorporated for momentum, continuity, turbulence kinetic energy etc. Mesh independence was performed before simulation of different cases.

IV. Results and Discussions

The structured mesh has been shown in Fig. 1. The residual diagram for this mesh has been shown in Fig. 2. This diagram shows that there is a good convergence history for this mesh type. Fig. 3 represents the contour plots of primary velocity vectors over different sections along the span of the channel. From this diagram it is very clear that velocity was uniform at the inlet and then gradually develops as we moved downstream of the channel. The numerical model captured these aspects with much accuracy. The velocity profiles are shown on half of the channel due to symmetric cross-section of the channel. Doing so reduces the cost and time consumption required for simulation.

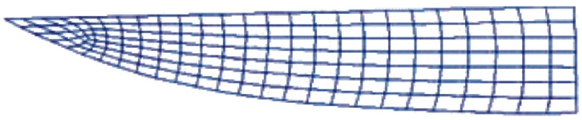

Fig. 1. Structured mesh over the cross section

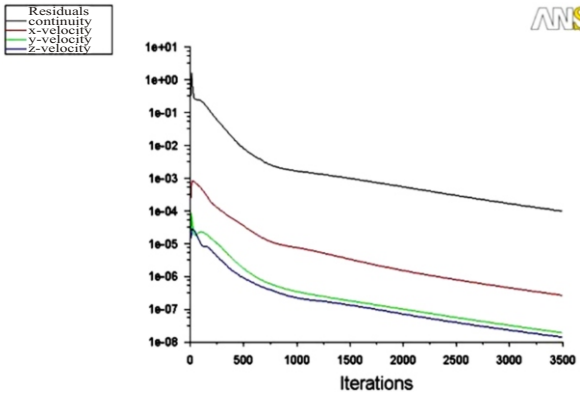

Fig. 2. Residuals for structured mesh

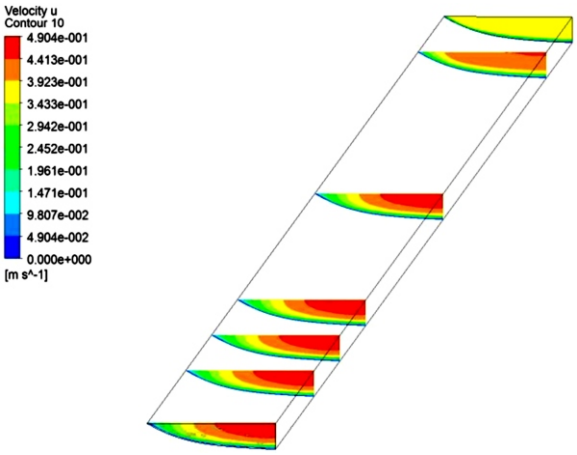

Fig. 3. Contour plots for primary velocities along the span of the channel

The above mentioned velocity profiles are perpendicular to mid section and free surface because these have been taken as axis of symmetry. The mesh shown in Fig. 4 is an unstructured mesh comprised of triangular elements. The corresponding velocity contours obtained by simulating this mesh are shown in Fig. 5. The results are not so good indicating poor performance of the mesh. This might be due to misappropriation of mesh elements for this case.

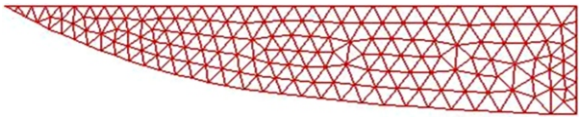

Fig. 4. Unstructured mesh over the cross section

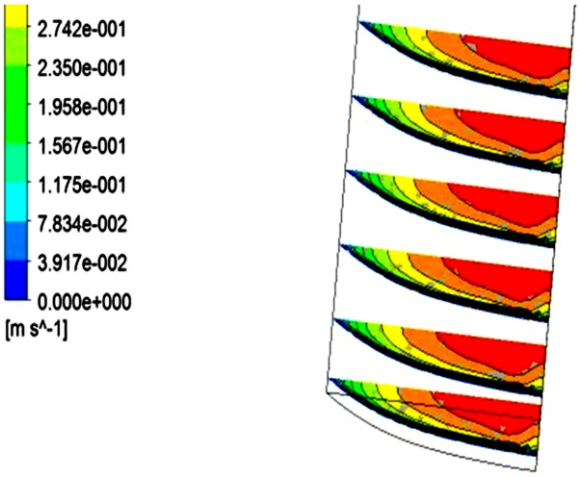

Fig. 5. Contour plots for primary velocities along the span of the channel for unstructured mesh

The Fig. 6 shows third type of mesh tested in this research work. It is comprised of boundary layer region close to bed of the channel whereas in the inner and upper regions, the quadrilateral elements have been used. Results from this mesh have been shown in Fig. 7 which are of good quality. These are also perpendicular to mid section and free surface due to condition of symmetry boundary condition employed there.

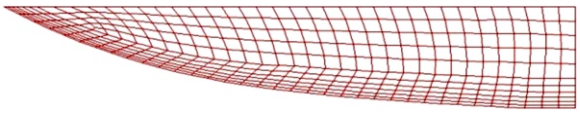

Fig. 6. Structured mesh with boundary layer over the cross section

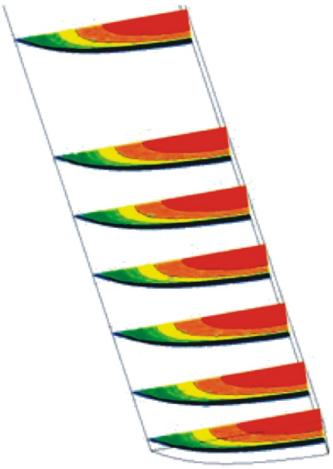

Fig. 7. Contour plots for primary velocities along the span of the channel for structured/boundary layer mesh

As far as periodic boundary condition is concerned, it was employed on the meshes of Fig. 1, 4 and 6 but with a reduced domain. The channel length for this case was reduced to only 1 m. With periodic boundary condition applied at inlet and outlet for these cases, the fully developed flow was achieved quickly. The results of primary velocity contours obtained for structured and boundary layer regions are similar to the one obtained previously however for unstructured it was slightly better but in all these cases, simulation converged quickly due to reduced domain. The results for these cases have been shown in Fig. 8-10.

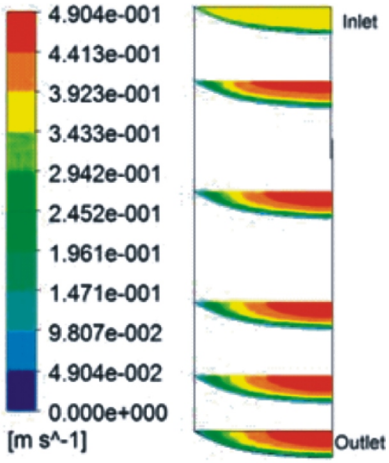

Fig. 8. Contour plots for primary velocities along the span of the channel with periodic boundary conditions for structured mesh

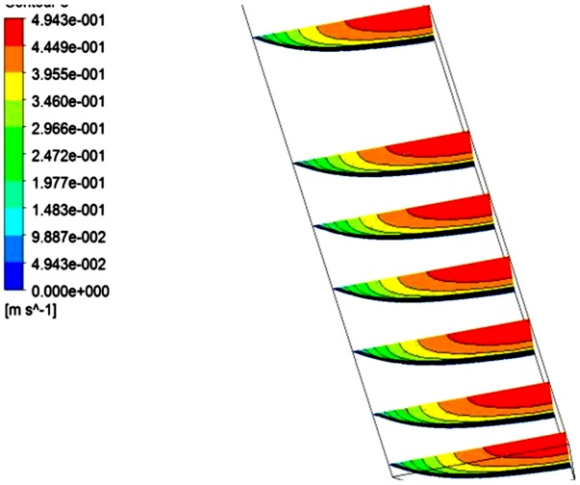

Fig. 9. Contour plots for primary velocities along the span of the channel with periodic boundary conditions for unstructured mesh

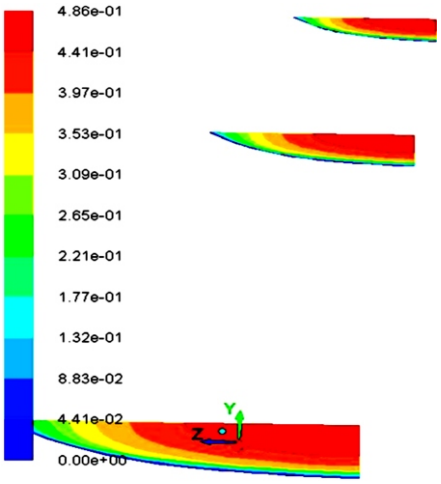

Fig. 10. Contour plots for primary velocities along the span of the channel with periodic boundary conditions for structured/boundary layer mesh

V. Conclusions

The results from a numerical investigation have been given in this research paper. It included the investigation regarding suitability of mesh type and boundary condition on simulation process of a curved open channel. It was observed that structured and boundary layer meshes produced similar results but unstructured gave poor results. As far boundary condition is concerned it was found that periodic boundary was helpful in reducing number of cells, time consumption due to less number of cells, and thus less cost of simulation was required for this case without compromising the accuracy of the results. So it can be concluded that boundary layer structured mesh with periodic boundaries will be most suitable for this type of open channel flow.

Refrerences

[i] B. Ataie-Ashtiani, C. T. Simmons, and A. D. Werner, Influence of Boundary Condition Types on Unstable Density-Dependent Flow. Journal of Groundwater, 2014. 52(3): p. 378-387.

[ii] G. Desrayaud, E. Chénier, A. Joulin, A. Bastide, B. Brangeon, J. P. Caltagirone, Y. Cherif, R. Eymard, C. Garnier, S. Giroux-Julien, Y. Harnane, A. Sergent, S. Xin, and A. Zoubir, Benchmark solutions for natural convection flows in vertical channels submitted to different open boundary conditions. International Journal of Thermal Sciences, 2013. 72: p. 18-33.

[iii] A. Bousquet, M. Marion, M. Petcu, and R. Temam, Multilevel finite volume methods and boundary conditions for geophysical flows". Journal of Computers & Fluids, 2013. 74: p.66-90.

[iv] J. Nycander, A. M. Hogg, and L. M. Frankcombe, Open boundary conditions for nonlinear channel flow. Journal of Ocean Modelling, 2008. 24: p. 108-121.

[v] M. H. Yu, Y. Deng, L. Qin, D. Wang, Y. Chen, Numerical Simulation of Levee Breach Flows Under Complex Boundary Conditions. Journal of Hydrodynamics, Ser. B, 2009. 21 (5): p.633-639.

[vi] J. Zhang, Y. P. Wang, A method for inversion of periodic open boundary conditions in two-dimensional tidal models. Journal of Computer Methods in Applied Mechanics and Engineering, 2014. 275: p. 20-38.

[vii] S. M. Hosseini, and J. J. Feng, Pressure boundary conditions computing incompressible flows with SPH. Journal of Computational Physics, 2011. 230 (19): p. 7473-7487.

[viii] S. K. Choi, M. Park, and H. Kang, Numerical simulations of cellular secondary currents and suspended sediment transport in open channel flows over smooth-rough bed strips. Journal of Hydraulic Research, 2007. 45(6): p. 829-840.

[ix] S. R. McLean, The role of non-uniform roughness in the formation of sand ribbons. Journal of Marine Geology, 1981. 42: p. 49-74.

[x] A. Muller, and X. Studerus, Secondary flow in an open channel. Proceedings of 18th IAHR Congress, 1979. 3: p. 19-24.

[Xi] W. Rodi, Turbulence Models and Their Applications in Hydraulics, A State of the art Review. IAHR Monograph series Delft, Netherland, 1980.

[xii] User Guide Gambit 2.3. Gnterra Resources Park 10 Cavendish Court, Lebanon: New Hamshire, USA, 2010.

[xiii] User Guide Fluent 12. Lebnon: FLUENT 12 Incorporated Lebanon, New Hamshire, USA, 2011.

Design and Development of Environment Friendly Textile Dyeing Machine

N. Ahmad[1], I. A. Shaikh[2], S. Munir[3], E. Suhail[4], I. Ahmad[5]

[1]*Institute of Geology, University of the Punjab, Lahore*
[2,3,4,5]*College of Earth & Environmental Science, University of the Punjab, Lahore*
[2]textilemaster@gmail.com

Abstract-This work describes the novel development, installation, and operation of a textile dyeing machine that used one of the most emerging technologies based on Advanced Oxidation Processes (AOPs). The new machine was found to be capable of reducing water consumption by 57% and process time by 40%, without compromising textile dyeing quality. Different shades were dyed on newly built dyeing machine using three different types of reactive dyes, Vinylsulphone, Monofluorotriazine, and Monochlorotriazine. The washing and rinsing of dyed fabrics were carried out at the completion of dyeing, both in conventional and newly developed dyeing machines. Fabrics washed in both machines was compared in terms of color fastness, color alteration, color fading, and final appearance. Overall results from the environment point of view have indicated that the new dyeing machine is a promising alternative to the conventional machine because its wastewater exhibited lower pH, conductivity, and colour strength.

Keywords-Jet Dyeing Machine, AOPs, Ozone, Reactive Dyes, Washing

I. INTRODUCTION

In recent years, environment seems to be the driving force for the development of new technologies which should not only consume less energy and water, but should also reduce wastewater quantity and toxicity. Textile industry is no exception and number of efforts have been made in the past for the reduction of pollution load in terms of several parameters such as chemical oxygen demand (COD), biological oxygen demand (BOD), total suspended solids (TSS), colour strength, pH, and temperature [i, ii].

Application of ozone (O_3) in various industrial applications has been widely investigated [iii]. The high oxidation potential of ozone (2.07 V) is found to be capable to degrade aromatic structures and unsaturated bonds, such as -C=C- or -N=N-, which are commonly found in chemical structures of textile dyes[iv]. The oxidation power of ozone is the result of extra oxygen atom that can easily breakdown these chemical structures into simpler biodegradable products [v]. Moreover, reactions of ozone with other chemicals, such as textile dyes, do not produce any sludge [vi] or toxic by-products [vii]. Ozone also lowers COD of the effluent making it suitable to discharge into water streams [viii]. Another merit of using ozone in industrial applications is that ozone is always applied in its gaseous state, and thus it does not increase the volume of sludge and wastewater.

Ozone can react with organic materials using two different pathways, firstly by direct oxidation as molecular O_3, and secondly by indirect reaction through hydroxyl (OH) radicals [ix, x]. In water, ozonation process may undergo following reactions:

$$O_3 + OH^- \rightarrow HOO\bullet + O_2 \quad \text{(i)}$$

$$O_3 + O^{-2} \rightarrow O\bullet_3 + O_2 \quad \text{(ii)}$$

$$O\bullet_3 + H^+ \rightarrow HO\bullet_3 \quad \text{(iii)}$$

$$HO\bullet_3 \rightarrow HO\bullet + O_2 \quad \text{(iv)}$$

The reaction between OH ions and O_3 can lead to the generation of super oxides anion radicals O_2 and hydroperoxyl radicals HOO• [xi]. When the pH of aqueous solution is acidic, O_3 is available in molecular form [xii].

This pilot-scale study investigated the efficiency of a newly developed textile dyeing machine equipped with ozone application. The application of ozone gas in the machine effectively decolorized the used washing and rinsing wastewater. This wastewater can then be subsequently reused in the same process.

II. MATERIALS AND METHODS

2.1 MATERIALS

2.1.1 Textile material, dyes and chemicals

A textile knitted fabric (100% cotton) having 200 gsm and made out with 21/s ring-spun yarn was used throughout the study. Selected commercial reactive dyes (Dystar, Pakistan) used in the study are summarized in Table I.

TABLE I
REACTIVE DYES AND RECIPES USED IN THE EXPERIMENTAL WORK

Dye Commercial Name	Colour strength (% owf)	C.I. Name	Type of Reactive dye
Shade: RED			
Remazol Red RR	5	Mixed dye	Vinylsulfone
Remazol Brillian Blue BB	0.5	C.I. Reactive Blue 220	
Remazol Golden Yellow RNL	0.5	C.I. Reactive Orange 107	
Shade: Yellow			
Cibacron Yellow F-3R	5	C. I. Reactive Orange 91	Monofluorotriazine
Cibacron Red F-B	0.5	C. I. Reactive Red 184	
Cibacron Blue F-R	0.5	C. I. Reactive Blue 182	
Shade: Blue			
Procion Yellow H-EXL	0.5	C. I. Reactive Yellow 138	Monochlorotriazine
Procion Brilliant Red H-EGXL	0.5	C. I. Reactive Red 231	
Procion Blue H-EXL	5	C. I. Reactive Blue 198	

Chemical auxiliaries like sodium sulphate (Na_2SO_4) and sodium carbonate (Na_2CO_3) used were of commercial grade and used without any further purification.

2.1.2 Development of dyeing machine

Newly developed dyeing machine Fig. 1 was consisted of a regular 10 kg jet machine (Thies GmbH & Co. KG, Germany), equipped with an O_3 generator (Kaufman, OZ-50, Germany), O_3 analyzer (Ozonova, UVP 200, Germany), injector pump, O_3 catalyst (destroyer), O_3 gas leak detector, ORP meter, and ambient air O_3 monitor (Gfg, Micro III, Germany).

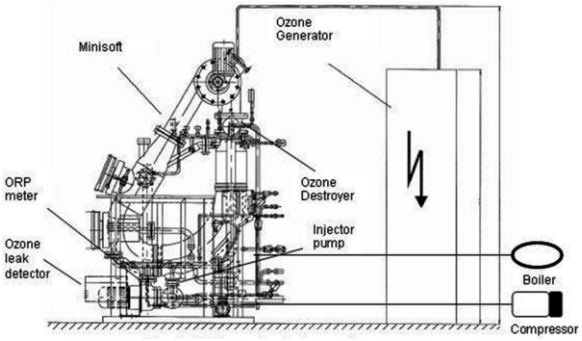

Fig. 1. Schematic diagram of newly developed textile dyeing machine

Fig. 2. Picture of newly developed textile dyeing machine

The O_3 gas was generated using the ozone generator designed to produce up to 50g /hr of O_3. The flow rate O_3 gas was kept at the rate of 500 L/min. To avoid heating up of ozone generator, cooling water was circulated in the generator. The transfer of O_3 gas from the ozone generator to the dyeing machine was carried out with the help of an injector pump connected to machine through a stainless pipe (2-inch internal diameter). The O_3 was injected at the bottom of dyeing machine, next to the suction of main water pump to get homogenous mixing of O_3 with the used washing and rinsing wastewater. Injection of O_3 at this location of the machine can ensure maximum mass transfer of O_3 gas into the wastewater. Unused and non-reacted O_3 gas from the machine was destroyed using a catalyst destructor. In order to monitor the dissolved O_3 in the machine, a self-cleaning ORP (Oxidation-Reduction Potential) meter (RAB automation, Model 39300, Germany) was also installed. The ORP meter measured the dissolved O_3 with the help of electrodes. An ozone leak detector (SK 110, Germany) was also installed on the machine to detect the O_3 gas around the machine.

2.3 METHODS

2.3.1 Color removal efficiency

Dyed fabrics in newly developed dyeing machine were subjected to O_3 application. This treatment was continued until the wastewater is decolorized around 95%. The color removal (%) was determined using the following equation:

$$D = \frac{C_0 - C_t}{C_0} \times 100$$

D = decolorization (%), C_0 = initial concentration of dye,
C_t = concentration of dye at time t

2.3.1 Evaluation of color differences and fastness properties

The color fastnesses of dyed fabrics were assessed using AATCC test methods. AATCC 61-2001-2A and AATCC Test Method 8-2001 were used to evaluate color change and rubbing fastness, respectively [xiii, xiv]. The CIELAB color values of dyed fabrics were measured using spectrophotometer (Spectraflash SF 600 PLUS CT, Datacolor, USA).

III. Results and Discussions

3.1 Machine efficiency

After loading 5kg of fabric in the dyeing machine, it was filled with 50 liters of fresh water at liquor ratio (L:R) of 1: 10 and ozone application was initiated. Characteristics of treated wastewater and experimental conditions for various shades are summarized in Table II.

TABLE II
CONDITIONS AND EFFICIENCIES OF THE MACHINE

Shade	Ozone Dose (mg/m) ppm	Ozone Exposure Time (min)	Conductivity (µS/cm)	pH	Temp. (°C)	Color removal (%)
RED	167	0	9	9.98	42	-
		10	17	9.65	41	67
		20	25	9.1	39	84
		30	27	8.5	37	91
		40	31	8.25	34	94
		50	38	7.8	32	96
Yellow	133	0	11	10.1	48	-
		10	21	9.51	44	75
		20	27	9.18	37	87
		30	31	8.2	35	99
Blue	167	0	6	9.81	41	-
		10	10	9.12	39	77
		20	13	8.68	37	84
		30	21	8.21	34	89
		40	28	7.7	32	93
		50	29	7.48	30	97

For Red shade, the O_3 dose and air flow were set to 10g/hr and 600 LPM, respectively. This particular flow rate maintained the differential pressure (ΔP) of the machine on negative side to avoid build-up of O_3 in the machine. At this particular flow rate, O_3 concentration in the feed gas was found to be 0.22 mg/l. There was no adjustment in the pH of the wastewater before or during the ozonation. However, pH was observed to be changing during ozonation. After 50 minute of O_3 treatment, the colour of wastewater was significantly reduced to almost colourless solution yielding 96% colour removal. In case of Yellow shade, 99% colour removal was achieved after 30 minutes of treatment using 133 mg/m of O_3 dose. Similar trend was observed in Blue shade.

The pH values of wastewaters were also measured and displayed in Fig. 3.

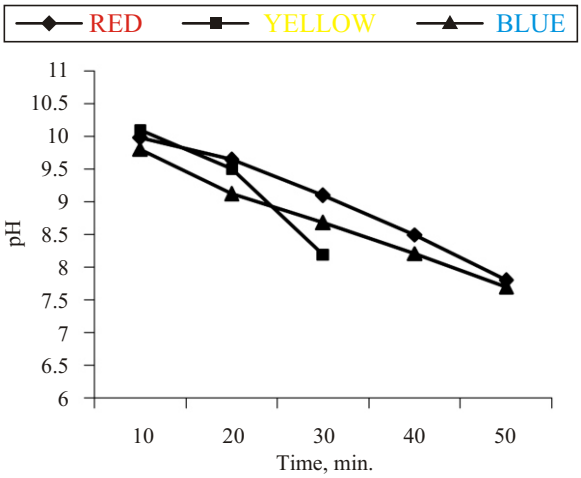

Fig. 3. Effect of treatment time on

At the start of O_3 application, the starting pH of the wastewater was around 10, which gradually dropped to around 7.5 in 30-50 minutes. This drop in pH during O_3 application was in line with similar studies [xv, xvi, xvii].

3.2 Colour difference values

The colour difference values between reference fabric and those washed in new are summarized in Table III.

TABLE III
COLOR DIFFERENCES OF REFERENCE AND NEW MACHINE WASHED FABRICS

Shade	ΔL*	Δa*	Δb*	ΔC*	Δh*	ΔE^*_{cmc}
Red	-0.86	-0.19	0.11	-0.03	0.22	0.89
Yellow	0.03	0.00	0.10	-0.09	0.01	0.10
Blue	-0.56	0.41	0.20	0.41	-0.20	0.72

The results pertinent to RED shade clearly indicate that minor differences in lightness (ΔC*= -0.03), Hue (ΔH* = 0.22), and total difference (ΔE*cmc=0.89) were noticed. Similarly, negligible colour differences were observed in Yellow and Blue shades.

3.3 Fastness properties

The fastness results are summarized in Table IV. The results clearly show that fabrics processed on conventional and newly developed machines exhibited identical fastness properties, and most ratings were found to be in the range of 4.5 to 5, which indicates commercially acceptable results.

TABLE IV
COLOR FASTNESS AND CHANGE OF SHADE PROPERTIES OF REFERENCE AND NEW MACHINE WASHED FABRICS

Shade	Dyes fabrics	Rubbing		Colour Staining			Change of Shade
		Dry	Wet	Cotton	Nylon	PES	
Red	Reference	5	4.5	4.5	5	5	-
	New Machine Washed	4	5	4.5	5	5	4.5
Yellow	Reference	5	5	5	5	5	-
	New Machine Washed	5	5	5	5	5	4.5
Blue	Reference	5	4.5	4.5	5	5	-
	New Machine Washed	5	5	4.55	5	5	5

The change of shade data for all three shades confirms the fact that new machine provided similar dyeing results.

IV. CONCLUSION

It is observed that new machine would require far less O_3, compared to conventional O_3 applications that were tried as an end-of-pipe treatments to remove colour in final, complex, and highly coloured wastewater. A comparative analysis pertaining to water consumption in new machine also showed that 57% less water was used in new machine. This saving of water due to the fact that rinsing process in new machine was completed with 3 fills and drains as opposed to 7 in conventional machine. Consequently, if the new machine is used in the industry at liquor ratio of 1:8, it is possible to use only 24 L water for one kilogram of fabric, instead of using 56 L water in conventional machine. The new machine also did not use any steam, and thus proved to be a low energy intensive compared to the conventional machine.

ACKNOWLEDGEMENT

The authors wish to thank Thies GmbH & Co. (Germany) for their support to design and develop new machine.

REFERENCES

[i] H. Selcuk. (2005, Mar.). Decolorization and detoxification of textile wastewater by ozonation and coagulation processes. *Dyes Pigments.* [Online]. *64(3),* pp. 217-222. Available:http://www.sciencedirect.com/science/article/pii/S0143720804001147

[ii] I. Arslan-Alaton. (2007, Jan.). Degradation of a commercial textile biocide with advanced oxidation processes and ozone. *J. Environ Manage.* [Online]. *82*(2), pp.145-154. Available:http://www.sciencedirect.com/science/article/pii/S0301479706000193

[iii] H. Zhou and D. W. Smith. (2002, Jul.). Advanced technologies in water and wastewater treatment. *J. ENVIRONENG SCi.* [online]. *1(4),* pp. 27-264. Available:http://www.nrcresearchpress.com/doi/abs/10.1139/s02-020#.U6CVDfmSzX9

[iv] A. C. Silva, J. S. Pic, G. L. Sant'Anna Jr & M. Dezotti. (2009, Sep.). Ozonation of azo dyes (Orange II and Acid Red 27) in saline media. *J. of Hazard. Mater.*[Online].*169(13),* pp.965-971. Available:http://www.sciencedirect.com/science/article/pii/S030438940900613X

[v] C. C. Alton. (1983). Recycling dye wastewater through ozone treatment. *Text. Ind. 7,* pp. 26-30.

[vi] N. H. Ince and D. T. Gonenc. (1997). Treatability of a textile azo dye by UV/H_2O_2. *Environ. Technol.* [Online]. *18(2)*, pp. 179-185. Available:http://www.tandfonline.com/doi/pdf/10.1080/09593330.1997.9618484

[vii] F. Gahr, F. Hermanutz and W. Opperman. (1994). Ozonation an important technique to comply with new German law for textile wastewater treatment. *Water Sci. Technol.30* pp. 255-263.

[viii] Y. Xu, R. E. Lebrun, P. J. Gallo & P. Blond. (1999). Treatment of textile dye plant effluent by nanofiltration membrane. *Sep. Sci. Tech.* [Online]. *34(13),* pp. 2501-2519. Available:http://www.tandfonline.com/doi/pdf/10.1081/SS-100100787

[ix] I. Arslan, I. Akmehmet Balcioglu & T. Tuhkanen. (1999, Dec.). Oxidative treatment of simulated dyehouse effluent by uv and near-UV light assisted Fenton's reagent. *Chemosphere,* [Online]. *39(15),* pp. 2767-2783. Available:http://www.sciencedirect.com/science/article/pii/S0045653599002118

[x] S. Baig & P. Liechti. (2001). Ozone treatment for biorefractory COD removal. *Water Sci. Technol.* [Online]. *43*(2), pp.197-204. Available:http://www.iwaponline.com/wst/04302/wst043020197.htm

[xi] C. Gottschalk, J. A. Libra & A. Saupe. (2009). *Ozonation of water and waste water: A practical guide to understanding ozone and its applications*. (2nd ed.) [Online]. Available:http://books.google.com.pk/books?hl=en&lr=&id=MGpBHLw2POsC&oi=fnd&pg=PR5&dq=Ozonation+of+Water+and+Waste+Water.&ots=INij_yLMc3&sig=HZC7ei1Rm3CaFKjQWF60YYy62f0#v=onepage&q=Ozonation%20of%20Water%20and%20Waste%20Water.&f=false

[xii] W. Chu & C. W. Ma (2000, Aug.). Quantitative prediction of direct and indirect dye ozonation kinetics. *Water Res.* [Online]. *34(12),* pp. 3153-3160. Available:http://www.sciencedirect.com/science/article/pii/S0043135400000439

[xiii] *Colorfastness to Laundering*, AATCC Testing Method 61-2001-2A, 2001.

[xiv] *Colorfastness to Crocking*, AATCC Testing Method 8-2001,2001.

[xv] U. K. Khare, P. Bose & P. S. Vankar. (2007, Nov.). Impact of ozonation on subsequent treatment of azo dye solutions. *J. Chem. Tech. Biot.* [Online]. *82(11),* pp.1012-1022. Available:http://onlinelibrary.wiley.com/doi/10.1002/jctb.1785/full

[xvi] E. Oguz & B. Keskinler. (2008, Mar.). Removal of colour and COD from synthetic textile wastewaters using O_3, PAC, H_2O_2 and HCO_3^-. *Journal of Hazardous Materials,* [Online]. *151(23),* pp. 753-760. Available:http://www.sciencedirect.com/science/article/pii/S0304389407009090

[xvii] O. Avinc, H. A. Eren & P. Uysal. (2012, Dec.). Ozone applications for after-clearing of disperse-dyed poly (lactic acid) fibres. *Color. Technol.* [Online]. *128(6),* pp. 479-487. Available:http://onlinelibrary.wiley.com/doi/10.1111/j.1478-4408.2012.00403.x/full

Variations in Return Loss of Patch Antennas in the Close Proximity of Human Body and Rectangular and Cylindrical Phantoms at 1.8 GHz

M. I. Khattak[1], M. Shafi[1], N. Khan[1], R. Edwards[2], Nasim Ullah[3], M. Saleem[4]

[1]University of Engineering and Technology Peshawar, Pakistan
[2]Electrical and Electronic Engineering Department, Loughborough University, LE11 3TU, UK
[3]Smart PCB Ghouri Town Rawalpindi, Pakistan
[4]Ghulam Ishaq Khan Institute of Engineering Sciences and Technology, Pakistan
M.I.Khattak@nwfpuet.edu.pk

Abstract-The performance evaluation of an antenna in the presence of human body is attracting considerable interest due to the increasing use of Body Area Networks (BAN). This study investigates the variations in matching of linearly polarised and circularly polarised patch antennas due to the presence of human body and glass fibre Specific Anthropomorphic Mannequin (SAM). The return loss at 1.8GHz is measured at varying distances to study the matching behaviour. It was found that flat section phantom gave optimal return loss closer to its surface than an actual human. Also the optimal return loss for a circularly polarised antenna is at a distance that is double than that for a linearly polarised antenna. The findings of this research are particularly useful when considering the separation distance between wearable antenna and human body in both intra and inter body wireless connectivity.

Keywords-Linear and Circular Polarised Patch Antenna, Losses, Patch Antennas, Phantoms, Propagation and Specific Anthropomorphic Mannequin (SAM)

I. INTRODUCTION

An ongoing trend in communications is the incorporation of technology both onto and into the human body [i, ii]. Medical imaging techniques for the early detection of problem matter in the body can benefit from this technology[iii, iv]. With the increasing usage of cell phones and personal digital assistants (PDAs), research on the microwave interactions with the users (humans) has received a great amount of interest in recent years[v, vi]. It is now accepted that lossy biological tissue has a serious impact on the performance of an on-body antenna. However, using volunteers during the design process is not always sensible and therefore the need for body simulating phantoms that closely exhibit the properties of human tissues in the frequency ranges used for on-body networks has increased. Examples of such Tissue-mimicking (TM) phantoms can be found in [vii-x]. However, these phantoms involve complicated fabrication methods as well as chemicals that may be difficult to obtain.

Measured values for Specific absorption rate (SAR) are important in wearable antennas as it gives an insight of the interaction of fields with body tissues. The lossy nature of biological tissue makes a human body to absorb a major portion of energy which is produced by the antenna. Authors of [xi-xiii] have worked on calculations of SAR levels for mobile phones at different environments near the SAM. Note that fairly generic phantoms such as SAM are useful both as standards and for prototyping on-body antennas. They consist of a rigid outer shell, filled with a phaseless tissue simulating liquid [xiv].

It has been proved that humans are not an ideal medium for radio frequency propagation [xv-xix]. Body behaves as partially conductive medium that consists of approximately thirty different tissue types, each of which has its own different electrical properties. The dispersive and lossy nature of humans means that resonance and absorption can quickly lead to far field pattern distortion of on-body antennas [xx, xxi]. Propagation on the surface of the body is more complex than that of free space, so simple path loss rules cannot be applied to on-body propagation. On-body propagation may be considered as a combination of free space propagation, diffraction (creeping waves) and reflections from the environment. However, the properties of wearable antennas are strongly linked to the degree of closeness (proximity) to the body and to be effective a wearable antenna must be separated at some isolation distance from the human body on which it is to be analyzed. This study is therefore, concerned with the optimal separation distance between the body surface and the antenna.

In this paper, we measure the effects of a fibre glass phantom and the human body on the return loss of a linearly polarised and a circular polarised patch antenna. Both probe fed (with main beam towards the skin/shell) and planar fed (with main beam away from the skin/shell) versions of the antenna are considered.

The objective of the experiments carried out in this research is to assess the extent to which a simple SAM like phantom can be relied upon to predict an optimal distance of the wearable antenna from the body during antenna design.

II. Technical Description of the Experimental Setup

A. Antenna Design

Simple patch antennas fabricated on FR4 were used in the experiments. The antenna designs [xxii]were modified using CST Microstripes. To maintain a proper distance above SAM and Human chest and back spacers were used. Fig. 1 gives a line demonstration of antennas and the positioning spacer.

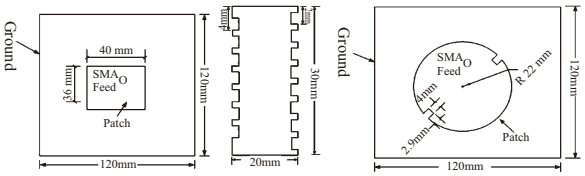

Fig. 1. An unscaled line diagram of patch antennas and experimental spacer

A particular care was given for the accurate calibration and minimized cable disturbance. A combination of metallic cap [xxiii] and ferrite beads were used for the purpose of chocking any surface currents on the coax because of the mismatch in impedance at the feeding point. This concept of metallic cap at the end of the coaxial cable is shown in Fig. 2.

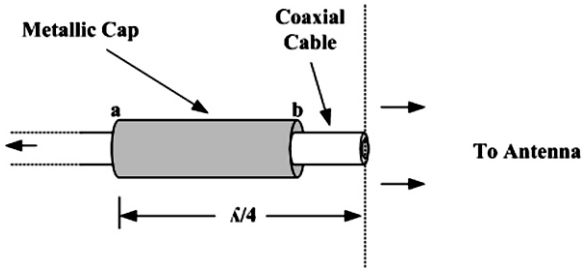

Fig. 2. Quarter wave current choke used for surface currents at the cable

The repeatability of the experiments was ensured by performing them repeatedly for few days. It was also observed that a variation of ± 0.5-to-1dB in S_{11}(dB) was monitored due to any flexing in the coaxial cable during the experiments. A Portable Network Analyzer operated on batteries was used in all measurements. To test the behaviour of an antenna with its main beam directed away from the surface of the human body and the SAM, a microstrip line, linear polarised [xxii] and circular polarised [xxiv] patch antennas were used as shown in Fig. 3.

B. The Phantom Muscle Simulating Dielectric Liquid

The phantoms were manufactured from 2mm thick glass fibre and are shown in Fig. 4. The dimensions of these phantoms were so selected to closely match with the size of human body. Note that in microwave measurements use of glass fibre as a phantom material is a validated practice [xxv-xxvii].

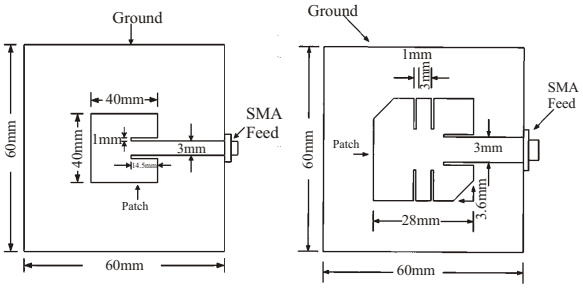

Fig. 3. A line diagram of a microstrip line patch antennas

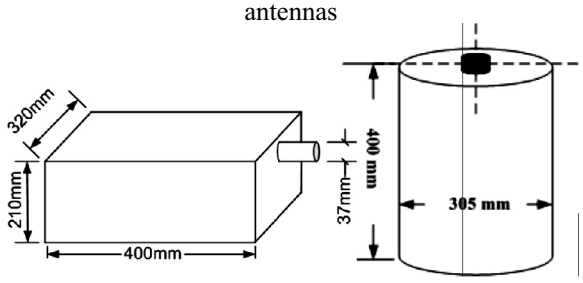

Fig. 4. An unscaled line diagram of Phantoms

The electrical properties of the SAM and the dielectric fluid used to simulate human muscle are given in Table I. A comprehensive procedure for making the muscle simulating liquid can be found in [xiv]. The volume of the phantom could accommodate approximately 10 liters of liquid and special care was taken to avoid air pockets while filling the phantoms. This was achieved by slow filling and settling of the liquid.

TABLE I
Electrical Properties of Material Used in Experiments

	ε_r	$\sigma(S/m)$
Muscle Simulating Dielectric Liquid (MSL)	55.15	1.47
FR4 chip	4.5	0
Glass Fibre	4.5	6e(-3)
PVC Spacer	4.0	10.01e (-6)

C. Measurement Procedure

The measurements were performed for the separation distance of 3cm from the surface of the body which is nearly equivalent to the several layers of usual clothing (T-Shirt) and may be an outer garment such as a coat. Previously research work at Loughborough University [xxviii, xxix] had mentioned that dielectric constants for most of the garments varies from 1 to 2.5 and are low loss, so the clothing effect can be neglected. Therefore, The two main reasons associated with the variation in the return loss of the wearable antennas are as follows:

The reflection from the surface of the human body or SAM and

Losses in the skin and muscle of the human body and the dielectric liquid used in the phantoms

Standard calibration technique was adopted for the calibration to normalize the cable losses. The S_{11}(dB) measurements were taken for a range of 2 to 30mm with 2mm steps in every interval. The antenna was not allowed to touch the human skin while measuring the return loss to avoid the shortening of the antenna with the human skin because of the finite conductivity of skin at the intended operational frequency of 1.8GHz. Fig. 5 shows the experimental setup.

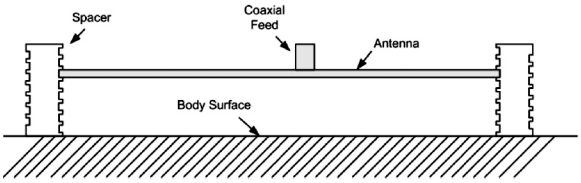

Fig. 5. Antenna positioning with respect to the surface of a Human Body and Phantoms

It can be seen that the phantom is fully planar and the human mid top back is approximately considered to be planar. All volunteers were male and were in their mid-twenties. Since the effects measured are only sensitive in the very near field, so the measurements were taken in a laboratory. For authentication, another experimental setup inside in an anechoic chamber was designed to further reduce the reflections by using RF absorbers. This is setup is shown in Fig. 6.

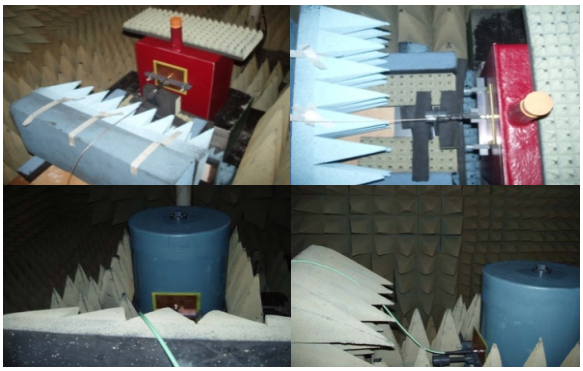

Fig. 6. Antenna positioning on the Phantoms inside the Anechoic Chamber

D. Antennas, Human Torso and Phantoms Models

The simulated linear and circular polarised patch antennas at 1.8GHz are shown in Fig. 7 (a) and 7 (b) respectively. The dimensions of their patches are given in Table II. The ground plane in each case was 120x120x1.6 mm^3.

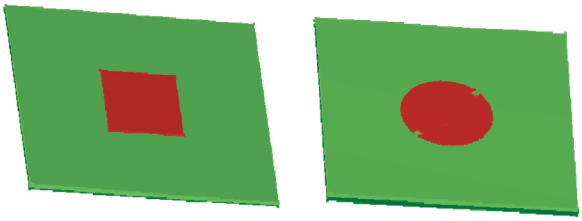

Fig. 7. (a) Linear polarised rectangular patch antenna, (b) Circular polarised circular patch antenna

TABLE II
DIMENSIONS OF THE PATCHES AND GROUND PLANES OF RECTANGULAR AND CIRCULAR PATCH ANTENNAS AT 1.8GHZ

Antenna type	Ground Plane (mm^3)	Patch Dimensions
Rectangular Patch	120x120x1.6	Length=36mm Width=40mm
Circular Patch	120x120x1.6	Radius=22mm

Simple three layer human body model was created in CST Microstripes. These kind of layered models are common in practice [xxx-xxxii]. The simulated model contained layers of muscle, dry skin and wet skin. The dimensions of the cylindrical model approximated the human torso, 290mm from stomach to back, 418mm from shoulder to shoulder and 450mm for vertical height from shoulder to waist. Similarly, 2mm thick fibre glass models of rectangular and cylindrical phantoms were also created and their dimensions were carefully chosen so as to match the human body model dimensions as given above. These models with an antenna on the top are shown in Fig. 8. The parametric study was carried out by changing the distance between antenna and human body models.

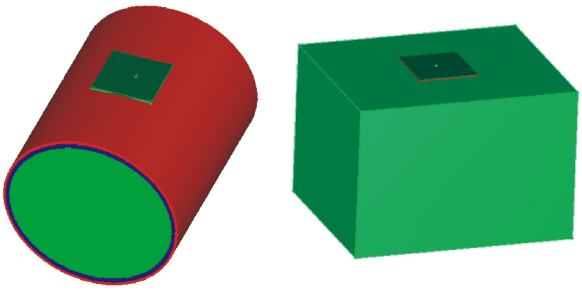

Fig. 8. Simulated (a) human body and (b) rectangular phantom models in CST Microstripes with patch antenna on their top at 1.8GHz

III. RESULTS

A. Experimental Results

To get the maximal amplitude of the reflected waves and surface currents, probe fed linear and circular polarised antennas were used, with their main beam directed towards the surface of the rectangular phantom and human body. This may not be typical in wearable antennas but may be such in medical imaging. The measured S_{11}(dB) at varying distances from the surface of the human body and muscle simulating liquid (MSL) filled phantom at operational frequency of 1.8GHz for linear and circular polarised patch antennas is shown in Fig. 9 and Fig. 10 respectively. It can be observed that for rectangular phantom, the best match occurs at a distance of 15mm from the phantom and for the human body it occurs at a distance of 26mm from the surface. When compared, the variations in the match resemble each other; but for human body it occurs right shifted, approximately 10mm.

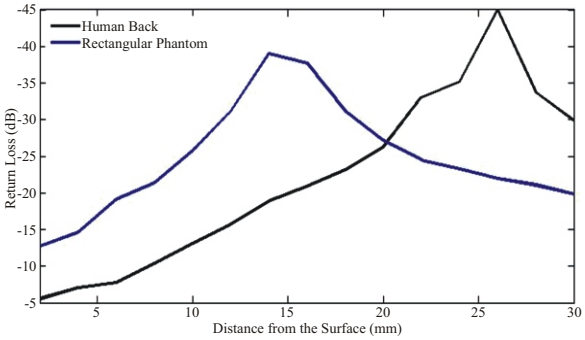

Fig. 9. Recorded S_{11}(dB) Variations for Rectangular SAM and Back of a Human Body.
Antenna Type: Linear Polarised Operational Frequency: 1.8GHz

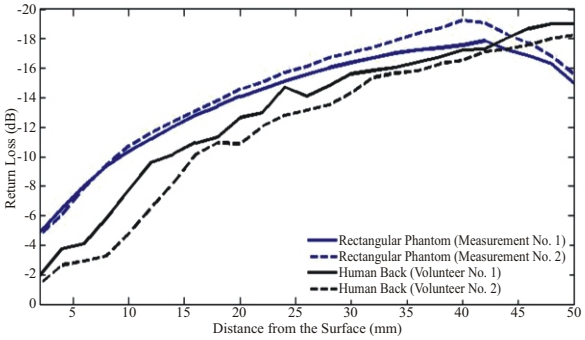

Fig. 10. Recorded S_{11}(dB) Variations for Rectangular SAM and Back of a Human Body.
Antenna Type: Circular Polarised Operational Frequency: 1.8GHz

In the 2nd set of experiments, both rectangular and cylindrical phantoms were used in comparison to the human body, for linear and circular polarised antennas at 1.8GHz inside in an anechoic chamber. The measured S_{11}(dB) at varying distances from the surface of the human body and muscle simulating liquid (MSL) filled rectangular and cylindrical phantoms at operational frequency of 1.8GHz for linear and circular polarised patch antennas is shown in Fig. 11and Fig. 12 respectively. It can be observed that when compared with rectangular phantom, both human body and cylindrical phantom resonates the antennas exactly at the same distance, and right shifted by 6-10mm.

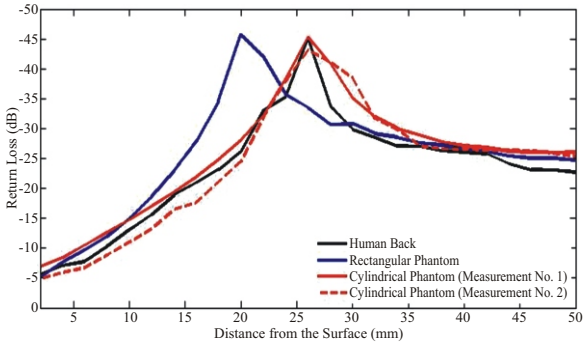

Fig. 11. Recorded S_{11}(dB) Variations for Rectangular and Cylindrical SAM and Back of a Human Body.
Antenna: Linear Polarised
Operational Frequency: 1.8GHz

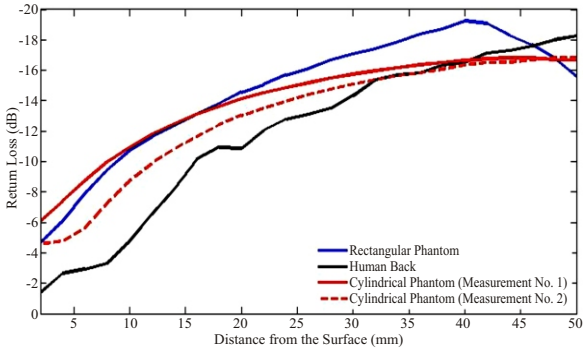

Fig. 12. Recorded S_{11}(dB) Variations for Rectangular and Cylindrical SAM and Back of a Human Body.
Antenna: Circular Polarised Operational Frequency: 1.8GHz

In 3rd set of experiments, microstrip line patch antennas shown in Fig. 3, were used with their main beam directed away from the surface of the human body and phantom. The radiations in this case are mainly blocked by the ground plane, and only reduced back lobe interacts with the human body. Therefore, there is no considerable change in return loss versus distance from the surface, as shown in Fig. 13 and Fig. 14. The knee of the response in Fig. 13 and Fig. 14 (demonstrated with the help of arrows) reflects that both for linear and circular polarised antennas, null in the match occurs 10mm before for rectangular phantom as compared to that of the human body and cylindrical phantom. It shows that the conclusions drawn from the 1st and 2nd set of experiments are correct.

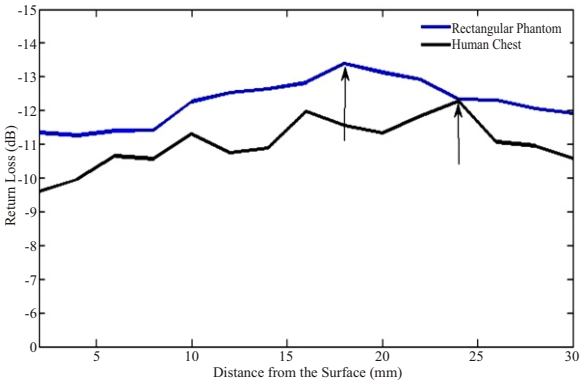

Fig. 13. Comparison of S_{11}(dB) Measurements for a Dielectric Liquid filled Rectangular Phantom and Chest of a Human Body for a Microstrip Line Linear Polarised Antenna at 1.8GHz

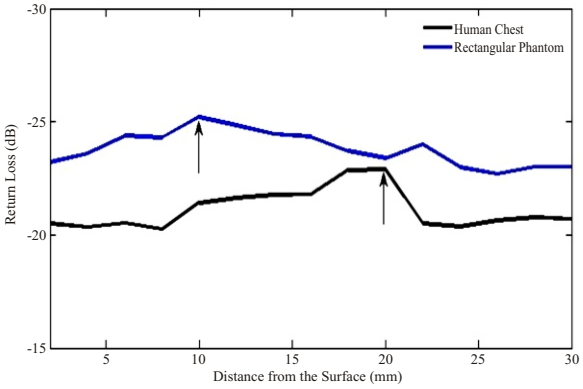

Fig. 14. Comparison of S_{11}(dB) Measurements for a Dielectric Liquid filled Rectangular Phantom and Chest of a Human Body for a Microstrip Line Circular Polarised Antenna at 1.8GHz

B. Simulation Results

As discussed earlier, to strengthen our experimental results and conclusions, CST Microstripes was used to simulate antennas, 2mm glass fibre rectangular and cylindrical phantoms and human body models.

Fig. 15 shows the variation in return loss of the linear polarised antenna at different distances from the surfaces of glass fibre rectangular phantom and human body models. Similarly, Fig. 16 shows variations in return loss of circular polarised antenna when its distance is varied from the surfaces of glass fibre rectangular and cylindrical phantom and human body model. It can be observed clearly in and Fig. 16 that when considered against human body and cylindrical phantom, there is always a right shift in the resonance of linear and circular polarised antennas.

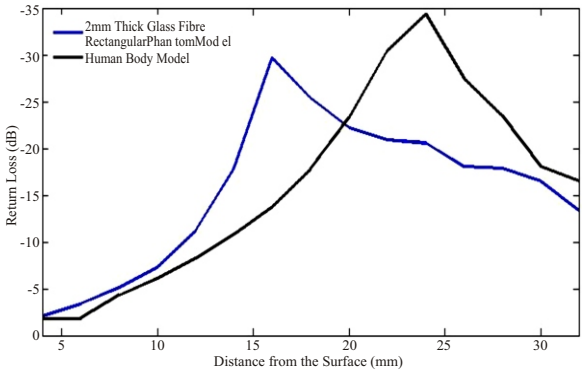

Fig. 15. Comparison of S_{11}(dB) Measurements for a 2mm Glass Fibre Rectangular Phantom and a Human Body Model for Linear Polarised Antenna at 1.8GHz

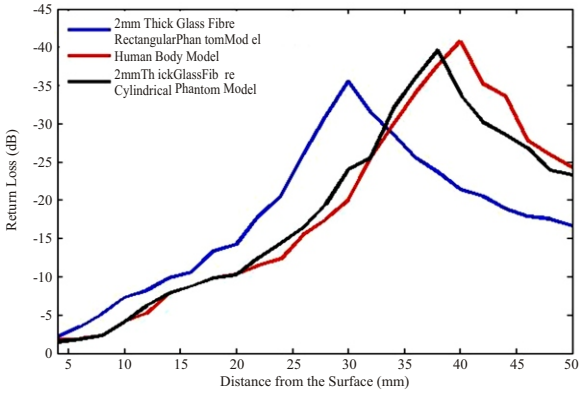

Fig. 16. Comparison of S_{11}(dB) Measurements for a 2mm Glass Fibre Rectangular and Cylindrical Phantom and a Human Body Model for Circular Polarised Antenna at 1.8GHz

IV. CONCLUSIONS

This paper investigates the mismatch variations of the patch antennas placed close to the biological tissue and fiberglass made rectangular and cylindrical phantoms. Just according to the expectations both human body as well as the phantoms changes the resonance to a low frequency.

A number of experiments were performed to draw thorough conclusions. In every set of experiments, it was found that the resonance of a patch antenna, whether linear polarised or circular polarised, occur approximately 10mm before for rectangular phantom as compared to that of the human body and cylindrical phantom. The only reason to the cause seems to be the edges of the rectangular phantom. So the recommended option in shapes of the phantom is the cylindrical one in antenna measurements inside or outside the anechoic chamber. Furthermore, the results suggest that *null* of the match for circular polarised antenna occurs at approximately double the distance as compared to the linear polarised antenna, both for the rectangular and the cylindrical phantom. The outcomes of the experiments were also verified when main beam of the

antenna was directed away from the body surface. In this set of experiments as shown in Fig. 13 and Fig. 14, the variations in mismatch were not noticeable when the distance from the surface was varied; yet a closer view of the mismatch patterns shows that *null* of the resonance curve in case of rectangular phantom occurs at approximately 10mm before that of the human body model for linear and circular polarised antennas. Also the best match for circular polarised antenna occurs at nearly double the distance of the linear polarised antenna. At the end, the simulation results as shown in Fig. 15 and Fig. 16, also confirmed the afore-mentioned conclusions.

Based on the experimental results obtained in this research, it is recommended that the separation distance must be increased while using rectangular phantoms in wearable antenna measurements.

REFERENCES

[i] J. W. Hines, "Medical and surgical applications ofspace biosensor technology", *Acta Astronaut.,* vol. 38, pp. 261-267, 1996.

[ii] S. Park and S. Jayaraman, "Enhancing the quality of life through wearable technology", *IEEE Engineering in Medicine and Biology Magazine,* vol. 22, pp. 41-48, 2003.

[iii] E. Fear, S. Hagness, P. Meaney, M. Okoniewski and M. Stuchly, "Enhancing breast tumor detection with near-field imaging", *IEEE Microwave Magazine,* vol. 3, pp. 48-56, 2002.

[iv] S. C. Hagness, A. Taflove and J. E. Bridges, "Two-dimensional FDTD analysis of a pulsed microwave confocal system for breast cancer detection: Fixed-focus and antenna-array sensors", *IEEE Transactions on Biomedical Engineering,* vol. 45, pp. 1470-1479, 1998.

[v] R. W. Y. Habash, *Electromagnetic Fields and Radiation: Human Bioeffects and Safety.* CRC, 2001.

[vi] D. Poljak, A. Sarolic and V. Roje, "Human interaction with the electromagnetic field radiated from a cellular base station antennas", in *EMC EUROPE 2002 International Symposium on Electromagnetic Compatibility,* 2002.

[vii] A. Guy, "Analyses of electromagnetic fields induced in biological tissues by thermographic studies on equivalent phantom models", *IEEE Transactions on Microwave Theory Tech.,* vol. 19, pp. 205-214, 1968.

[viii] A. Surowiec, P. Shrivastava, M. Astrahan and Z. Petrovich, "Utilization of a multilayer polyacrylamide phantom for evaluation of hyperthermia applicators", *International Journal of Hyperthermia,* vol. 8, pp. 795-807, 1992.

[ix] C. McCann, J. Kumaradas, M. Gertner, S. Davidson, A. Dolan and M. Sherar, "Feasibility of salvage interstitial microwave thermal therapy for prostate carcinoma following failed brachytherapy: studies in a tissue equivalent phantom", *Phys. Med. Biol.,* vol. 48, pp. 1041-1052, 2003.

[x] S. Davidson and M. Sherar, "Measurement of the thermal conductivity of polyacrylamide tissue-equivalent material", *International Journal of Hyperthermia,* vol. 19, pp. 551-562, 2003.

[xi] C. J. Panagamuwa, et al. "Experimental verification of a modified specific anthropomorphic mannequin (SAM) head used for SAR measurements", *Antennas and Propagation Conference, LAPC 2007. Loughborough.* IEEE, 2007.

[xii] W. G Whittow, C. J. Panagamuwa, R. M. Edwards and P. McEvoy, "*Investigating the Effect of Adding a Seam Along the Nose of the SAM Phantom to Allow Excitation from the Front*", *March 2006, pp 1-9, Reports for EPSRC Grant no EP/C517490/1.*

[xiii] W. G Whittow, et al. "On the effects of straight metallic jewellery on the specific absorption rates resulting from face-illuminating radio communication devices at popular cellular frequencies", *Physics in medicine and biology* 53.5 (2008): 1167.

[xiv] "Schmid & partner engineering AG, DASY4 manual V4.1, march 2003."

[xv] E. Reusens, W. Joseph, G. Vermeeren and L. Martens, "On-body measurements and characterization of wireless communication channel for arm and torso of human", in *IFMBE PROCEEDINGS*, pp. 264, 2007.

[xvi] A. Fort, J. Ryckaert, C. Desset, P. De Doncker, P. Wambacq and L. Van Biesen, "Ultra-wideband channel model for co mm un ic at io n around the human body", *IEEE J. Select. Areas Commun.,*vol. 24, pp. 927, 2006.

[xvii] H. Ghannoum, C. Roblin and X. Begaud, *Investigation of the UWB on-Body Propagation Channel,* 2005.

[xviii] A. Fort, C. Desset, J. Ryckaert, P. De Doncker, L. Van Biesen and P. Wambacq, "Characterization of the ultra wideband body area propagation channel", in *2005 IEEE International Conference on Ultra-Wideband, 2005. ICU 2005,* 2005, pp. 6.

[xix] A. Alomainy, Y. Hao, X. Hu, C. Parini and P. Hall, "UWB on-body radio propagation and system modelling for wireless body-centric networks", *IEE Proceedings-Communications,* vol. 153, pp. 107-114, 2006.

[xx] O. P. Gandhi, *Biological Effects and Medical Applications of Electromagnetic Energy.* Prentice-Hall Englewood Cliffs, NJ, 1990.

[xxi] R. Adey, E. Albert, S. Allen, J. Allis, P. Barber, H. Bassen, E. Berman, C. Blackman, R. Carpenter and K. Chen, "Biological effects and medical applications of electromagnetic energy", *Proc IEEE,* vol. 68, pp. 5, 1980.

[xxii] C. A. Balanis, "Antenna theory analysis and design", *John Wily & Sons Inc,* 1997.

[xxiii] C. Icheln, J. Ollikainen and P. Vainikainen, "Reducing the influence of feed cables on small antenna measurements", *Electronic Letert.,* vol. 35, pp. 1212, 1999.

[xxiv] W. S. Chen, "Inset-microstripline-fed circularly polarised microstrip antennas", in *IEEE Antennas and Propagation Society International Symposium,,1999 Digest. Held in conjunction with: USNC/ URSI National Radio Science Meeting*, 1:260-3, 1999.

[xxv] Y. Koyanagi, H. Kawai, K. Ogawa and K. Ito, "Consideration of the local SAR and radiation characteristics of a helical antenna using a cylindroid whole body phantom at 150 MHz", *Electronics and Communications in Japan (Part I: Communications),* vol. 87, 2004.

[xxvi] W. G. Whittow, et al. "Specific absorption rates in the human head due to circular metallic earrings at 1800MHz", *Antennas and Propagation Conference, LAPC 2007. Loughborough.* IEEE, 2007.

[xxvii] V. Hombach, et al. "The dependence of EM energy absorption upon human head modeling at 900 MHz", *IEEE Transactions onMicrowave Theory and Techniques,* 44.10 (1996): 1865-1873.

[xxviii] L. Ma, R. M. Edwards, W. G. Whittow, "A Mult-band Printed Monopole Antenna", *EUCAP2009*, Berlin, Germany, pp.1-3, ISBN: 9781424447534.

[xxix] L. Ma, R. M. Edwards, S. Bashir and M. I. Khattak, "A Wearable Flexible Multi-Band Antenna Based On A Square Slotted Printed Monopole", *Antennas and Propagation Conference, 2008. LAPC 2008*, Loughborough, pp. 345-348.

[xxx] Z. Hu, M. Gallo, Q. Bai, Y. Nechayev, P. Hall and M. Bozzettit, "Measurements and simulations for on-body antenna design and propagation studies",*EuCAP 2007. the Second European Conference on Antennas and Propagation, pp. 1-7, 2007.*

[xxxi] Y. Hao, A. Alomainy, Y. Zhao, C. G. Parini, Y. Nechayev, P. Hall and C. C. Constantinou, "Statistical and deterministic modelling of radio propagation channels in WBAN at 2.45 GHz", in *IEEE Antennas and Propagation Society International Symposium 2006, pp. 2169-2172, 2006.*

[xxxii] A. Christ, T. Samaras, A. Klingenbock and N. Kuster, "Characterization of the electromagnetic near-field absorption in layered biological tissue in the frequency range from 30 MHz to 6000 MHz", *Phys. Med. Biol.,* vol. 51, pp. 4951-4966, 2006.

A Secure Cyclic Steganographic Technique for Color Images Using Randomization

K. Muhammad[1], J.Ahmad[2], N. U. Rehman[3], Z. Jan[4], R. J. Qureshi[5]

[1,2,3,4,5]Computer Science Department, Islamia College Peshawar, Pakistan
Khan.muhammad.icp@gmail.com

***Abstract*-**Information Security is a major concern in today's modern era. Almost all the communicating bodies want the security, confidentiality and integrity of their personal data. But this security goal cannot be achieved easily when we are using an open network like Internet. Steganography provides one of the best solutions to this problem. This paper represents a new Cyclic Steganographic Technique (CST) based on Least Significant Bit (LSB) for true color (RGB) images. The proposed method hides the secret data in the LSBs of cover image pixels in a randomized cyclic manner. The proposed technique is evaluated using both subjective and objective analysis using histograms changeability, Peak Signal-to-Noise Ratio (PSNR) and Mean Square Error (MSE). Experimentally it is found that the proposed method gives promising results in terms of security, imperceptibility and robustness as compared to some existent methods and vindicates this new algorithm.

***Keywords*-**Steganography, Least Significant Bit, Cyclic Steganographic Technique

I. INTRODUCTION

Steganography is a Greek origin word meaning "Concealed Writing". It can be considered as a way to hide secret information in cover image pixels such that it cannot be detected by Human Visual System (HVS) and nobody know about its existence without the intended sender and receiver. Steganography requires three main components named as carrier object, secret data and steganographic algorithm. Sometimes a secret key and cryptographic algorithm is also required in order to increase the security levels and introduce multiple barriers in the way of an attacker. Steganography can be used for many useful applications like online voting security, secure transmission of top-secret data between national and international governments, online banking security, military and intelligent agencies security and safe circulation of secret documents among defense organizations. On the other hand, Steganography is also very nefarious; it is used by terrorists and criminals for their secure communication and sending viruses and Trojan horses to compromise machines. [i-iv].

1.1 Types of Steganography w.r.t Carrier Object

There are five different types of steganography based on the carrier object that is used for embedding the secret information. The carrier object may be images, text, videos, audios or network protocol packets. If the image is used as a carrier, it is called image steganography. Similarly if video is used for hiding secret messages, we call it video steganography and so on[i, v]. The diagrammatic representation of different types of steganography is shown in Fig. 1.The types of steganography are:

a. Audio Steganography
b. Image Steganography
c. Video Steganography
d. Text Steganography
e. Network Steganography

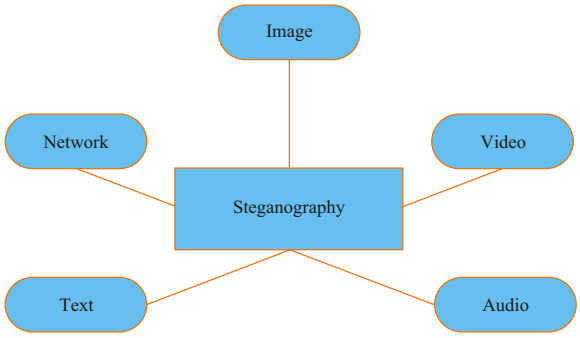

Fig. 1. Types of Steganography w.r.t carrier object

1.2 Types of Steganography w.r.t Key Exchange

To make the steganographic algorithm more robust against different fraudulent behaviors, the idea of using secret key and public key was introduced. When secret key and public keys are used in steganography, a mechanism should be there via which these keys can be securely exchanged. Usually one or two keys are used in the process of steganography; public key that is used to embed secret information into the carrier object and secret or private key that has a mathematical relationship with public key and is used for extraction of secret data from stego object [vi]. On the basis of exchange of keys, there are three types of steganography as shown in Fig. 2.

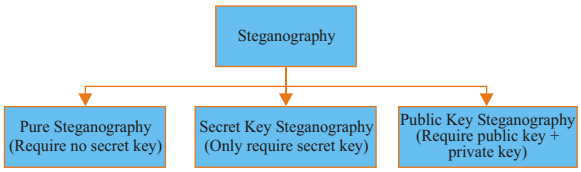

Fig. 2. Types of steganography w.r.t Key Exchange

1.3 Classifications of Steganographic Techniques

The classification of steganographic techniques can be performed using different approaches. One approach is to classify them on the basis of carrier object that is used at the time of embedding the secret data into the carrier object. Another approach is to categorize them on the basis of cover modification in the process of hiding secret information. We use the second approach and classify steganographic techniques into two broad domains.

1.3.1 Spatial Domain Techniques

In spatial domain techniques, the carrier object (image, video etc) pixels are directly changed in order to hide secret data inside it. These techniques have high payload and bring minor changes in the carrier object but are vulnerable to even simple statistical attacks like cropping, scaling, rotating, compression etc. Some of the techniques that belong to spatial domain are:

a. Least Significant Bit (LSB)
b. Gray-Level Modification (GLM)
c. Pixel Value Differencing (PVD)
d. Edges based Embedding (EBE)

1.3.2 Transform Domain Techniques

In transform domain techniques, the carrier object (image, video etc) is first transformed from spatial domain to transform domain and then its frequencies are used to hide the secret data. After embedding the secret data, the object is again transformed into spatial domain. These techniques have lower payload but are robust against statistical attacks. Some techniques of transform domain are[vii]:

i. Discrete Wavelet Transform Technique (DWTT)
ii. Discrete Fourier Transform Technique (DFTT)
Iii. Discrete Cosine Transform Technique (DCTT)

In this paper, color image has been selected as a carrier object because it contains more redundant bits and color image provide more pixels to increase the payload capacity. The remaining of the paper is organized as fellows. Section 2 describes some existence related approaches whose limitations led us towards current proposed work. Section 3 briefly discusses the proposed technique. Section 4 discusses experimental results and discussion and section 5 concludes the paper.

II. Literature Review

Steganography was first started by ancient Greeks in (484-425 BC). Histaeus, the ruler of Miletus shaved the head of his honest slave and then tattooed a secret text or a symbol on his head. When the slave's hair grew back, the slave was sent to Aristagorus in order to provide him the hidden text. When the slave arrived at his destination, his head was shaved again in order to read the secret message. From that time to till now many technical, linguistics and modern steganographic techniques have been developed and used for steganography. All the techniques have their corresponding pros and cons. Some techniques have high payload capacity and good imperceptibility depending upon the selected cover for secret data hiding (Spatial domain techniques) but more vulnerable to attacks (Noise throwing, cropping, rotation, resizing etc) while others techniques are more robust against statistical attacks but they have lower payload capacity. This means that there is always a tradeoff between the three factors (Payload, Imperceptibility and Robustness). As an example a few techniques of steganography are critically discussed below [vii-x].

The most basic technique used for steganography is LSB technique in which the least significant bit of carrier image pixels are replaced with the bits of secret message. To clarify the concept of LSB method, consider the pixels below and hide a secret character (S.C) "B" inside it.

Decimal	Binary	S.C	Binary
143	10001111	B	01000010
134	10000110		
126	01111110		
99	01100011		
44	00101100		
134	10000110		
79	01001111		
127	01111111		

Now replace the LSBs of the given pixels with the secret message bits as shown.

Decimal	Binary
142	1000111**0**
135	1000011**1**
126	01111110
98	0110000**1**
44	00101100
134	10000110
79	01001011
126	0111011**0**

The bold face LSBs are changed which shows that approximately half of the pixels changes so the resultant stego image slightly changes from the original cover image.

In [xi], the authors propose a robust method which embeds variable bits in image pixels depending on the pixel value and value of mean and standard deviation

(SD). Two bits are inserted in the image pixel if (meanSD/2) is greater than pixel value; 3 bits are stored if (mean +SD/2) is greater than pixel value otherwise 4 bits are stored in each pixel value. Chaotic effect is also obtained in the proposed method by using random traversing path which make the attack loathsome but nothing is given about generating the random traversing path which is its major weak point.

Reference [xii] presents pixel indicator technique (PIT) in which one channel is used for indication while other two channels are used for embedding secret data in a predefined cycle manner which enhances the robustness of proposed method. The experimental results demonstrate the larger payload and enhanced imperceptibility of the proposed method. This method also eliminates the stego key exchange overhead. The major limitation of this technique is the fixed number of bits embedded in each gray level of the host image which may cause noticeable distortion if we increase the number of embedded bits. Furthermore, the payload of this method is absolutely dependent on the carrier image and indicator bits which may be reduced.

In [xiii], the authors proposed a new method to embed secret data in the GREEN or BLUE channel of carrier image on the basis of secret key bits and RED channel LSB. This method adds one more level security to the existing LSB method by utilization of secret key. The RED channel LSB and secret key bit is xored and then a decision is taken on the basis of its result to replace the LSB of GREEN or BLUE channel. The proposed method has the same payload, more robustness and better security as compared to simple LSB method. However the secure key exchange of secret key is an open challenge and is an extra overhead of proposed method.

III. Proposed Method

In this paper, a more secure steganographic technique is presented which hides secret data in the LSBs of cover image pixels in a randomized cyclic manner. The order in which secret bits are embedded in cover image pixels' planes is RED, GREEN, BLUE, RED, GREEN, and BLUE and so on. This randomized and cyclic approach increases the robustness of the proposed algorithm and randomly disperses the secret data inside the cover image pixels. Due to this reason it is difficult for a malicious user to extract the original secret data from the stego image. The embedding and extraction algorithm for the proposed method are given below.

3.1 Embedding Algorithm

Input: Color Image and secret data

Output: Stego Image

Step 1: Take the cover color image and secret data.

Step 2: Separate the RED, GREEN and BLUE planes from the cover image.

Step 3: Convert secret data into 1-D array of bits.

Step 4: Set channelFlag = 1 initially (channelFlag determines the channel for embedding).

Step 5: If channelFlag = 1
Replace the LSB of RED channel with secret bit Else if channelFlag = 2
Replace the LSB of GREEN channel with secret bit Else if channelFlag = 3
Replace the LSB of BLUE channel with secret bit End

Step 6: Increment channelFlag by 1.

Step 7: If channelFlag = 3
Set channelFlag = 1;
End

Step 8: Repeat Step 5 to Step 7 until all secret data bits are embedded.

Step 9: Combine all three planes to form the resultant stego image.

<Fig. 3: Embedding Algorithm Flowchart >

3.2 Extraction Algorithm

Input: Stego Image

Output: Secret data

Step 1: Take the stego image and separate the RED, GREEN and BLUE planes from it.

Step 2: Set channelFlag = 1 initially.

Step 3: If channelFlag = 1
Extract the LSB of RED channel.
Else if channelFlag = 2
Extract the LSB of GREEN channel.
Else if channelFlag = 3
Extract the LSB of BLUE channel.
End

Step 4: Increment the channelFlag by 1.

Step 5: If channelFlag = 3
Set channelFlag = 1;
End

Step 6: Repeat Step 3 to Step 5 until all secret data bits are extracted.

Step 7: Convert the extracted secret bits into its original secret data format.

<Fig. 4: Extraction Algorithm Flowchart >

IV. Experimental Results and Discussion

The proposed algorithm, LSB algorithm and Karim's algorithm[xiii] are simulated using MATLAB R2013a. The standard color images used for experiments of implemented three techniques are Lena, baboon, trees etc. Experimentally, these three algorithms are evaluated by three different perspectives:

a. Embedding same amount of cipher in different standard color images of same dimensions.
b. Hiding same amount of secret data in the same

Image of different dimensions.

c. Embedding variable amount of cipher in the same image of same dimensions.

4.1 Comparison of proposed method and existing methods

The comparison of proposed technique with existing techniques is based on two types of analysis known as subjective and objective analysis. Subjective analysis is done using Human Visual System (HVS) to notice the changes between the cover and stego images and their corresponding histograms. A few samples of standard color cover and stego images and their histograms for the proposed method are shown below in Fig. 5-7. From figures it is observed that there is no noticeable change in the cover and stego images and their histograms which shows the effectiveness of the proposed method.

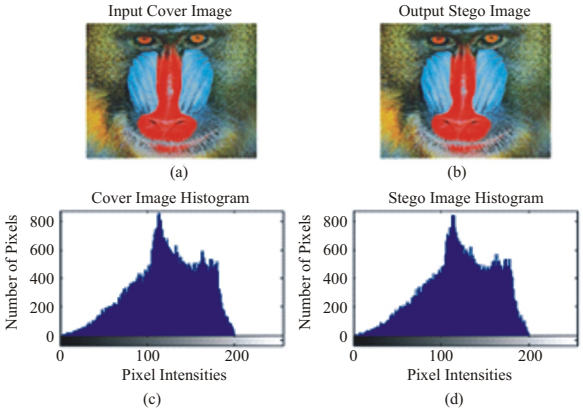

Fig. 5. baboon cover and stego image and their histograms

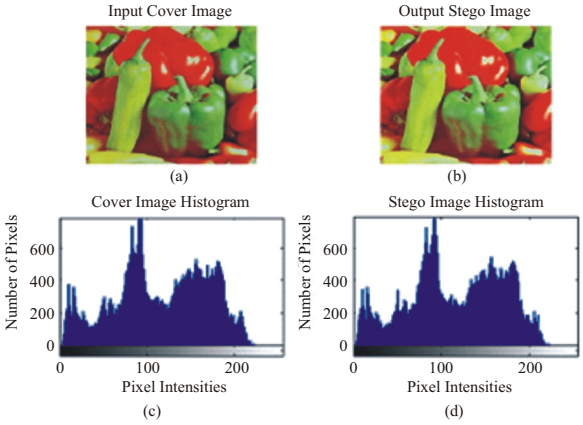

Fig. 6. Peppers cover and stego image and their histograms

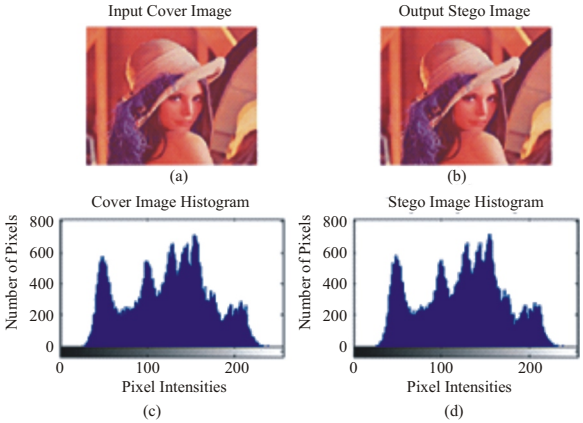

Fig. 7. Lena cover and stego image and their histograms

Objective analysis is the second mathematical standard for measuring the distortion that occurs in the cover image after embedding secret data. Objective analysis is performed on the proposed method using Peak Signal-to-Noise Ratio (PSNR) and Mean Square Error (MSE). PSNR and MSE are calculated using equations (1) and (2).

$$PSNR = 10log_{10}\left(\frac{{C_{max}}^2}{MSE}\right) \quad (1)$$

$$MSE = \frac{1}{MN}\sum_{x=1}^{M}\sum_{y=1}^{N}(S_{xy} - C_{xy}) \quad (2)$$

Here M and N are image dimensions, x and y are loop variables, S is stego image, C is cover image and C_{max} is the maximum pixel intensity among both images. The experimental results of the proposed method, LSB and method in [xiii] are shown in Table I, Table II and Table III respectively.

TABLE I
COMPARISON BASED ON PSNR

Image Name	LSB Method	Karim's Method [13]	Proposed Method
	PSNR (dB)	PSNR (dB)	PSNR (dB)
baboon.png	61.8784	48.558	52.5573
lena.png	42.6331	42.6204	71.8865
building.png	51.4677	47.0305	63.4042
parrot.png	49.708	49.8421	49.8417

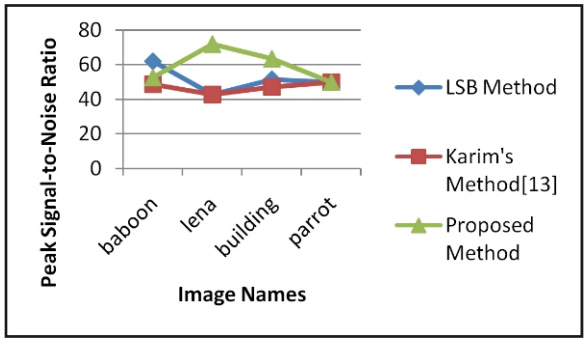

Fig. 8. Comparison based on PSNR with different images of dimension 256×256

TABLE II
PSNR BASED COMPARISON OF EXISTING AND PROPOSED METHOD

Image Dimensions	LSB Method	Karim's Method [13]	Proposed Method
	PSNR(dB)	PSNR(dB)	PSNR(dB)
128×128	70.3187	65.5328	65.5474
256×256	61.8784	50.8811	52.5573
512×512	52.4555	37.2456	48.8123
1024×1024	59.204	41.9577	49.7897

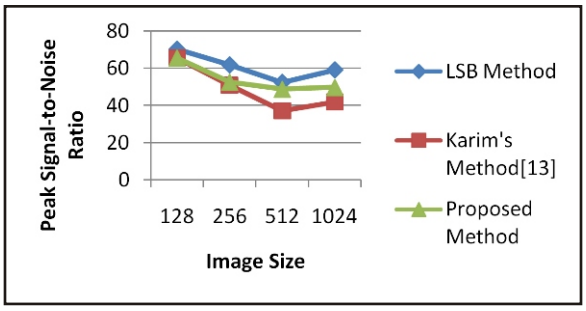

Fig. 9. PSNR based comparison with same size cipher & different image dimensions

TABLE III
COMPARISON BASED ON PSNR WITH VARIABLE AMOUNT OF CIPHER EMBEDDED

Image Name	Cipher size in (KBs)	LSB Method	Karim's Method [13]	Proposed Method
		PSNR(dB)		
baboon with dimension 256×256	2	63.3775	52.0373	52.0668
	4	61.8442	51.6345	51.6853
	6	60.4909	51.1776	51.2539
	8	59.7481	50.8811	51.0035

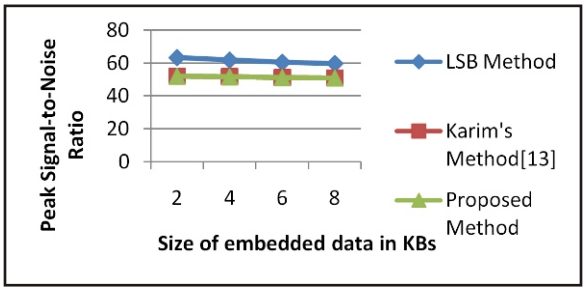

Fig. 10. Comparison based on PSNR with same image dimension and variable amount of cipher

4.2 Performance Analysis of the proposed method

The performance of a steganographic technique is measured using three metrics; payload, robustness and imperceptibility. An algorithm is considered to be best if it has high imperceptibility, more robustness and larger payload. The payload of all three mentioned approaches is same i.e. 1bpp (bits per pixel). The proposed scheme is better than classical LSB scheme in terms of robustness because the classical LSB method directly hides data in only blue channel which can be easily detected while the proposed method scatters it in all three channels and hence increases the robustness. In contrast to Karim's method, the proposed method gives better imperceptibility as indicated by larger PSNR values in Table I-III.

4.3 Advantages and limitations of the proposed method

The proposed method embeds the secret data inside the gray levels of the host image in a randomized cyclic manner which increases its robustness and makes the extraction difficult. Furthermore, the proposed scheme gives better imperceptibility as compared to existing methods which can be also confirmed by larger values of PSNR. The major weakness of the proposed method is its vulnerability to different image processing and statistical attacks such as image cropping, scaling and noise attacks. Since spatial domain is used for the proposed scheme, therefore the embedded data will be lost like other schemes if the stego image is compressed, rotated or attacked with different types of noises (pepper noise, salt and pepper, speckle noise etc).

V. CONCLUSIONS

In this paper, we proposed a more secure cyclic steganographic algorithm for RGB images using the concept of randomization with enough robustness, imperceptibility and security. An average PSNR above 50dB is achieved by the proposed algorithm which describes its superioty as compared to some existing steganographic algorithms. The proposed method hides the same amount of secret data as LSB and Karim's method but scatters it inside the whole image pixels to increase the robustness. The utilization of randomization and cyclicness makes the extraction of original secret information from the stego image more difficult for a malicious user. Hence the proposed technique gives promising results in terms of robustness, imperceptibility and security.

VI. ACKNOWLEDGMENT

The authors wish to thank all the contributors for their critical and technical review of the proposed work and their valuable support and guidance. Special thanks to Mr. Zahid Khan for his valuable help and support during this research work

REFERENCES

[i] S. Roy and P. Venkateswaran, "Online payment system using steganography and visual cryptography," in *Electrical, Electronics and Computer Science (SCEECS), 2014 IEEE Students' Conference on*, 2014, pp. 1-5.

[ii] P. Pathak, A. K. Chattopadhyay, and A. Nag,

"A new audio steganography scheme based on location selection with enhanced security," in *Automation, Control, Energy and Systems (ACES), 2014 First International Conference on*, 2014, pp. 1-4.

[iii] I. Diop, S. Farss, K. Tall, P. Fall, M. Diouf, and A. Diop, "Adaptive Steganography scheme based on LDPC codes," in *Advanced Communication Technology (ICACT), 2014 16th International Conference on*, 2014, pp. 162-166.

[iv] A. Sharp, Q. Qi, Y. Yang, D. Peng, and H. Sharif, "A video steganography attack using multi-dimensional Discrete Spring Transform," in *Signal and Image Processing Applications (ICSIPA), 2013 IEEE International Conference on*, 2013, pp. 182-186.

[v] J. Kodovsky and J. Fridrich, "Steganalysis in resized images," in *Acoustics, Speech and Signal Processing (ICASSP), 2013 IEEE International Conference on*, 2013, pp. 2857-2861.

[vi] F. Wang, L. Huang, Z. Chen, W. Yang, and H. Miao, "A novel text steganography by context-based equivalent substitution," in *Signal Processing, Communication and Computing (ICSPCC), 2013 IEEE International Conference on*, 2013, pp. 1-6.

[vii] F. Rezaei, T. Ma, M. Hempel, D. Peng, and H. Sharif, "An anti-steganographic approach for removing secret information in digital audio data hidden by spread spectrum methods," in *Communications (ICC), 2013 IEEE International Conference on*, 2013, pp. 2117-2122.

[viii] J. Fridrich, "Effect of cover quantization on steganographic fisher information," *Information Forensics and Security, IEEE Transactions on,* vol. 8, pp. 361-373, 2013.

[ix] C. Qin, C.-C. Chang, Y.-H. Huang, and L.-T. Liao, "An inpainting-assisted reversible steganographic scheme using a histogram shifting mechanism," *Circuits and Systems for Video Technology, IEEE Transactions on,* vol.23, pp. 1109-1118, 2013.

[x] S. Grabski and K. Szczypiorski, "Steganography in OFDM Symbols of Fast IEEE 802.11 n Networks," in *Security and Privacy Workshops (SPW), 2013 IEEE*, 2013, pp. 158-164.

[xi] R. Amirtharajan, P. Archana, V. Rajesh, G. Devipriya, and J. Rayappan, "Standard deviation converges for random image steganography," in *Information & Communication Technologies (ICT), 2013 IEEE Conference on*, 2013, pp. 1064-1069.

[xii] A. A.-A. Gutub, "Pixel indicator technique for RGB image steganography," *Journal of Emerging Technologies in Web Intelligence,* vol. 2, pp. 56-64, 2010.

[xiii] M. Karim, "A new approach for LSB based image steganography using secret key," in *14th International Conference on Computer and Information Technology (ICCIT 2011)*, 2011, pp. 286-291.

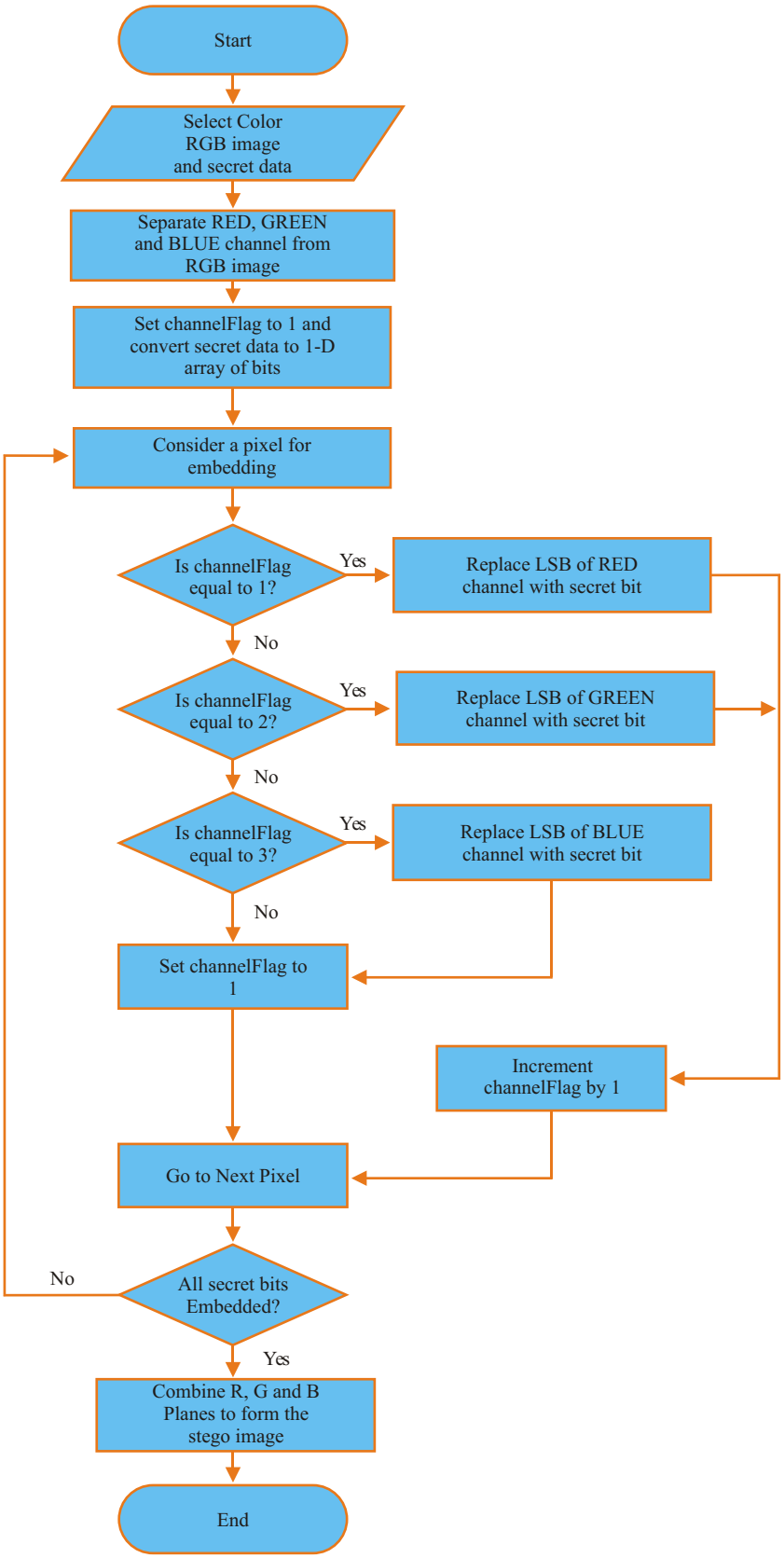

Fig. 3. Embedding Algorithm Flowchart

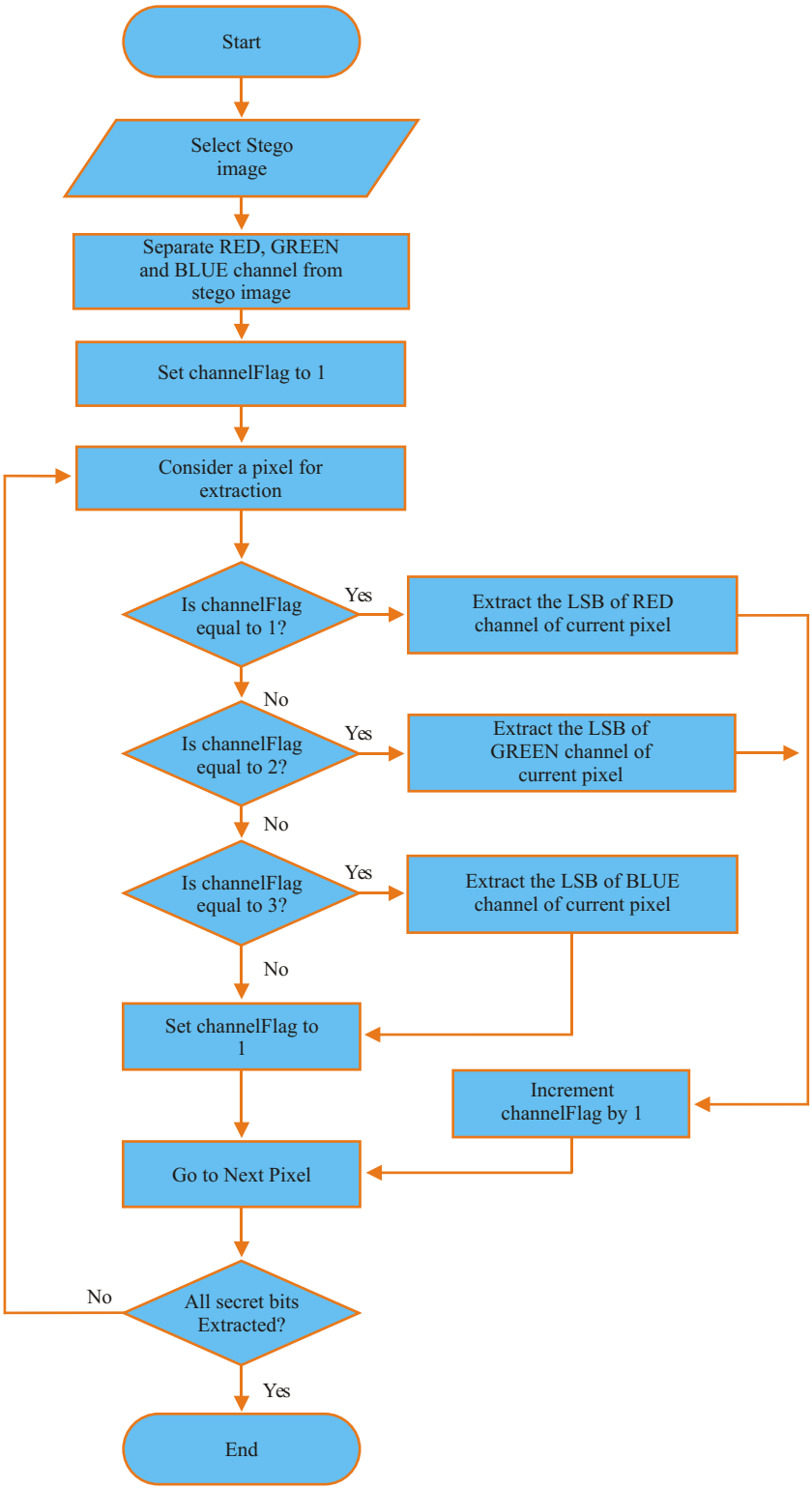

Fig. 4. Extraction Algorithm Flowchart

Technical Journal
University of Engineering and Technology, Taxila
Website: www.uettaxila.edu.pk.

CALL FOR PAPERS

Researchers and Academia are invited to submit the research articles to Technical Journal of UET Taxila. It is a broad-based open access journal. It covers all areas of science, engineering and management.

Technical Journal is a quarterly publication of UET Taxila recognized by HEC in "Y" category. It is published regularly with a key objective to provide the visionary wisdom to academia and researchers to disseminate novel knowledge and technology for the benefit of society. Technical Journal is indexed by well recognized international database such as PASTIC Science Abstracts, AGRIS Data Base and ProQuest Products.

For enquiries, submissions of articles or any other information please visit our website http://web.uettaxila.edu.pk or contact the Editorial Office on the following numbers:

+92-51-9047455, +92-51-9047298
E-mail: technical.journal@uettaxila.edu.pk

It will be highly appreciated if the information is forward to interested colleagues from Pakistan as well as abroad.

Looking forward to receiving the research papers on behalf of Technical Journal Editorial Office.

Prof. Dr. Abdul Razzaq Ghumman
Chief Editor
Technical Journal,
UET, Taxila

Instruction for authors for publishing in Technical Journal UET Taxila

General

Papers may be submitted any time throughout the year. After receipt of paper it will be sent to three referees, at least one from a technology advanced countries. Papers reviewed and declared fit for publication will be published in the coming issue. The journal is quarterly publication, having four issues annually. Two copies of the manuscript should be submitted on the corresponding address given at the end and a soft copy must be submitted through e-mail to the following address:-

technical.journal@uettaxila.edu.pk

Authors are required to read the following carefully for writing a paper.

Manuscript Preparation

Text should be type-written with M.S word, Times New Roman Font size 10, at single space and with margins as 1 inch top,1 inch left, 0.5 inch right, and 1 inch bottom, on an A-4 size paper. The manuscript should be compiled in following order:-

Title Page

The Title page should contain:

- Paper title
- Author names and affiliations
- Postal and email addresses
- Telephone/Cell and fax numbers
- One author should be identified as the Corresponding Author

Abstract

An abstract up to maximum of 200 words should be written in the start of paper. The abstract should give a clear indication of the objectives, scope, methods, results and conclusions.

Keywords

Include at least five keywords (Title Case) in a separate line at the end of the abstract.

Body of the Paper

Body of the paper may include introduction and literature review, materials and methods, modeling/experimentation, results-discussions and conclusions.

- Define abbreviations and acronyms the first time they are used in the text, even after they have already been defined in the abstract. Do not use abbreviations in the title unless they are Unavoidable.
- Use zero before decimal places: "0.24" not ".24".
- Avoid contractions; for example, write "do not" instead of "don't."
- If you are using *Word,* use either the Microsoft Equation Editor or the *MathType* add-on (http://www.mathtype.com) for equations in your paper (Insert | Object | Create New | Microsoft Equation *or* MathType Equation). Number equations consecutively with equation numbers in parentheses flush with the right margin, as in (1). Refer to "(1)," not "Eq. (1)" or "equation (1)," except at the beginning of a sentence: "Equation (1) is ... ."
- Symbols used in the equations must be defined before or immediately after it appears.
- Use SI units only.

Originality

Only original contributions to Engineering, Science and Management literature should be submitted for publication. It should incorporate substantial information not previously published.

Length

Research paper should be consisting of 5-8 pages as per specifications given above.

Accuracy

All the technical, scientific and mathematical information contained in the paper should be checked with great care.

Figures

All figures should be at least 300 dpi in JPG format. It is to be also ensured that lines are thick enough to be reproduced conveniently after size reduction at the stage of composing. All figures (graphs, line drawings, photographs, etc.) should be numbered consecutively and have a caption consisting of the figure number and a brief title or description of the figure. This number should be used when referring to the figure in the text. Figure may be referenced within the text as "Fig. 1" etc.

Tables

Tables should be typed in a separate file using M.S. Word 'table' option. All tables should be numbered in Roman numerals consecutively. Tables should have a caption in Upper Case, must be centered and in 8 pt. consisting of the table number and brief title. This number should be used when referring to the table in text. Table should be inserted as part of the text as close as possible to its first reference.

When referencing your figures and tables within your paper, use the abbreviation "Fig." Even at the beginning of a sentence. Do not abbreviate "Table." Tables should be numbered with Roman Numerals.

Acknowledgments
All individuals or institutions not mentioned elsewhere in the work who have made an important contribution should be acknowledged.

References
Reference may be cited with number in square brackets, e.g. "the scheme is discussed in [3]". Multiple references are each numbered with separate brackets.

Do not use "Ref." or "reference" except at the beginning of a sentence: "Reference [11] illustrates... ." Please do not use automatic endnotes in Word, rather, type the reference list at the end of the paper using the "References" style.

Note: For template of paper please visit our journal's page:
http://web.uettaxila.edu.pk/techjournal/index.html

EDITORIAL OFFICE: Correspondences should be made on the following address:
Asif Ali Editor Technical Journal
Central Library, University of Engineering and Technology (UET) Taxila, Pakistan
Tel**:** +92 (51) 9047298 Email**:**technical.journal@uettaxila.edu.pk